Chapter 2

2.0 PRINCIPAL DESIGN CRITERIA

The Universal Storage System is a canister-based spent fuel dry storage cask system that is designed to be compatible with the Universal Transportation System. It is designed to store a variety of intact PWR and BWR fuel assemblies. This chapter presents the design bases, including the principal design criteria, limiting load conditions, and operational parameters of the Universal Storage System. The principal design criteria are summarized in Table 2-1.

Table 2-1 Summary of Universal Storage System Design Criteria

Parameter	Criteria
Design Life	50 years
Design Code - Confinement	ASME Code, Section III, Subsection NB [1] for confinement boundary
Design Code - Nonconfinement	
Basket	ASME Code, Section III, Subsection NG [2] and NUREG/CR-6322 [3]
Vertical Concrete Cask	ACI-349 [4], ACI-318 [5]
Transfer Cask	ANSI N14.6 [6] and NUREG-0612 [7]
Maximum Weight:	
Canister with Design Basis PWR Fuel Assembly (dry, including inserts) (Class 2)	72,900 lbs.
Canister with Design Basis BWR Fuel (dry) (Class 5)	75,600 lbs.
Vertical Concrete Cask (loaded) (Class 5)	313,900 lbs.
Transfer Cask (Class 3)	121,500 lbs.
Thermal:	
Maximum Fuel Cladding Temperature:	
PWR Fuel	Variable Based on Fuel Type, Burnup and Cool Time. See Table 4.4.7-5 for Temperature Limits. 1058°F (570°C) Off-Normal/Accident/Transfer [21]
BWR Fuel	Variable Based on Fuel Type, Burnup and Cool Time. See Table 4.4.7-5 for Temperature Limits. 1058°F (570°C) Off-Normal/Accident/Transfer [21]
Ambient Temperature:	
Normal (average annual ambient)	76°F
Off-Normal (extreme cold; extreme hot)	-40°F; 106°F
Accident	133°F
Concrete Temperature:	
Normal Conditions	≤ 150°F (bulk); ≤ 300°F (local) [24]
Off-Normal/Accident Conditions	≤ 350°F local/ surface [4]
Cavity Atmosphere	Helium

2.5 References

1. ASME Boiler and Pressure Vessel Code, Division I, Section III, Subsection NB, "Class 1 Components," 1995 Edition with 1995 Addenda.

2. ASME Boiler and Pressure Vessel Code, Division I, Section III, Subsection NG, "Core Support Structures," 1995 Edition with 1995 Addenda.

3. Nuclear Regulatory Commission, "Buckling Analysis of Spent Fuel Basket," NUREG/CR-6322, May 1995.

4. American Concrete Institute, "Code Requirements for Nuclear Safety Related Concrete Structures (ACI 349-85) and Commentary (ACI 349R-85)," March 1986.

5. American Concrete Institute, "Building Code Requirements for Structural Concrete (ACI 318-95) and Commentary (ACI 318R-95), October 1995.

6. ANSI N14.6-1993, "American National Standard for Radioactive Materials - Special Lifting Devices for Shipping Containers Weighing 10,000 Pounds (4,500 kg) or More," American National Standards Institute, Inc., June 1993.

7. Nuclear Regulatory Commission, "Control of Heavy Loads at Nuclear Power Plants," NUREG-0612, July 1980.

8. Levy, et al., Pacific Northwest Laboratory, "Recommended Temperature Limits for Dry Storage of Spent Light-Water Zircalloy Clad Fuel Rods in Inert Gas," PNL-6189, May 1987.

9. Nuclear Regulatory Commission, "Design Basis Tornado for Nuclear Power Plants," Regulatory Guide 1.76, April 1974.

10. Nuclear Regulatory Commission, "Standard Review Plan," NUREG-0800, April 1996.

11. Code of Federal Regulations, "Licensing Requirements for the Independent Storage of Spent Nuclear Fuel and High-Level Radioactive Waste," Part 72, Title 10, January 1996.

12. ANSI/ASCE 7-93 (formerly ANSI A58.1), "Minimum Design Loads for Buildings and Other Structures," American Society of Civil Engineers, May 1994.

13. ANSI/ANS-57.9-1992, "Design Criteria for an Independent Spent Fuel Storage Installation (Dry Type)," American Nuclear Society, May 1992.

14. ASHRAE Handbook, "Fundamentals," American Society of Heating, Refrigeration, and Air Conditioning Engineers, 1993.

15. Code of Federal Regulations, "Packaging and Transportation of Radioactive Materials," Part 71, Title 10, April 1996.

16. Nuclear Regulatory Commission, "Load Combinations for the Structural Analysis of Shipping Casks for Radioactive Material," Regulatory Guide 7.8, March 1989.

17. Nuclear Regulatory Commission, "Establishing Quality Assurance Programs for Packaging Used in the Transport of Radioactive Material," Regulatory Guide 7.10, June 1986.

18. Nuclear Regulatory Commission, "Classification of Transportation Packaging and Dry Spent Fuel Storage System Components According to Importance to Safety," NUREG/CR-6407, February 1996.

19. Code of Federal Regulations, "Standards for Protection Against Radiation," Part 20, Title 10, January 1991.

20. Department of Energy, "Multi-Purpose Canister (MPC) Subsystem Design Procurement Specification," Document No. DBG000000-01717-6300-00001, Rev. 6, June 1996.

21. Johnson, A.B., and Gilbert, E.R., Pacific Northwest Laboratory, "Technical Basis for Storage of Zircaloy-Clad Spent Fuel in Inert Gases," PNL-4835, September, 1983.

22. Garde, M., "Hot Cell Examination of Extended Burnup Fuel from Fort Calhoun," DOE/ET/34030-11, CEND-427A, September 1986.

23. Newman, L. M., "The Hot Cell Examination of Oconee 1 Fuel Rods after Five Cycles of Irradiation," DOE/ET/34212-50, BAW-1874L, October 1986.

24. Nuclear Regulatory Commission, "Standard Review Plan for Dry Cask Storage Systems," NUREG-1536, January 1997.

Chapter 3

Table of Contents

3.0 STRUCTURAL EVALUATION 3.1-1

3.1 Structural Design 3.1-1
- 3.1.1 Discussion 3.1-2
- 3.1.2 Design Criteria 3.1-6

3.2 Weights and Centers of Gravity 3.2-1

3.3 Mechanical Properties of Materials 3.3-1
- 3.3.1 Primary Component Materials 3.3-1
- 3.3.2 Fracture Toughness Considerations 3.3-16

3.4 General Standards 3.4.1-1
- 3.4.1 Chemical and Galvanic Reactions 3.4.1-1
  - 3.4.1.1 Component Operating Environment 3.4.1-1
  - 3.4.1.2 Component Material Categories 3.4.1-2
  - 3.4.1.3 General Effects of Identified Reactions 3.4.1-12
  - 3.4.1.4 Adequacy of the Canister Operating Procedures 3.4.1-12
  - 3.4.1.5 Effects of Reaction Products 3.4.1-12
- 3.4.2 Positive Closure 3.4.2-1
- 3.4.3 Lifting Devices 3.4.3-1
  - 3.4.3.1 Vertical Concrete Cask Lift Evaluation 3.4.3-6
  - 3.4.3.2 Canister Lift 3.4.3-19
  - 3.4.3.3 Standard Transfer Cask Lift 3.4.3-26
  - 3.4.3.4 Advanced Transfer Cask Lift 3.4.3-54
- 3.4.4 Normal Operating Conditions Analysis 3.4.4-1
  - 3.4.4.1 Canister and Basket Analyses 3.4.4-1
  - 3.4.4.2 Vertical Concrete Cask Analyses 3.4.4-63
- 3.4.5 Cold 3.4.5-1

3.5 Fuel Rods 3.5-1

Table of Contents (Continued)

3.6 Structural Evaluation of Site Specific Spent Fuel 3.6-1
3.6.1 Structural Evaluation of Maine Yankee Site Specific Spent Fuel for Normal Operating Conditions 3.6-1
3.6.1.1 Maine Yankee Intact Spent Fuel 3.6-1
3.6.1.2 Maine Yankee Damaged Spent Fuel 3.6-2

3.7 References 3.7-1

3.8 Carbon Steel Coatings Technical Data 3.8-1
3.8.1 Carboline 890 ..... 3.8-2
3.8.2 Keeler & Long E-Series Epoxy Enamel 3.8-4
3.8.3 Description of Electroless Nickel Coating 3.8-8
3.8.4 Keeler & Long Kolor-Poxy Primer No. 3200 ..... 3.8-12
3.8.5 Acrythane Enamel Y-1 Series Top Coating 3.8-14

List of Figures

Figure 3.1-1 Principal Components of the Universal Storage System 3.1-7
Figure 3.4.2-1 Universal Storage System Welded Canister Closure 3.4.2-2
Figure 3.4.3-1 Standard Transfer Cask Lifting Trunnion 3.4.3-3
Figure 3.4.3-2 Canister Hoist Ring Design 3.4.3-4

Figure 3.4.3.1-1 Base Weldment Finite Element Model 3.4.3-18
Figure 3.4.3.2-1 Canister Lift Finite Element Model 3.4.3-24
Figure 3.4.3.2-2 Canister Lift Model Stress Intensity Contours (psi) 3.4.3-25
Figure 3.4.3.3-1 Finite Element Model for Standard Transfer Cask Trunnion and Shells 3.4.3-44
Figure 3.4.3.3-2 Node Locations for Standard Transfer Cask Outer Shell Adjacent to Trunnion 3.4.3-45
Figure 3.4.3.3-3 Node Locations for Standard Transfer Cask Inner Shell Adjacent to Trunnion 3.4.3-46
Figure 3.4.3.3-4 Stress Intensity Contours (psi) for Standard Transfer Cask Outer Shell Element Top Surface 3.4.3-47
Figure 3.4.3.3-5 Stress Intensity Contours (psi) for Standard Transfer Cask Outer Shell Element Bottom Surface 3.4.3-48
Figure 3.4.3.3-6 Stress Intensity Contours (psi) for Standard Transfer Cask Inner Shell Element Top Surface 3.4.3-49
Figure 3.4.3.3-7 Stress Intensity Contours (psi) for Standard Transfer Cask Inner Shell Element Bottom Surface 3.4.3-50
Figure 3.4.3.4-1 Advanced Transfer Cask Finite Element Model 3.4.3-71
Figure 3.4.3.4-2 Node Locations for Advanced Transfer Cask Outer Shell Adjacent to Trunnion 3.4.3-72
Figure 3.4.3.4-3 Node Locations for Advanced Transfer Cask Inner Shell Adjacent to Trunnion 3.4.3-73
Figure 3.4.3.4-4 Node Locations for Advanced Transfer Cask Stiffener Plate Above Trunnion 3.4.3-74
Figure 3.4.3.4-5 Stress Intensity Contours (psi) for Advanced Transfer Cask Outer Shell Element Top Surface 3.4.3-75
Figure 3.4.3.4-6 Stress Intensity Contours (psi) for Advanced Transfer Cask Outer Shell Element Bottom Surface 3.4.3-76

List of Figures (Continued)

Figure 3.4.3.4-7 Stress Intensity Contours (psi) for Advanced Transfer Cask Inner Shell Element Top Surface 3.4.3-77
Figure 3.4.3.4-8 Stress Intensity Contours (psi) for Advanced Transfer Cask Inner Shell Element Bottom Surface 3.4.3-78
Figure 3.4.3.4-9 Stress Intensity Contours (psi) for Advanced Transfer Cask Stiffener Plate Element Top Surface 3.4.3-79
Figure 3.4.3.4-10 Stress Intensity Contours (psi) for Advanced Transfer Cask Stiffener Plate Element Bottom Surface 3.4.3-80
Figure 3.4.4.1-1 Canister Composite Finite Element Model 3.4.4-20
Figure 3.4.4.1-2 Weld Regions of Canister Composite Finite Element Model at Structural and Shield Lids 3.4.4-21
Figure 3.4.4.1-3 Bottom Plate of the Canister Composite Finite Element Model 3.4.4-22
Figure 3.4.4.1-4 Locations for Section Stresses in the Canister Composite Finite Element Model 3.4.4-23
Figure 3.4.4.1-5 BWR Fuel Assembly Basket Showing Typical Fuel Basket Components 3.4.4-24
Figure 3.4.4.1-6 PWR Fuel Basket Support Disk Finite Element Model 3.4.4-25
Figure 3.4.4.1-7 PWR Fuel Basket Support Disk Sections for Stress Evaluation (Left Half) 3.4.4-26
Figure 3.4.4.1-8 PWR Fuel Basket Support Disk Sections for Stress Evaluation (Right Half) 3.4.4-27
Figure 3.4.4.1-9 PWR Class 3 Fuel Tube Configuration 3.4.4-28
Figure 3.4.4.1-10 PWR Top Weldment Plate Finite Element Model 3.4.4-29
Figure 3.4.4.1-11 PWR Bottom Weldment Plate Finite Element Model 3.4.4-30
Figure 3.4.4.1-12 BWR Fuel Basket Support Disk Finite Element Model 3.4.4-31
Figure 3.4.4.1-13 BWR Fuel Basket Support Disk Sections for Stress Evaluation (Quadrant I) 3.4.4-32
Figure 3.4.4.1-14 BWR Fuel Basket Support Disk Sections for Stress Evaluation (Quadrant II) 3.4.4-33
Figure 3.4.4.1-15 BWR Fuel Basket Support Disk Sections for Stress Evaluation (Quadrant III) 3.4.4-34
Figure 3.4.4.1-16 BWR Fuel Basket Support Disk Sections for Stress Evaluation (Quadrant IV) 3.4.4-35

List of Figures (Continued)

Figure 3.4.4.1-17 BWR Class 5 Fuel Tube Configuration 3.4.4-36
Figure 3.4.4.1-18 BWR Top Weldment Plate Finite Element Model 3.4.4-37
Figure 3.4.4.1-19 BWR Bottom Weldment Plate Finite Element Model 3.4.4-38
Figure 3.4.4.2-1 Concrete Cask Thermal Stress Model 3.4.4-70
Figure 3.4.4.2-2 Concrete Cask Thermal Stress Model - Vertical and Horizontal Rebar Detail 3.4.4-71
Figure 3.4.4.2-3 Concrete Cask Thermal Stress Model Boundary Conditions 3.4.4-72
Figure 3.4.4.2-4 Concrete Cask Thermal Model Axial Stress Evaluation Locations 3.4.4-73
Figure 3.4.4.2-5 Concrete Cask Thermal Model Circumferential Stress Evaluation Locations 3.4.4-74

List of Tables

Table 3.2-1 Universal Storage System Weights and CGs – PWR Configuration 3.2-2
Table 3.2-2 Universal Storage System Weights and CGs – BWR Configuration 3.2-3
Table 3.2-3 Calculated Under-Hook Weights for the Standard Transfer Cask 3.2-3
Table 3.2-4 Calculated Under-Hook Weights for the Advanced Transfer Cask 3.2-4
Table 3.3-1 Mechanical Properties of SA-240 and A-240, Type 304 Stainless Steel 3.3-3
Table 3.3-2 Mechanical Properties of SA-479, Type 304 Stainless Steel 3.3-4
Table 3.3-3 Mechanical Properties of SA-240, Type 304L Stainless Steel 3.3-5
Table 3.3-4 Mechanical Properties of SA-564 and SA-693, Type 630, 17-4 PH Stainless Steel 3.3-6
Table 3.3-5 Mechanical Properties of A-36 Carbon Steel 3.3-7
Table 3.3-6 Mechanical Properties of A-615, Grade 60 and A-706 Reinforcing Steel 3.3-7
Table 3.3-7 Mechanical Properties of SA-533, Type B, Class 2 Carbon Steel 3.3-8
Table 3.3-8 Mechanical Properties of A-588, Type A or B Low Alloy Steel 3.3-9
Table 3.3-9 Mechanical Properties of SA-350/A-350, Grade LF 2, Class 1 Low Alloy Steel 3.3-10
Table 3.3-10 Mechanical Properties of SA-193, Grade B6, High Alloy Steel Bolting Material 3.3-11
Table 3.3-11 Mechanical Properties of 6061-T651 Aluminum Alloy 3.3-12
Table 3.3-12 Mechanical Properties of Concrete 3.3-13
Table 3.3-13 Mechanical Properties of NS-4-FR and NS-3 ..... 3.3-14
Table 3.3-14 Mechanical Properties of SA-516, Grade 70 Carbon Steel 3.3-15
Table 3.4.3.3-1 Top 30 Stresses for Standard Transfer Cask Outer Shell Element Top Surface 3.4.3-51
Table 3.4.3.3-2 Top 30 Stresses for Standard Transfer Cask Outer Shell Element Bottom Surface 3.4.3-52
Table 3.4.3.3-3 Top 30 Stresses for Standard Transfer Cask Inner Shell Element Top Surface 3.4.3-53
Table 3.4.3.3-4 Top 30 Stresses for Standard Transfer Cask Inner Shell Element Bottom Surface 3.4.3-54

List of Tables (Continued)

Table 3.4.3.4-1 Top 30 Stresses for Advanced Transfer Cask Outer Shell Element Top Surface 3.4.3-81
Table 3.4.3.4-2 Top 30 Stresses for Advanced Transfer Cask Outer Shell Element Bottom Surface 3.4.3-82
Table 3.4.3.4-3 Top 30 Stresses for Advanced Transfer Cask Inner Shell Element Top Surface 3.4.3-83
Table 3.4.3.4-4 Top 30 Stresses for Advanced Transfer Cask Inner Shell Element Bottom Surface 3.4.3-84
Table 3.4.3.4-5 Top 30 Stresses for Advanced Transfer Cask Stiffener Plate Element Top Surface 3.4.3-85
Table 3.4.3.4-6 Top 30 Stresses for Advanced Transfer Cask Stiffener Plate Element Bottom Surface 3.4.3-86
Table 3.4.4.1-1 Canister Secondary (Thermal) Stresses (ksi). 3.4.4-39
Table 3.4.4.1-2 Canister Dead Weight Primary Membrane (P_m) Stresses (ksi), $P_{internal}$ = 0 psig 3.4.4-40
Table 3.4.4.1-3 Canister Dead Weight Primary Membrane plus Bending ($P_m + P_b$) Stresses (ksi), $P_{internal}$ = 0 psig 3.4.4-41
Table 3.4.4.1-4 Canister Normal Handling With No Internal Pressure Primary Membrane (P_m) Stresses, (ksi) 3.4.4-42
Table 3.4.4.1-5 Canister Normal Handling With No Internal Pressure Primary Membrane plus Bending ($P_m + P_b$) Stresses (ksi) 3.4.4-43
Table 3.4.4.1-6 Summary of Canister Normal Handling plus Normal Internal Pressure Primary Membrane (P_m) Stresses (ksi). 3.4.4-44
Table 3.4.4.1-7 Summary of Canister Normal Handling, Plus Normal Pressure Primary Membrane plus Bending ($P_m + P_b$) Stresses (ksi). 3.4.4-45
Table 3.4.4.1-8 Summary of Maximum Canister Normal Handling, plus Normal Pressure, plus Secondary (P + Q) Stresses (ksi) 3.4.4-46
Table 3.4.4.1-9 Canister Normal Internal Pressure Primary Membrane (P_m) Stresses (ksi) 3.4.4-47
Table 3.4.4.1-10 Canister Normal Internal Pressure Primary Membrane plus Bending ($P_m + P_b$) Stresses (ksi) 3.4.4-48
Table 3.4.4.1-11 Listing of Sections for Stress Evaluation of PWR Support Disk 3.4.4-49
Table 3.4.4.1-12 $P_m + P_b$ Stresses for PWR Support Disk - Normal Conditions (ksi) 3.4.4-52

List of Tables (Continued)

Table 3.4.4.1-13 $P_m + P_b + Q$ Stresses for the PWR Support Disk - Normal Conditions (ksi) 3.4.4-53
Table 3.4.4.1-14 Listing of Sections for Stress Evaluation of BWR Support Disk 3.4.4-54
Table 3.4.4.1-15 $P_m + P_b$ Stresses for BWR Support Disk — Normal Conditions (ksi) 3.4.4-60
Table 3.4.4.1-16 $P_m + P_b + Q$ Stresses for BWR Support Disk - Normal Conditions (ksi) 3.4.4-61
Table 3.4.4.1-17 Summary of Maximum Stresses for PWR and BWR Fuel Basket Weldments - Normal Conditions (ksi) 3.4.4-62
Table 3.4.4.2-1 Summary of Maximum Stresses for Vertical Concrete Cask Load Combinations 3.4.4-75
Table 3.4.4.2-2 Maximum Concrete and Reinforcing Bar Stresses 3.4.4-76
Table 3.4.4.2-3 Concrete Cask Average Concrete Axial Tensile Stresses 3.4.4-77
Table 3.4.4.2-4 Concrete Cask Average Concrete Hoop Tensile Stresses 3.4.4-77

Transfer Cask

The transfer cask, with its lifting yoke, is primarily a lifting device used to move the canister. It provides biological shielding when it contains a loaded canister. The transfer cask is provided in the Standard configuration for canisters weighing up to 88,000 lbs, or in the Advanced configuration for canisters weighing up to 98,000 lbs. The transfer cask configurations have identical operational features. The transfer cask is a heavy lifting device that is designed, fabricated and load-tested to the requirements of NUREG-0612 [8] and ANSI N14.6 [9]. The transfer cask design incorporates a top retaining ring, which is bolted in place to prevent a loaded canister from being inadvertently lifted through the top of the transfer cask. The transfer cask has retractable bottom shield doors. During loading operations, the doors are closed and secured by bolts/pins, so they cannot inadvertently open. During unloading, the doors are retracted using hydraulic cylinders to allow the canister to be lowered into the storage or transport cask. The principal design parameters of the transfer casks are shown in Table 1.2-7.

Both transfer cask configurations are provided in five different lengths to accommodate the canisters containing one of the three classes of PWR fuel assemblies or two classes of BWR fuel assemblies.

The transfer cask is used for the vertical transfer of the canister between work stations and the concrete cask, or transport cask. It incorporates a multiwall (steel/lead/NS-4-FR/steel) design to provide radiation shielding.

Component Evaluation

The following components are evaluated in this chapter:

- canister lifting devices,
- canister shell, bottom, and structural lid,
- canister shield lid support ring,
- fuel basket assembly,
- transfer cask trunnions, shells, retaining ring, bottom doors, and support rails,
- vertical concrete cask body, and
- concrete cask steel components (reinforcement, inner shell, lid, bottom plate, bottom, etc.).

Other Universal Storage System components shown on the license drawings in Chapter 1 are included as loads in the evaluation of the components listed above, as appropriate.

The structural evaluations in this chapter demonstrate that the Universal Storage System components meet their structural design criteria and are capable of safely storing the design basis PWR or BWR spent fuel.

3.1.2 Design Criteria

The Universal Storage System structural design criteria are described in Section 2.2. Load combinations for normal, off-normal, and accident loads are evaluated in accordance with ANSI 57.9 [3] and ACI-349 [4] for the concrete cask (see Table 2.2-1), and in accordance with the 1995 edition of the ASME Code, Section III, Division I, Subsection NB [5] for Class 1 components of the canister (see Table 2.2-2). The basket is evaluated in accordance with ASME Code, Section III, Subsection NG [6], and NUREG-6322 [7]. The transfer cask and the lifting yoke are lifting devices that are designed to NUREG-0612 [8] and ANSI N14.6 [9].

Table 3.2-2 Universal Storage System Weights and CGs – BWR Configuration

Item Description	Class 4		Class 5	
	Calculated Weight (lb)	Center of Gravity[1]	Calculated Weight (lb)	Center of Gravity[1]
Fuel Contents (Including channels)	39,400	—	39,400	—
Concrete Cask Lid	2,500	—	2,500	—
Concrete Cask Shield Plug	4,900	—	4,900	—
Canister (empty, w/o lids)	8,800	—	9,000	—
Canister Structural Lid	3,000	—	3,000	—
Canister Shield Lid	7,000	—	7,000	—
Transfer Adapter Plate	11,200	—	11,200	—
Transfer Cask Lifting Yoke	6,000	—	6,000	—
Water in Canister	15,100	—	15,200	—
Basket	17,200	—	17,600	—
Canister (with basket, without fuel or lids)	25,900	—	26,500	—
Canister (with fuel, and shield and structural lids)	75,000	—	75,600	—
Concrete Cask (empty, with shield plug and lid, includes optional lift lugs)	233,700	—	238,400	—
Concrete Cask (with loaded Canister and lids, includes optional lift lug)[2]	308,700	113.7	313,900	115.8
Transfer Cask (empty)	118,000	—	120,700	—
Transfer Cask and Canister (empty, without lids)[3]	143,900	—	147,200	—
Transfer Cask and Canister (with fuel, water and shield lid)[3]	205,100	—	208,400	—
Transfer Cask and Canister (with fuel, dry with lids)[3]	193,000	—	196,200	—

General Note: All weights rounded to the next 100 lb.

1. Weights and CGs are calculated from nominal design dimensions.
2. Center of gravity is measured from the bottom of the concrete cask.

Table 3.2-3 Calculated Under-Hook Weights for the Standard Transfer Cask

Configuration	PWR Class 1	PWR Class 2	PWR Class 3	BWR Class 4	BWR Class 5
Transfer cask (empty)	112,300	117,300	121,500	118,000	120,700
Transfer cask, empty canister/basket and yoke	141,400	147,800	152,700	149,800	153,000
Transfer cask; wet, loaded canister (fuel, water and shield lid); and yoke	199,800	207,800	210,900	211,000	214,300
Transfer cask; dry, loaded canister; and yoke	188,700	196,000	198,000	198,900	202,100

General Note: All weights rounded to the next 100 lb.

Table 3.2-4 Calculated Under-Hook Weights for the Advanced Transfer Cask

Configuration	**PWR Class 1**	**PWR Class 2**	**PWR Class 3**
Advanced transfer cask (empty)	112,300	117,300	121,500
Transfer cask, empty canister, and yoke	143,000	149,200	154,600
Transfer cask; wet, loaded canister (fuel, water, and shield lid); and yoke	212,500	220,600	223,200
Transfer cask; dry, loaded canister; and yoke	202,900	210,300	211,700

Table 3.3-5 Mechanical Properties of A-36 Carbon Steel

Property	Value							
Temperature (°F)	100	200	300	400	500	600	650	700
Ultimate strength, S_u, (ksi) ***	58.0	58.0	58.0	58.0	—	—	—	—
Yield strength, S_y, (ksi) *	36.0	32.8	31.9	30.8	29.1	26.6	26.1	25.9
Design Stress Intensity, S_m,(ksi) *	19.3	19.3	19.3	19.3	19.3	17.7	17.4	17.3
Modulus of Elasticity, E ($\times 10^3$ ksi) *	29.0	28.8	28.3	27.7	27.3	26.7	26.1	25.5
Coefficient of Thermal Expansion, α ($\times 10^{-6}$ in/in/°F) *	5.53	5.89	6.26	6.61	6.91	7.17	7.30	7.41
Poisson's Ratio*	0.31							
Density**	0.284 lbm/in^3							

* ASME Code, Section II, Part D [10].

** Metallic Materials Specification Handbook [12].

*** ASME Code Case, Nuclear Components, N-71-17 [13].

Table 3.3-6 Mechanical Properties of A-615, Grade 60 and A-706 Reinforcing Steel

Property	A-615, Grade 75	A-706
Ultimate Strength ** (ksi)	90.0	80.0
Yield Strength ** (ksi)	60.0	60.0
Coefficient of Thermal Expansion, * α (in/in/°F)	6.1×10^{-6}	6.1×10^{-6}
Density [12] lbm/in^3	0.284	0.284

* Metallic Materials Specification Handbook [12].

** Annual Book of ASTM Standards [14].

Table 3.3-6 Mechanical Properties of SA-533, Type B, Class 2 Carbon Steel

Property	Value							
Temperature (°F)	-20	70	200	300	400	500	750	800
Ultimate strength S_u, (ksi) *	90.0	90.0	90.0	90.0	90.0	90.0	87.2	81.8
Yield strength, S_y, (ksi) *	70.0	70.0	65.5	64.5	63.2	62.3	59.3	58.3
Design Stress Intensity, S_m,(ksi) *	30.0	30.0	30.0	30.0	30.0	30.0	—	—
Modulus of Elasticity E, ($\times 10^3$ ksi) *	29.9	29.2	28.5	28.0	27.4	27.0	24.6	23.9
Alternating Stress @ 10 cycles (ksi) **	465.0	465.0	453.8	435.0	436.3	429.9	391.7	—
Alternating Stress @ 10^6 cycles (ksi) **	15.8	15.8	15.4	15.2	14.8	14.6	13.3	—
Coefficient of Thermal Expansion, α ($\times 10^{-6}$ in/in/°F) *	—	7.02	7.25	7.43	7.58	7.70	8.00	8.05
Poisson's Ratio *	0.31							
Density *	503 lbm/ft^3(0.291 lbm/in^3)							

* ASME Code, Section II, Part D [10].

** ASME Code, Section III, Appendix I [11].

3.4.3 Lifting Devices

To provide more efficient handling of the Universal Storage System, different methods of lifting are designed for each of the components. The transfer cask, the transportable storage canister, and the concrete cask, are handled using trunnions, hoist rings, and a system of jacks and air pads, respectively.

The designs of the UMS® Universal Storage System and Universal Transport System components address the concerns identified in U.S. NRC Bulletin 96-02, "Movement of Heavy Loads Over Spent Fuel, Over Fuel in the Reactor Core, or Over Safety-Related Equipment" (April 11, 1996) as follows:

(1) The UMS® lifting and handling components satisfy the requirements of NUREG-0612 and ANSI N14.6 for safety factors on redundant or nonredundant load paths as described in this chapter.

(2) Transfer or transport cask lifting in the spent fuel pool or cask loading pit or transfer or transport cask lifting and movement above the spent fuel pool operating floor will be addressed on a plant-specific basis.

The transfer cask is provided in either the Standard configuration for canisters weighing up to 88,000 lbs or in the Advanced configuration for canisters weighing up to 98,000 lbs. The two configurations have identical operating features. The transfer casks are lifted by trunnions located near the top of each cask. The Standard transfer cask trunnions are attached by full-penetration welds to both the inner and the outer shells (Figure 3.4.3-1). The Advanced transfer cask trunnions are similarly attached, but incorporate a trunnion support plate at each trunnion for the additional load. The transfer casks are each designed as a heavy-lifting device that satisfies the requirements of NUREG-0612 and ANSI N14.6 for lifting the fully loaded canister of fuel and water, together with the shield lid, which is the maximum weight of the transfer cask during a lifting operation with a given configuration.

The transportable storage canister remains within the transfer cask during all preparation, loading, canister closure, and transfer operations. The canister is equipped with six hoist rings threaded into the structural lid to lift the loaded canister and to lower it into the concrete cask after the shield doors are opened. The hoist rings, shown in Figure 3.4.3-2, are also used for any subsequent lifting of the loaded dry canister.

The vertical concrete cask is moved by means of a system of air pads. The cask is raised approximately 3 in. by four lifting jacks placed at the jacking pads located near the end of each air inlet. A system consisting of 4 air pads is then inserted under the concrete cask. The cask is lowered onto the uninflated air pads, the jacks are removed, and the air pads are inflated to lift the concrete cask and position it as required on the storage pad or transport vehicle. When positioning is complete, the jacks are used to support the cask as the air pads are removed.

As an option, the loaded concrete cask may also be lifted and moved using lifting lugs at the top of the cask. The top lifting lugs are described in Section 3.4.3.1.3.

The structural evaluations in this section consider the bounding conditions for each aspect of the analysis. Generally, the bounding condition for lifting devices is represented by the heaviest component, or combination of components, of each configuration. The bounding conditions used in this section are:

Section	Evaluation	Bounding Condition	Configuration
3.4.3.1	Concrete Cask Lifting Jacks	Heaviest loaded Concrete Cask + 10% dynamic load factor	BWR Class 5
	Pedestal Loading	Heaviest loaded Canister + 10% dynamic load factor	BWR Class 5
	Concrete Cask Air Pads (Lifting)	Heaviest loaded Concrete Cask	BWR Class 5
	Concrete Cask Top Lifting Lugs (Lifting)	Heaviest loaded Concrete Cask + 10% dynamic load factor	BWR Class 5
3.4.3.2	Canister Lift	Heaviest loaded Canister + 10% dynamic load factor	BWR Class 5
3.4.3.3	Transfer Cask Lift	Heaviest loaded Transfer Cask + 10% dynamic load factor	BWR Class 5
3.4.3.3.3	Transfer Cask Shield Doors and Rails	Heaviest loaded Canister + water, shield doors and 10% dynamic load factor	BWR Class 5

3.4.3.3.5 PWR Class 1 Standard Transfer Cask with Transfer Cask Extension

The PWR Class 1 standard transfer cask, baseline weight of 112,300 lb. empty, can be equipped with a Transfer Cask extension to accommodate the loading of a PWR Class 2 canister. The purpose of the extended transfer cask configuration is to permit the loading of PWR Class 1 fuel assemblies with Control Element Assemblies inserted into a PWR Class 2 canister; the length of the control element assemblies requires the use of the longer PWR Class 2 canister. The weight of the transfer cask extension is 5,500 pounds. Therefore, the total weight of the PWR Class 1 transfer cask with extension would be:

$$W_{TC} = 112{,}300 + 5{,}500 = 117{,}800 \text{ lbs}$$

Standard Transfer Cask Shell and Trunnion

From the analysis in Section 3.4.3.3.1 for the Transfer Cask Shell and Trunnion, the heaviest loaded transfer cask weight used in the analysis was 210,000 pounds (Class 5 BWR). The total weight of the loaded transfer cask with extension is:

$$W_{TC\text{-}L} = 193{,}900 + 5{,}500 = 199{,}400 \text{ lbs}$$

where:

193,900 lbs = the weight of a PWR Class 1 transfer cask and canister (with fuel, water, and shield lid)

The Class 5 BWR transfer cask configuration bounds the PWR Class 1 transfer cask with extension; therefore, no additional handling analysis is required for the transfer cask shell and trunnions.

Retaining Ring and Bolts

From Section 3.4.3.3.2, the bounding transfer cask weight used was 124,000 pounds. As stated above, the weight of the PWR Class 1 transfer cask with extension is 117,800 pounds; therefore, the existing analysis in Section 3.4.3.3.2 bounds the PWR Class 1 transfer cask with extension and no additional analysis is required.

Standard Transfer Cask Extension Attachment Bolts

The transfer cask extension is attached to the transfer cask by 32 bolts that are identical to the Retaining Ring Bolts with the exception of bolt length. The retaining ring bolts are 2.25 inches long and the transfer cask extension attachment bolts are 9.0 inches long; the thread engagement lengths are identical. Since the transfer cask extension is 8.75 inches thick, the prying action is negligible for the transfer cask extension attachment bolts during an inadvertent lift of the transfer cask via the retaining ring during a canister handling operation. The PWR Class 1 transfer cask with extension weighs approximately 6,000 pounds less than the bounding analysis weight; therefore, no additional analysis of the attachment bolts is required.

Table 3.4.3.3-4 Top 30 Stresses for Standard Transfer Cask Inner Shell Element Bottom Surface

Node[1]	Principal Stresses(psi)			Nodal S.I. (psi)	F.S. on Yield S_y/S.I.[2]	F.S. on Ultimate (S_u/S.I.)[2]
	S1	S2	S3			
1869	18955.0	554.4	-1812.1	20768.0	N/A[3]	N/A[3]
1634	10094.0	530.6	-887.6	10982.0	N/A	N/A
1882	7550.5	886.3	-631.4	8181.8	N/A	N/A
1797	1147.8	143.2	-5927.0	7074.8	N/A	N/A
1731	2320.8	-75.8	-4368.2	6689.0	6.8	10.5
1884	6149.9	517.9	-483.4	6633.3	6.9	10.6
1725	1242.9	-392.2	-5118.9	6361.8	7.2	11.0
1729	3117.2	52.5	-3023.5	6140.7	7.4	11.4
1803	474.7	-3926.6	-5631.6	6106.3	7.5	11.5
1886	5973.5	2440.1	-81.0	6054.5	7.5	11.6
1801	457.4	-3130.0	-5557.0	6014.4	7.6	11.6
1742	1965.5	-0.9	-4026.8	5992.3	7.6	11.7
1782	2451.4	-0.2	-3512.8	5964.2	7.6	11.7
1799	543.1	-1622.2	-5294.3	5837.4	7.8	12.0
1822	1595.1	4.2	-4233.9	5829.0	7.8	12.0
1766	2666.8	-1.0	-2994.6	5661.4	8.1	12.4
1879	5157.5	127.0	-284.2	5441.6	8.4	12.9
1727	3646.3	282.8	-1615.2	5261.4	8.7	13.3
1838	1426.6	25.3	-3770.7	5197.3	8.8	13.5
1740	2367.5	-2.5	-2661.6	5029.1	9.1	13.9
1784	2285.8	-0.7	-2712.6	4998.4	9.1	14.0
1750	2342.2	-6.7	-2516.2	4858.4	9.4	14.4
1646	3727.5	676.6	-1129.4	4856.9	9.4	14.4
1806	3417.2	95.3	-827.4	4244.6	10.7	16.5
1824	2109.9	-2.3	-2106.6	4216.5	10.8	16.6
1768	1813.3	-0.4	-2337.6	4150.9	11.0	16.9
1854	1304.9	49.1	-2746.8	4051.6	11.3	17.3
1738	2231.7	1.0	-1617.9	3849.6	11.8	18.2
1786	1897.7	0.5	-1860.4	3758.2	12.1	18.6
1932	3722.3	1449.3	-8.2	3730.5	12.2	18.8

Notes:

1. See Figure 3.4.3.3-3 for node locations.
2. S_y = 45,600 psi, S_u = 70,000 psi.
3. Local stresses that are relieved by local material yielding. Therefore, stress design factors of 6 and 10 on material yield and ultimate strength are not applicable (ANSI N14.6, Section 4.2.1.2).

3.4.3.4 Advanced Transfer Cask Lift

The Advanced transfer cask and Standard transfer cask are identical in design, except that the Advanced transfer cask incorporates a 0.75-inch thick support plate positioned above each of the trunnions between the inner shell and the outer shell. The support plate allows the Advanced transfer cask to lifting canisters weighing up to 98,000, whereas the Standard transfer cask is limited to canisters weighing up to 88,000 pounds. The 0.75-inch thick support plate is welded to the inner and outer shells of the Advanced transfer cask, adding significant rigidity to the shell-trunnion juncture to resist the loads applied during the lifting operation of the transfer cask. The welds attaching the support plate to the shells are 0.375-inch double-sided fillet welds at each end of the plate. The support plate is not attached to the trunnion, which prevents any significant shear force from being developed in the welds. The Advanced transfer cask analysis is conservatively based on a transfer cask contents weight of 103,000 pounds.

The evaluation of the Advanced transfer cask presented here shows that the design meets NUREG-0612 [8] and ANSI N14.6 [9] requirements for nonredundant lift systems. The adequacy of the standard transfer cask is shown by evaluating the stress levels in all of the load-path components against the NUREG-0612 criteria.

3.4.3.4.1 Advanced Transfer Cask Shell and Trunnion

The adequacy of the trunnions and the cask shell in the region around the trunnions during lifting conditions is evaluated in this section in accordance with NUREG-0612 and ANSI N14.6.

A three-dimensional finite element model is used to evaluate the lifting of a fully loaded Advanced transfer cask. Because of symmetry, it was necessary to model only one-quarter of the Advanced transfer cask, including the trunnions and the shells at the trunnion region. The stiffener plate above the trunnions (between the two shells) is included in the model. The lead and the NS-4-FR between the inner and outer shells of the Advanced transfer cask are neglected, since they are not structural components. SOLID95 (20 noded brick element) and SHELL93 (8 noded shell element) elements are used to model the trunnion and shells, respectively. Due to the absence of rotational degrees of freedom for the SOLID95 elements, BEAM4 elements perpendicular to the shells are used at the interface of the trunnion and the shells to transfer moments from the SOLID95 elements to SHELL93 elements. The finite element model is shown in Figure 3.4.3.4-1.

The total weight of the heaviest loaded Advanced transfer cask (Advanced Class 3 PWR) is calculated at approximately 217,300 pounds. A conservative load of 225,000 lb., plus a 10% dynamic load factor, is used in the model. The 225,000-pound load corresponds to an assumed transfer cask contents weight of 103,000 pounds. The load used in the quarter-symmetry model is (225,000 × 1.1)/4 = 61,875 pounds. The load is applied upward at the trunnion as a "surface load" whose location is determined by the lifting yoke dimensions. The model is restrained along two planes of symmetry with symmetry boundary conditions. Vertical restraints are applied to the bottom of the model to resist the force applied to the trunnion.

The maximum temperature in the Advanced transfer cask shell/trunnion region is conservatively evaluated as 300°F. For the ASTM A-588 shell material, the yield strength, S_y, is 45.6 ksi, and the ultimate strength, S_u, is 70 ksi. The trunnions are constructed of ASTM A-350 carbon steel, Grade LF2, with a yield stress of 31.9 ksi and an ultimate stress of 70 ksi. The standard impact test temperature for ASTM A-350, Grade LF2 is -50°F. The NDT temperature range is -70°F to -10°F for ASTM A-588 with a thickness range of 0.625 in. to 3 in. [25]. Therefore, the minimum service temperature for the trunnion and shells is conservatively established as -10°F (40°F higher than the NDT test temperature, in accordance with Section 4.2.6 of ANSI N14.6 [9]).

Table 3.4.3.4-1 through Table 3.4.3.4-6 provide summaries of the top 30 maximum combined stresses (Equivalent von Misses stresses) for both surfaces of the outer shell, inner shell, and stiffener plate (see Figure 3.4.3.4-2 through Figure 3.4.3.4-4 for node locations for the outer shell, inner shell, and stiffener plate, respectively). Stress contour plots for the outer shell are shown in Figure 3.4.3.4-5 and Figure 3.4.3.4-6. Stress contours for the inner shell are shown in Figure 3.4.3.4-7 and Figure 3.4.3.4-8. Stress contours for the stiffener plate are shown in Figures 3.4.3.4-9 and 3.4.3.4-10. As shown in Table 3.4.3.4-1 through Table 3.4.3.4-6, all stresses, except local stresses, meet the NUREG-0612 and ANSI N14.6 criteria. That is, a factor of safety of 6 applies on material yield strength and 10 applies on material ultimate strength. The high local stresses, as defined in ASME Code Section III, Article NB-3213.10, which are relieved by slight local yielding, are not required to meet the 6 and 10 safety factor criteria [see Reference 9, Section 4.2.1.2].

The localized stresses occur at the interfaces of the trunnion with the inner and outer shells. In accordance with ASME Code, Article NB-3213.10, the area of localized stresses cannot be larger than:

$1.0\sqrt{Rt}$

where:

R is the minimum midsurface radius

t is the minimum thickness in the region considered

Based on this formula, the maximum distance from the discontinuity to the local high stress is less than 5.1 inches for the inner shell and 7.3 inches for the outer shell.

For the trunnion, the maximum tensile bending stress and average shear stresses occur at the interface with the outer shell. The linearized stresses through the trunnion are 4,260 psi in bending and 1,871 psi in shear. Comparing these stresses to the material allowable yield and ultimate strength (A350, Grade LF2), the factor of safety on yield strength is 7.5 (which is >6) and on ultimate strength is 16.4 (which is >10).

3.4.3.4.2 Advanced Transfer Cask Retaining Ring and Bolts

The Advanced transfer cask uses a retaining ring bolted to the top flange to prevent inadvertent lifting of the canister out of the transfer cask, which could increase the radiation exposure to nearby workers. In the event that the loaded transfer cask is inadvertently lifted by attaching to the canister eyebolts instead of the transfer cask trunnions, the retaining ring and bolts have sufficient strength to support the weight of the heaviest transfer cask, plus a 10% dynamic load factor.

Retaining Ring

To qualify the retaining ring, the equations for annular rings are used (Roark [26], Table 24, Case 1e). The retaining ring is represented as shown in the sketch below. The following sketch assists in defining the variables used to calculate the stress in the retaining ring and bolts. The model assumes a uniform annular line load *w* applied at radius r_o.

The boundary conditions for the model are outer edge fixed, inner edge free with a uniform annular line load w at radius r_o.

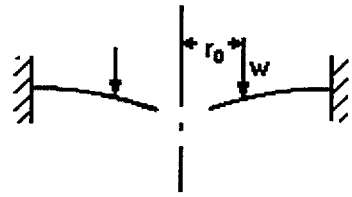

The material properties and parameters for the analysis are:

Plate dimensions:	
thickness:	$t = 0.75$ in
outer radius (bolt circle):	$a = 37.28$ in
outer radius (outer edge):	$c = 38.52$ in
inner radius:	$b = 32.37$ in
Weight of bounding transfer cask:	$wt = 124{,}000$ lb $\times$ 1.1
Radial location of applied load:	$r_o = 33.53$ in
Material:	ASTM A588
Modulus of elasticity:	$E = 28.3 \times 10^6$ psi
Poisson's ratio:	$\nu = 0.31$
Number of bolts:	$Nb = 32$
Radial length of applied load:	$L_r = 2\pi r_o$
	$L_r = 210.675$ in
Applied unit load:	$w \equiv \frac{wt}{L_r}$
	$w = 647.44$ psi

The shear modulus is:

$$G = \frac{E}{2 \cdot (1 + \nu)}$$

$$G = 1.08 \times 10^7 \text{ psi}$$

D is a plate constant used in determining boundary values; it is also used in the general equations for deflection, slope, moment and shear. K_{sb} and K_{sro} are tangential shear constants used in determining the deflection due to shear:

$$D = \frac{E \cdot t^3}{12 \cdot (1 - \nu^2)}$$

$$D = 1.101 \times 10^6 \quad \text{lb-in}$$

Tangential shear constants, K_{sb} and K_{sro}, are used in determining the deflection due to shear:

$$K_{sb} = K_{sro} = -1.2 \cdot \frac{r_o}{a} \cdot \ln\left(\frac{a}{r_o}\right)$$

$$= -0.114$$

Radial moment M_{rb} and M_{ra} at point s b and a (inner and outer radius, respectively) are:

M_{rb} (b,0) = 0 lb-in/in

M_{ra} (a,0) = 2207.86 lb-in/in

Transverse moment M_{tb} and M_{ta}, at points b and a (inner and outer radius, respectively) due to bending are:

M_{tb} (b,0) = -122.64 lb-in./in.

M_{ta} (a,0) = 684.44 lb-in./in.

The calculated shear stresses, τ_b and τ_a, at points b and a (inner and outer radius, respectively) are:

$\tau_b = 0$ psi

$$\tau_a = \frac{wt}{2\pi At}$$

$\tau_a = -776.42$ psi

The calculated radial bending stresses, σ_{rb} and σ_{ra}, at points b and a (inner and outer radius) are:

$$\sigma_{r(i)} = \frac{6M_{r(i)}}{t^2}$$

$\sigma_{rb} = 0$ psi

$\sigma_{ra} = 23{,}550$ psi

The calculated transverse bending stresses, σ_{tb} and σ_{ta}, at points b and a (inner and outer radius) are:

$$\sigma_{t(i)} = \frac{6M_{t(i)}}{t^2}$$

$\sigma_{tb} = -1308.2$ psi

$\sigma_{ta} = 7{,}300.7$ psi

The principal stresses at the outer radius are:

σ_{1a} = 23,590 psi
σ_{2a} = 7,263.6 psi
σ_{3a} = 0 psi

The stress intensity, SI_a, at the outer radius ($P_m + P_b$) is:

$$SI_a = \sigma_{1a} - \sigma_{3a}$$
$$SI_a = 23{,}590 \text{ psi}$$

The principal stresses at the inner radius are:

σ_{1b} = 0 psi
σ_{2b} = -1308.2 psi
σ_{3b} = 0 psi

The stress intensity, SI_b, at the inner radius ($P_m + P_b$) is:

$$SI_b = \sigma_{1b} - \sigma_{2b}$$
$$SI_b = 1308.2 \text{ psi}$$

The maximum stress intensity occurs at the outer radius of the retaining ring. For the off-normal condition, the allowable stress intensity is equal to the lesser of 1.8 S_m and 1.5 S_y. For ASTM A588, the allowable stress intensity at 300°F is 1.8(23.3) = 41.94 ksi. The calculated stress of 23.59 ksi is less than the allowable stress intensity and the margin of safety is:

$$MS = \frac{41.94}{23.59} - 1 = 0.78$$

<u>Retaining Ring / Canister Bearing</u>

The bearing stress, S_{brg}, between the retaining ring and canister is calculated as:

Weight of Transfer Cask (TFR) = 124,000 × 1.1 = 136,400 lbs.

Area of contact between retaining ring and canister:

$$S_{brg} = \frac{136{,}400}{240} = 568\,\text{psi}$$

$$A = \pi\left(33.53^2 - 32.37^2\right) = 240\,\text{in}^2$$

Bearing stress allowable is S_y. For ASTM A588, the allowable stress at 300°F is 45.6 ksi. The Calculated bearing stress is well below the allowable stress with a large margin of safety.

Shearing stress of Retaining Plate under the Bolt Heads

The shearing stress of the retaining plate under the bolt head is calculated as:

Outside diameter of bolt head d_b = 1.125 in.

Total shear area under bolt head = π (1.125) × 32 × 0.75

= 84.82 in^2.

$\tau_p = \frac{136{,}400}{84.82} = 1608\,\text{psi}$ Shear stress of retaining plate, τ_p, under bolt head is:

$$\tau_p = \frac{136{,}400}{84.82} = 1{,}608\,\text{psi}$$

Conservatively, the shear allowable for normal conditions is used.

$$\tau_{allowable} = (0.6)\,(S_m) = (0.6)\,(23.3\text{ ksi}) = 13.98\text{ ksi}$$

The Margin of Safety is: $\frac{13{,}980}{1{,}608} - 1 = +\text{large}$

Bolt Edge Distance

$\frac{77.04 - 74.56}{2} = 1.24\,\text{in} > 1.0\,\text{in}$ Using Table J3.5 "Minimum Edge Distance, in." of Section J3 from "Manual of Steel Construction Allowable Stress Design,"[23] the required saw-cut edge distance for a 0.75 inch bolt is 1.0 inch. The edge distance for the bolts that meets the criteria of the Steel Construction Manual is:

$$\frac{77.04 - 74.56}{2} = 1.24\,\text{in} > 1.0\,\text{in}$$

Retaining Ring Bolts

The load on a single bolt, F_F, due to the reactive force caused by inadvertently lifting the canister, is:

$$F_F = \frac{wt}{N_b} = 4{,}262 \text{ lb}$$

where:

N_b = number of bolts, 32, and

wt = the weight of the cask, plus a 10% load factor, 124,000 lb × 1.1 = 136,400 lb.

The load on each bolt, F_M, due to the bending moment, is:

$$F_M = \left(\frac{2 \cdot \pi \cdot a}{N_b}\right) \cdot \left(\frac{\sigma \cdot t^2}{6 \cdot L}\right)$$

$$F_M = 12{,}929 \text{ lb}$$

where:

a = the outer radius of the bolt circle, 37.28 in.,

t = the thickness of the ring, 0.75 in.,

σ = the radial bending stress at point *a*, σ_{ra} = 23,550 psi, and

L = the distance between the bolt centerline and ring outer edge, c - a = 1.25 in.

The total tension, F, on each bolt is

$$F = F_F + F_M = 17{,}191 \text{ lb}$$

Knowing the bolt cross-sectional area, A_b, the bolt tensile stress is calculated as:

$$\sigma_t = \frac{F}{A_b} = 38{,}912 \text{ psi}$$

where:

$A_b = 0.4418 \text{ in}^2$

For off-normal conditions, the allowable primary membrane stress in a bolt is $2S_m$. The allowable stress for SA-193 Grade B6 bolts is 54 ksi at 120°F, the maximum temperature of the transfer cask top plate. The margin of safety for the bolts is

$$MS = \frac{54{,}000}{38{,}912} - 1 = +0.38$$

Since the SA-193 Grade B6 bolts have higher strength than the top plate, the shear stress in the threads of the top plate is evaluated. The yield and ultimate strengths for the top plate ASTM 588 material at a temperature of 120°F are:

S_y = 49.5 ksi
S_u = 70.0 ksi

From Reference 27, the shear area for the internal threads of the top plate, A_n , is calculated as:

$$A_n = 3.1416\, n\, L_e\, D_s\min\left[\frac{1}{2n} + 0.57735\left(D_s\min - E_n\max\right)\right] = 1.525 \text{ in}^2$$

where:

D = 0.7482 in., basic major diameter of bolt threads,
n = 10, number of bolt threads per inch,
$D_s$min = 0.7353 in., minimum major diameter of bolt threads,
$E_n$max = 0.6927 in., maximum pitch diameter of lid threads, and
L_e = 1.625-0.74=0.885 in., minimum thread engagement.

The shear stress (τ_n) in the top plate is:

$$\tau_n = \frac{F}{A_n} = \frac{17{,}191 \text{ lb}}{1.525 \text{ in}^2} = 11{,}273 \text{ psi}$$

Where the total tension, F, on each bolt is

$$F = F_F + F_M = 17{,}191 \text{ lb}$$

The shear allowable for normal conditions is conservatively used:

$$\tau_{allowable} = (0.6)\ (S_m) = (0.6)\ (23.3\ ksi) = 13.98\ ksi$$

The Margin of Safety is:

$$MS = \frac{13{,}980}{11{,}273} - 1 = +0.24$$

Therefore, the threads of the top plate will not fail in shear.

3.4.3.4.3 Advanced Transfer Cask Bottom Plate Weld Analysis

The bottom plate is connected to the outer and inner shell of the transfer cask by full penetration welds. The weight of a loaded canister along with the shield door rail structure is transmitted from the bottom plate to the shell via the full penetration weld. For conservatism, only the length of the weld directly under the shell is considered effective in transmitting a load.

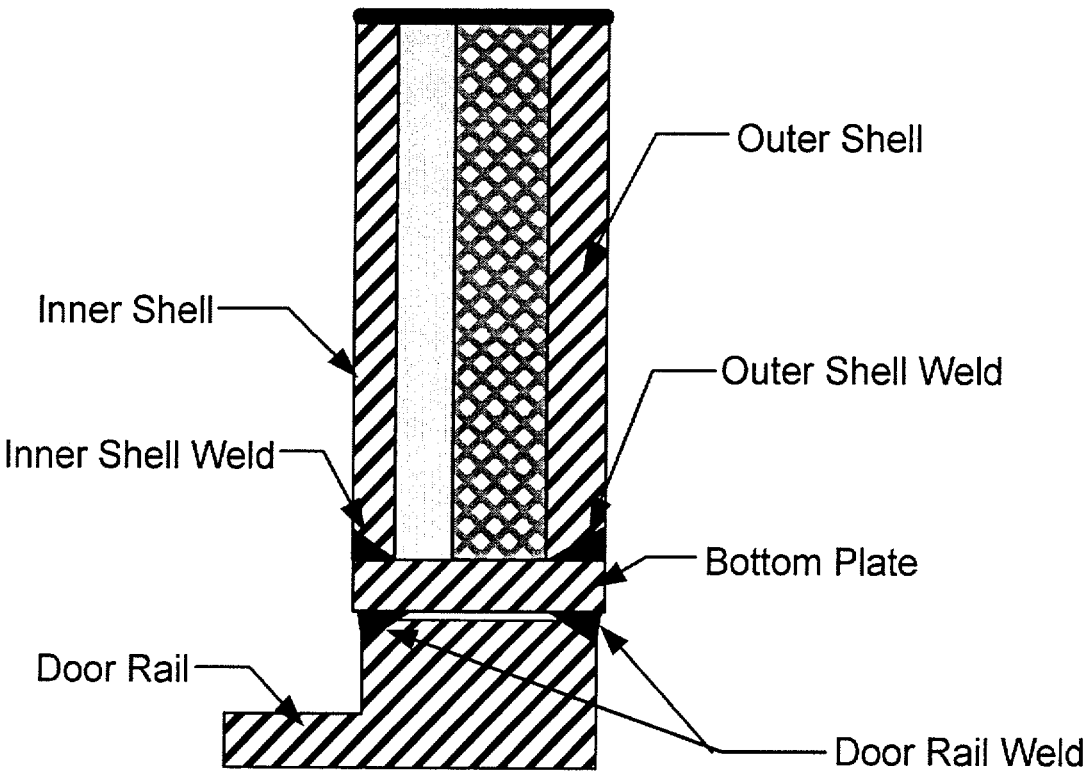

The weld connecting the outer and inner shell to the bottom plate has a length of approximately

l_w = (27.33 in. + 46.0 in.)/2 in. = 36.66 in.

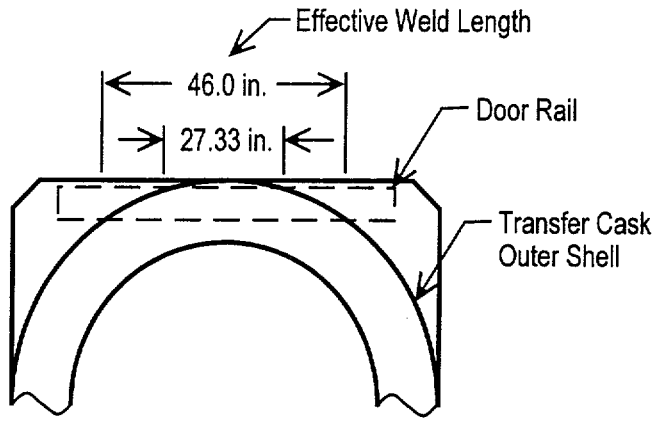

Stresses occurring in the outer shell to bottom plate weld are evaluated using a weight, W = 131,800 lb × 1.1 = 145,000 lb, which bounds the weight of the heaviest loaded canister, the weight of the water, and the weight of the shield doors and rails, with a 10% dynamic load factor.

The door rail structure and canister load will be transmitted to both the inner and outer shell via full penetration welds. The thickness of the two shells and welds are different; however, for conservatism, this evaluation assumes both shell welds are 0.75 in. groove welds.

Weld effective area = (36.66 in.)(0.75 in. + 0.75 in.) = 54.99 in^2

$$\sigma_{axial} = \frac{P}{A} = \frac{(145{,}000\,\text{lb})/(2)}{54.99\,\text{in}^2} = 1{,}318\,\text{psi}$$

For the bottom plate material (ASTM 588) at a bounding temperature of 400°F, the yield and ultimate stresses are:

$$FS_{yield} = \frac{43.0}{1.32} = +32.6 > 6$$

$$FS_{ultimate} = \frac{70.0}{1.32} = +53.0 > 10$$

where:

S_y = 43.0 ksi

S_u = 70.0 ksi

Thus, the welds in the bottom plate meet the ANSI N14.6 and NUREG-0612 criteria for nonredundant systems.

3.4.3.4.4 Advanced Transfer Cask Shield Door Rails and Welds

This section demonstrates the adequacy of the transfer cask shield doors, door rails, and welds in accordance with NUREG-0612 and ANSI N14.6, which require safety factors of 6 and 10 on material yield strength and ultimate strength, respectively, for nonredundant lift systems.

The shield door rails support the weight of a wet, fully loaded canister and the weight of the shield doors themselves. The shield doors are 9.0-in. thick plates that slide on the door rails. The rails are 9.38 in. deep × 6.5 in. thick and are welded to the bottom plate of the transfer cask. The doors and the rails are constructed of A-588 and A-350 Grade LF 2 low alloy steel, respectively.

The design weight used in this evaluation, $W = 131{,}800 \times 1.1 \approx 145{,}000$ pounds, is an assumed value that bounds the weight of the heaviest loaded canister, the weight of the water in the canister and the weight of the shield doors and rails. A 10% dynamic load factor is included to ensure that the evaluation bounds all normal operating conditions. This evaluation shows that the door rail structures and welds are adequate to support the design input.

Allowable stresses for the material are taken at 400°F, which bounds the maximum temperature at the bottom of the transfer cask under normal conditions. The material properties of A-588 and A-350 Grade LF 2 low alloy steel are provided in Tables 3.3-8 and 3.3-9, respectively. The standard impact test temperature for ASTM A-350, Grade LF2 is -50°F. The NDT temperature range is -70°F to -10°F for ASTM A-588 with a thickness range of 0.625 in. to 3 in. [28]. Therefore, the minimum service temperature for the trunnion and shells is conservatively established as 0°F (50°F higher than the NDT test temperature, in accordance with Section 4.2.6 of ANSI N14.6 [9]. For conservatism, the stress allowables for A-350 Grade LF 2 are used for all stress calculations.

Stress Evaluation for Door Rail

Each rail is assumed to carry a uniformly distributed load equal to 0.5W. The shear stress in each door rail bottom plate due to the applied load, W, is:

$$\tau = \frac{W}{A} = \frac{145{,}000\ \text{lb}}{281.25\ \text{in}^2} = 516\ \text{psi}$$

where:

$$A = 2.5\ \text{in.} \times 56.25\ \text{in. length/rail} \times 2\ \text{rails} = 281.25\ \text{in}^2.$$

The bending stress in each rail bottom section due to the applied load of W is:

$$\sigma_b = \frac{6M}{bt^2} = \frac{6 \times 86{,}275}{56.25 \times 2.5^2} = 1{,}472\ \text{psi},$$

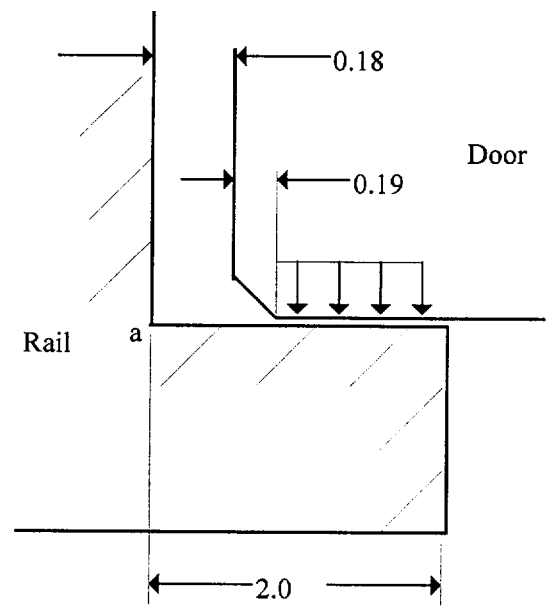

where:

$$M = \text{moment at } a,$$

$$= \frac{W}{2} \times L = \frac{145{,}000\ \text{lb.}}{2} \times 1.19\ \text{in.}$$

$$= 86{,}275\ \text{in-lb},$$

and,

$$L- = 2 - \frac{2-(0.18+0.19)}{2}$$

$$L = 1.19\ \text{in., applied load moment arm.}$$

The maximum principal stress in the bottom section of the rail is:

$$\sigma = \left(\frac{\sigma_b}{2}\right) + \sqrt{\left(\frac{\sigma_b}{2}\right)^2 + \tau^2}$$
$$= 1{,}635 \text{ psi}$$

The acceptability of the rail design is evaluated by comparing the allowable stresses to the maximum calculated stresses, considering the safety factors of NUREG-0612 and ANSI N14.6. For the yield strength criteria:

$$\frac{30{,}800 \text{ psi}}{1{,}635 \text{ psi}} = 18.8 > 6$$

For the ultimate strength criteria,

$$\frac{70{,}000 \text{ psi}}{1{,}635 \text{ psi}} = 42.8 > 10$$

The safety factors meet the criteria of NUREG-0612. Therefore, the rails are structurally adequate.

Stress Evaluation for the Shield Doors

The shield doors consist of a layer of NS-4-FR neutron shielding material sandwiched between low alloy steel plates (Note: steel bars are also welded on the edges of the doors so that the neutron shielding material is fully encapsulated). The door assemblies are 9-inch thick at the center and 6.75-inch thick at the edges, where they slide on the support rails. The stepped edges of the two door leaves are designed to interlock at the center and are, therefore, analyzed as a single plate that is simply supported on two sides.

The shear stress at the edge of the shield door where the door contacts the rail is:

$$\tau = \frac{W}{2 \times A_S} = \frac{145{,}000 \text{ lb}}{2 \times (49.2 \text{ in.} \times 4.75 \text{ in.})} = 310 \text{ psi}$$

where:

A = the total shear area, 4.75 in. thick × 49.2 in. long. Note that the effective thickness at the edge of the doors is taken as 4.75 in. because the neutron shield material and the cover plate are assumed to carry no shear load. The shear stress at the center of the doors approaches 0 psi.

The moment equation for the simply-supported beam with uniform loading is:

$$M = 72{,}500\ X - 2{,}031(X)(0.5\ X) = 72{,}500\ X - 1{,}015\ X^2$$

The maximum bending moment occurs at the center of the doors, X = 35.7 in. The bending moment at this point is:

$$M = 72{,}500 \text{ lb} \times (35.7 \text{ in.}) - 1{,}015 \text{ lb/in.} \times (35.7 \text{ in})^2$$
$$M = 12.95 \times 10^5 \text{ in.-lb.}$$

The maximum bending stress, σ_{max}, at the center of the doors, is

$$\sigma_{ax} = \frac{Mc}{I} = \frac{12.95 \times 10^5 \text{ in.} - \text{lb} \times 5.5 \text{ in.}}{2{,}378 \text{ in.}^4} = 2{,}995 \text{ psi}$$

where:

$$c = \frac{h}{2} = \frac{7 \text{ in.}}{2} + 2 \text{ in.} = 5.5 \text{ in., and}$$

$$I = \frac{bh^3}{12} = \frac{83.2 \text{ in.} \times 7^3 \text{ in}}{12} = 2{,}378 \text{ in}^4.$$

The acceptability of the door design is evaluated by comparing the allowable stresses to the maximum calculated stresses. As shown above, the maximum stress occurs for bending.

For the yield strength criteria,

$$\frac{30{,}800 \text{ psi}}{2{,}995 \text{ psi}} = 10.3 > 6$$

For the ultimate strength criteria,

$$\frac{70{,}000\ \text{psi}}{2{,}995\ \text{psi}} = 23.4 > 10$$

The safety factors satisfy the criteria of NUREG-0612. Therefore, the doors are structurally adequate.

Door Rail Weld Evaluation

The door rails are attached to the bottom of the transfer cask by 0.75-in. partial penetration bevel groove welds that extend the full length of the inside and outside of each rail. If the load is conservatively assumed to act at a point on the inside edge of the rail, the load, P, on each rail is,

$$P = \frac{W}{2} = \frac{145{,}000\ \text{lb}}{2} = 72{,}500\ \text{lb}$$

Summing moments about the inner weld location:

$$0 = P \times a - F_o \times (b) = 72{,}500\ \text{lb} \times 1.19\ \text{in.} - F_o\ (4.5\ \text{in.}),\ \text{or}$$

$$F_o = 19{,}172\ \text{lb}$$

Summing forces:

$$F_i = F_o + P = 19{,}172\ \text{lb} + 72{,}500\ \text{lb} = 91{,}672\ \text{lb}$$

The effective area of the inner weld is $0.75\ \text{in} \times .707 \times 56.25\ \text{in. long} = 29.83\ \text{in}^2$

The shear stress, τ, in the inner weld is

$$\tau = \frac{91{,}672\ \text{lb}}{29.83\ \text{in}^2} = 3{,}073\ \text{psi}$$

The factors of safety are

$$\frac{30{,}800\ \text{psi}}{3{,}073\ \text{psi}} = 10.0 > 6 \qquad \text{(for yield strength criteria)}$$

$$\frac{70{,}000\ \text{psi}}{3{,}073\ \text{psi}} = 22.8 > 10 \qquad \text{(for ultimate strength criteria)}$$

The safety factors meet the criteria of NUREG-0612.

Figure 3.4.3.4-1 Advanced Transfer Cask Finite Element Model

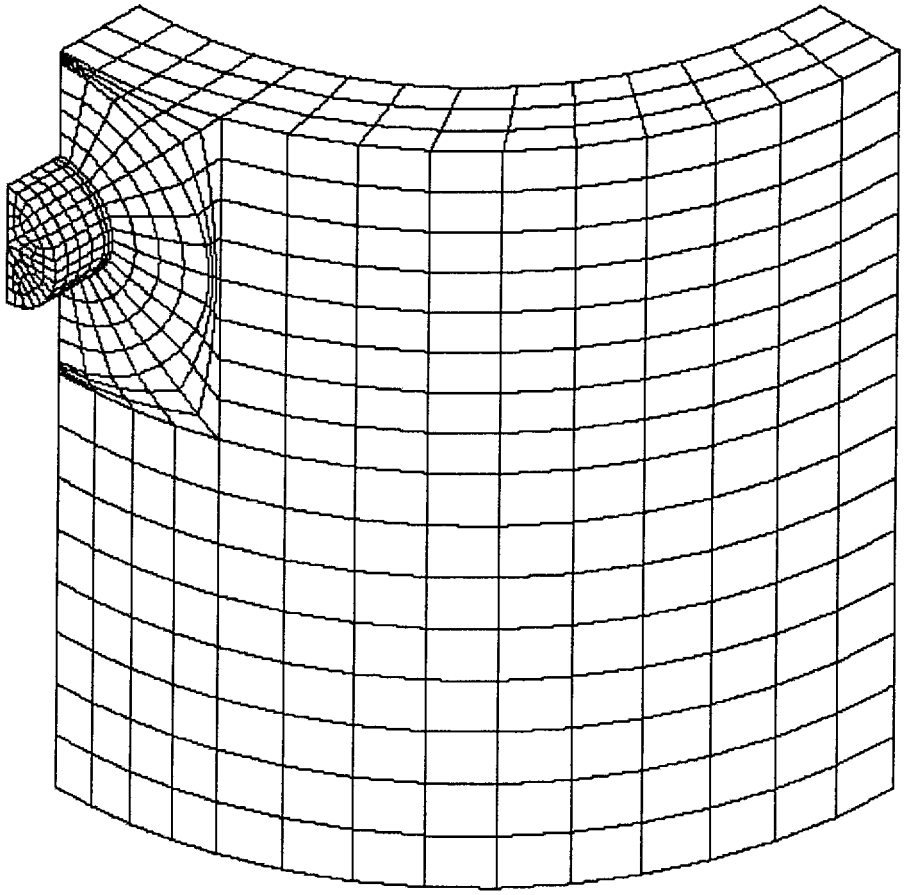

Figure 3.4.3.4-2 Node Locations for Advanced Transfer Cask Outer Shell Adjacent to Trunnion

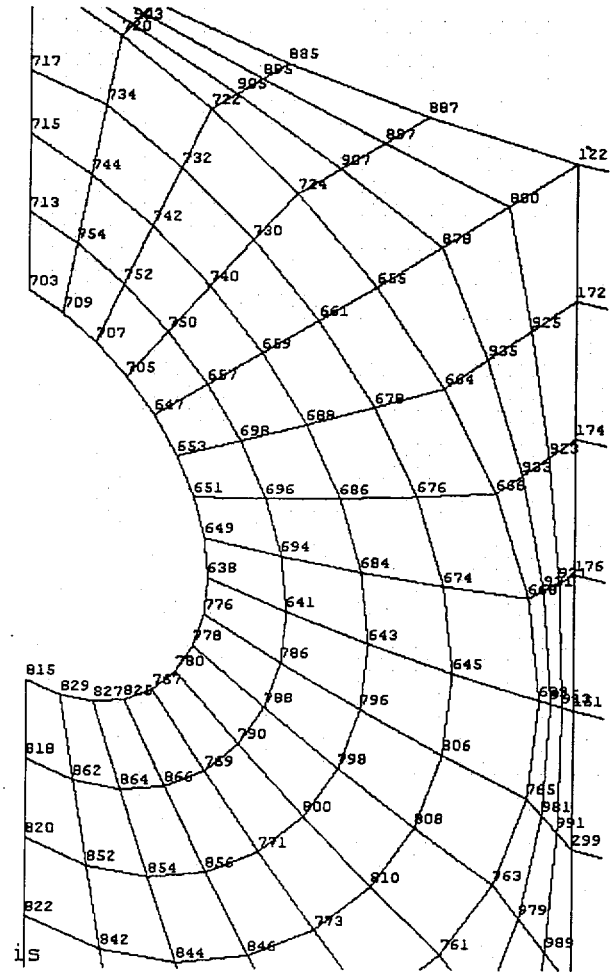

Figure 3.4.3.4-3 Node Locations for Advanced Transfer Cask Inner Shell Adjacent to Trunnion

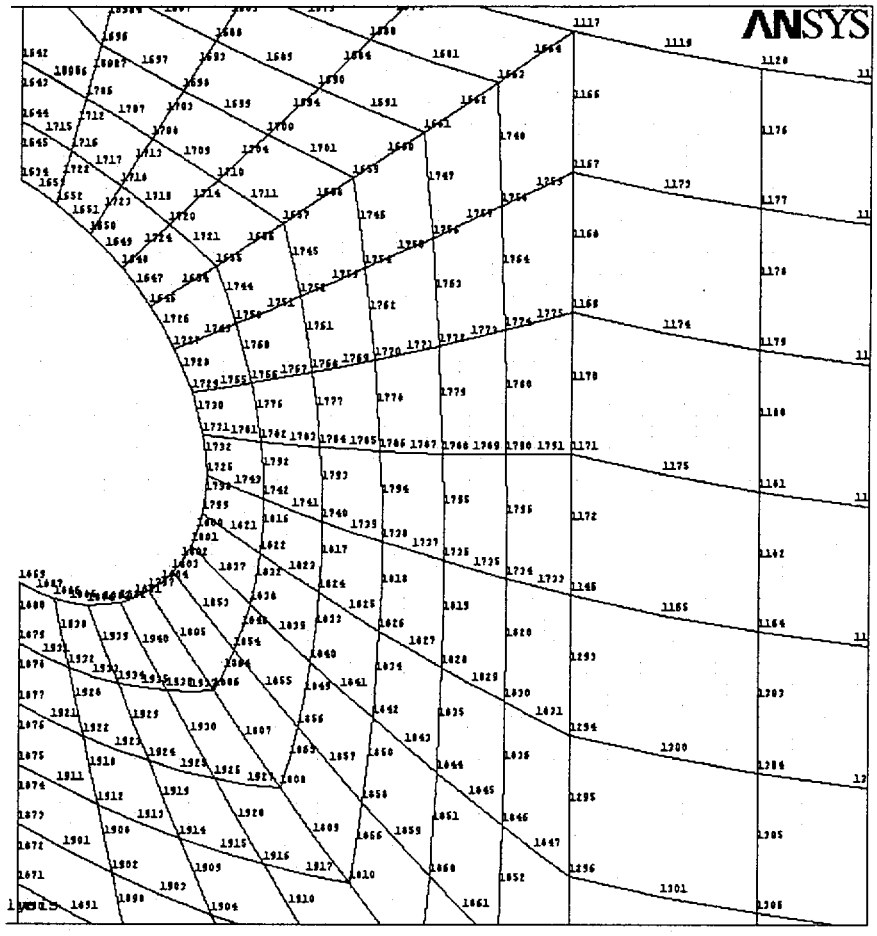

Figure 3.4.3.4-4 Node Locations for Advanced Transfer Cask Stiffener Plate Above Trunnion

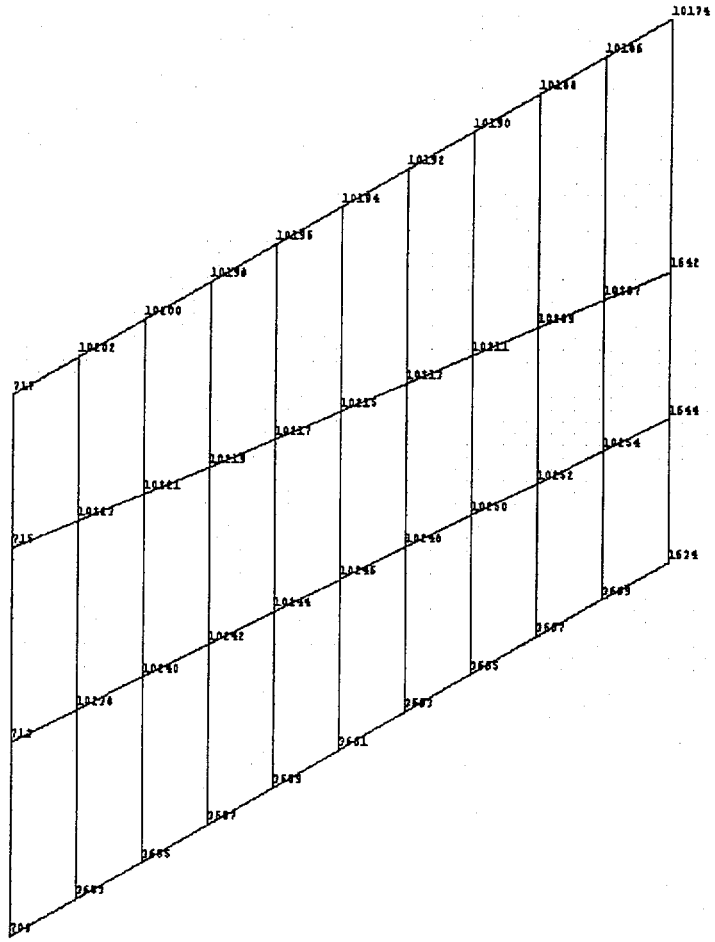

Figure 3.4.3.4-5 Stress Intensity Contours (psi) for Advanced Transfer Cask Outer Shell Element Top Surface

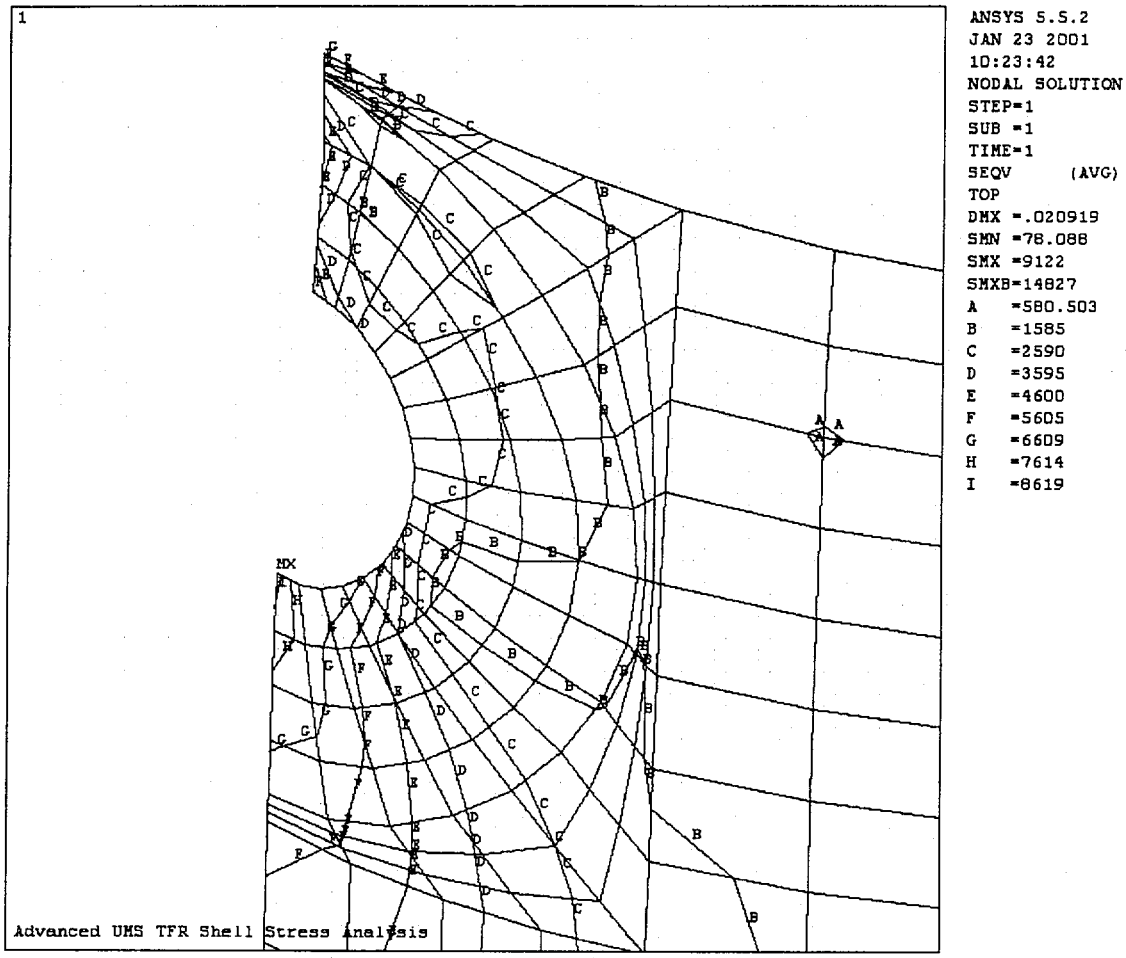

Figure 3.4.3.4-6 Stress Intensity Contours (psi) for Advanced Transfer Cask Outer Shell Element Bottom Surface

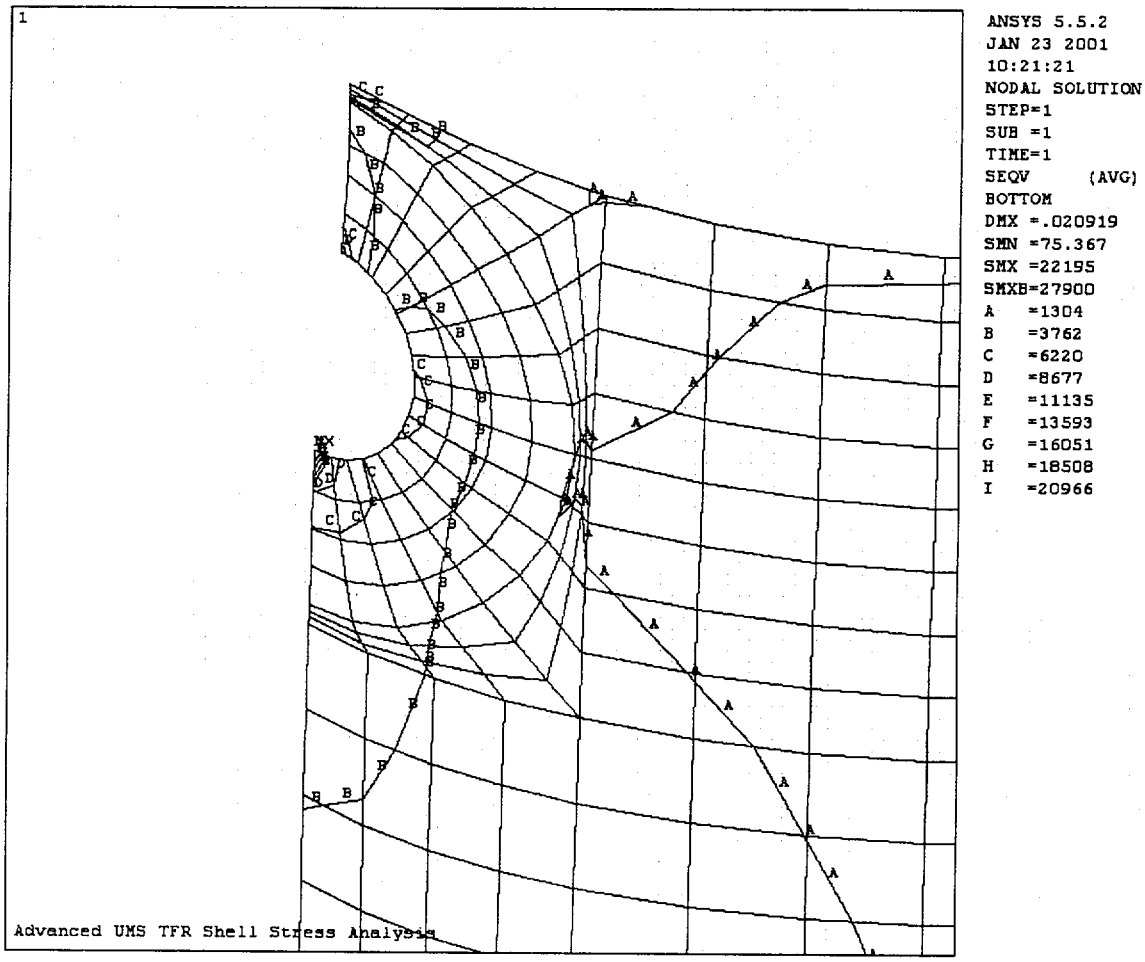

Figure 3.4.3.4-7 Stress Intensity Contours (psi) for Advanced Transfer Cask Inner Shell Element Top Surface

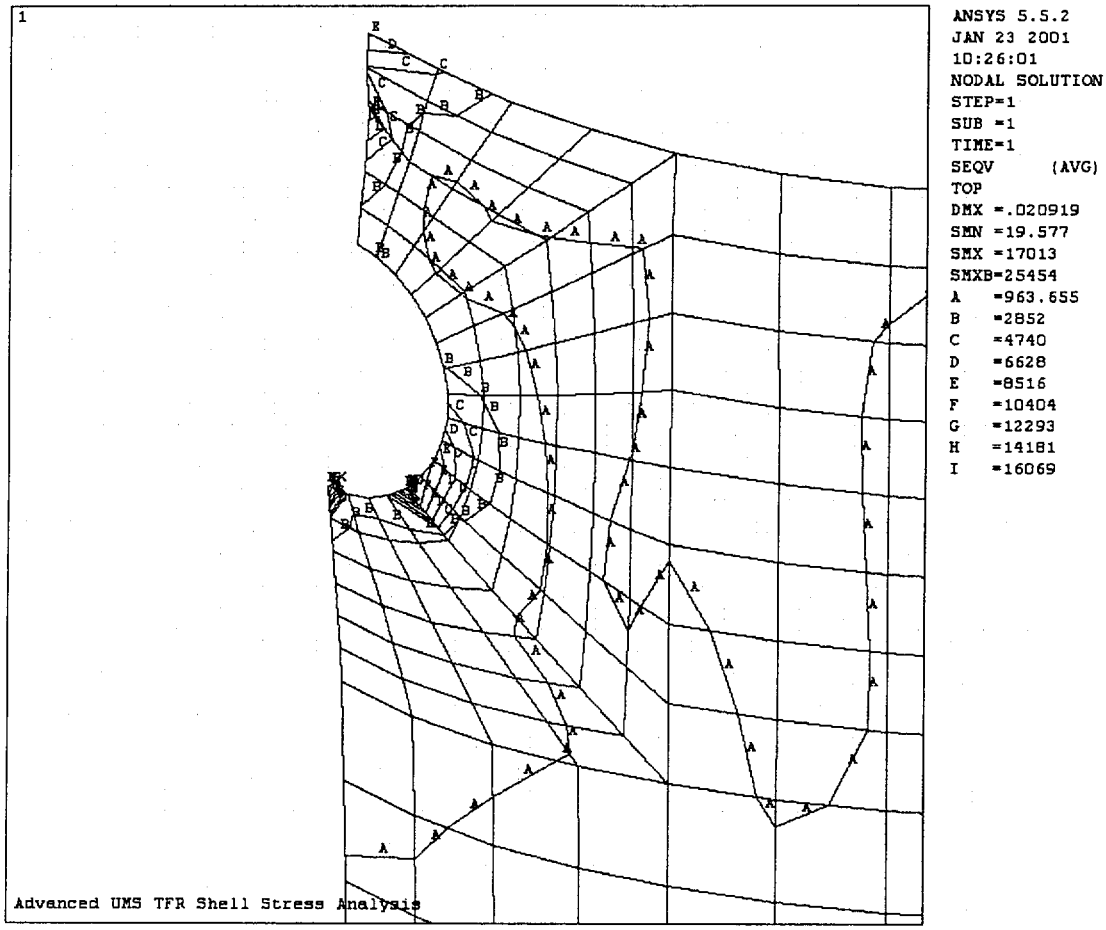

Figure 3.4.3.4-8 Stress Intensity Contours (psi) for Advanced Transfer Cask Inner Shell Element Bottom Surface

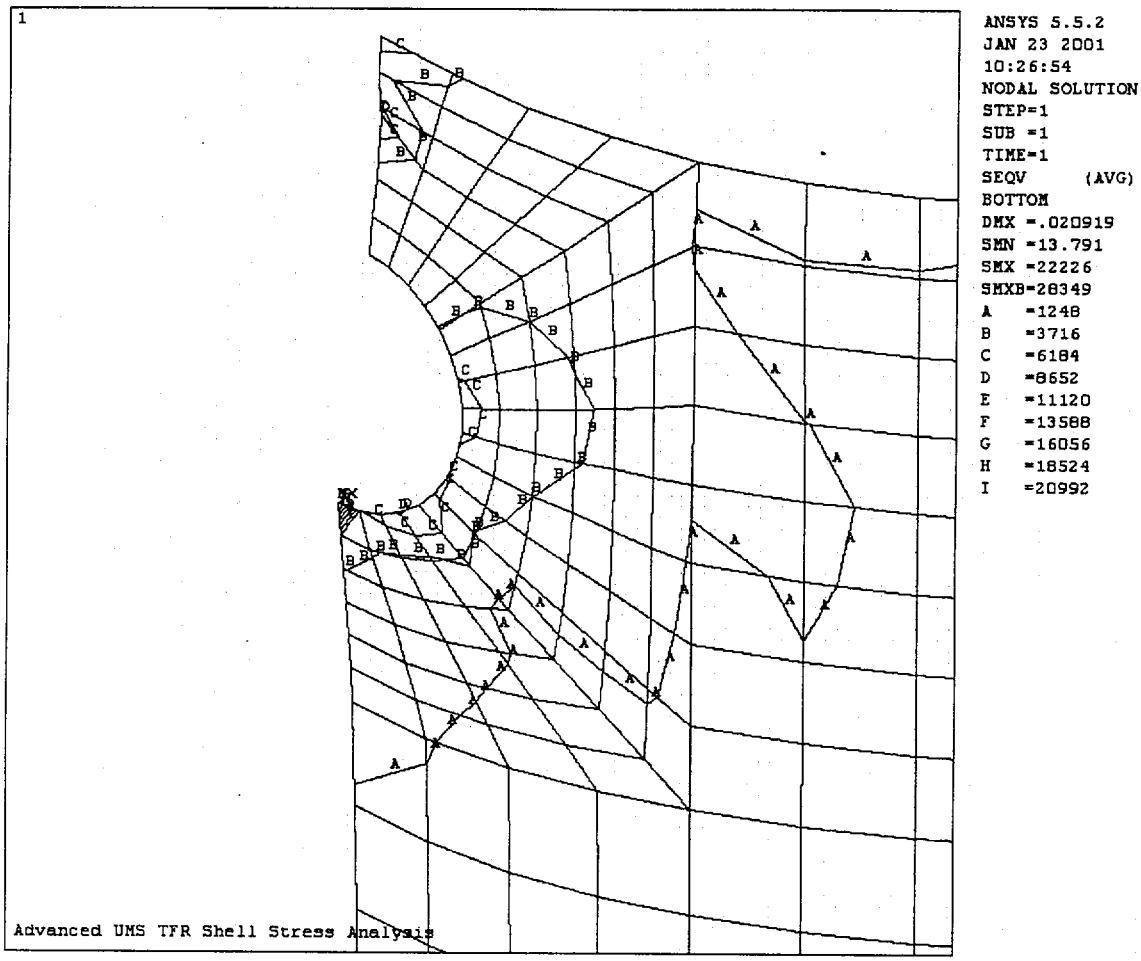

Figure 3.4.3.4-9 Stress Intensity Contours (psi) for Advanced Transfer Cask Stiffener Plate Element Top Surface

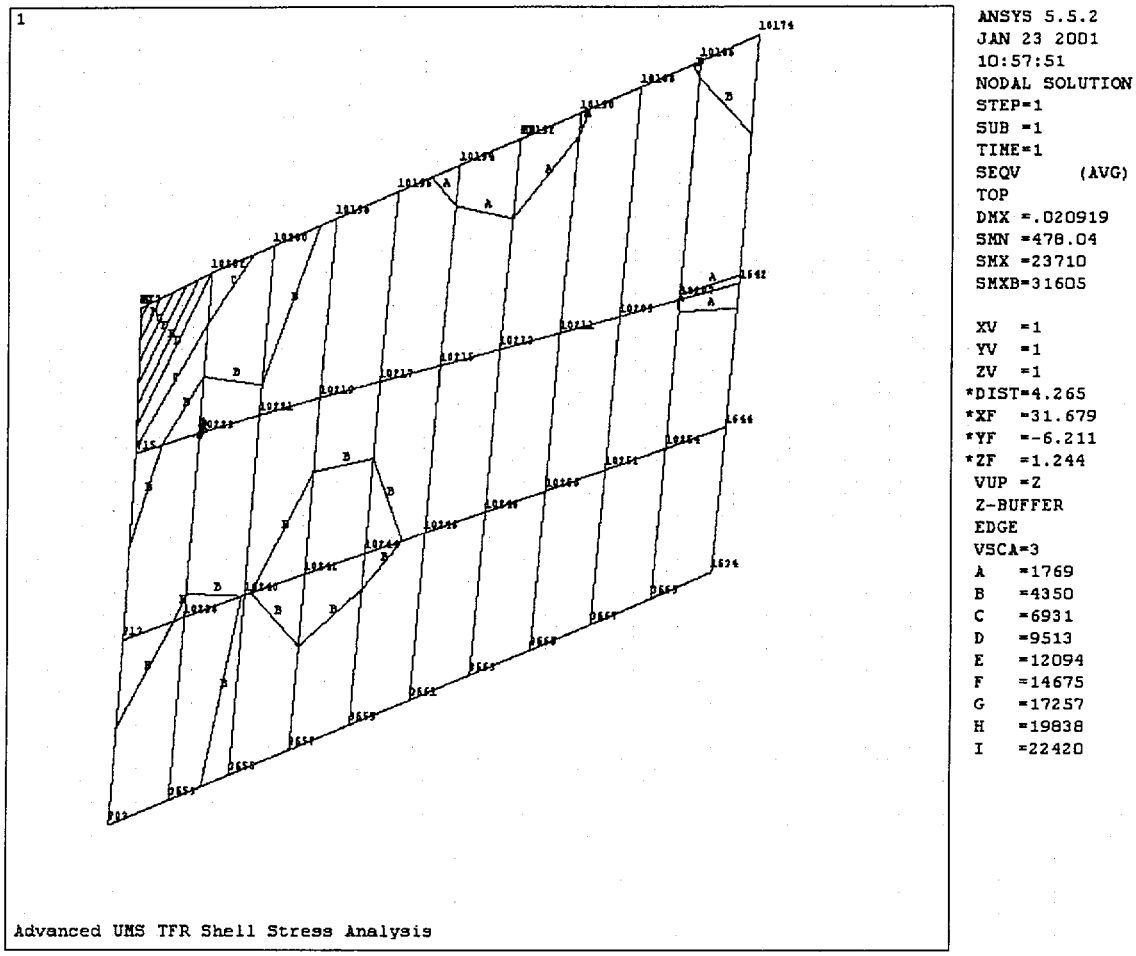

Figure 3.4.3.4-10 Stress Intensity Contours (psi) for Advanced Transfer Cask Stiffener Plate Element Bottom Surface

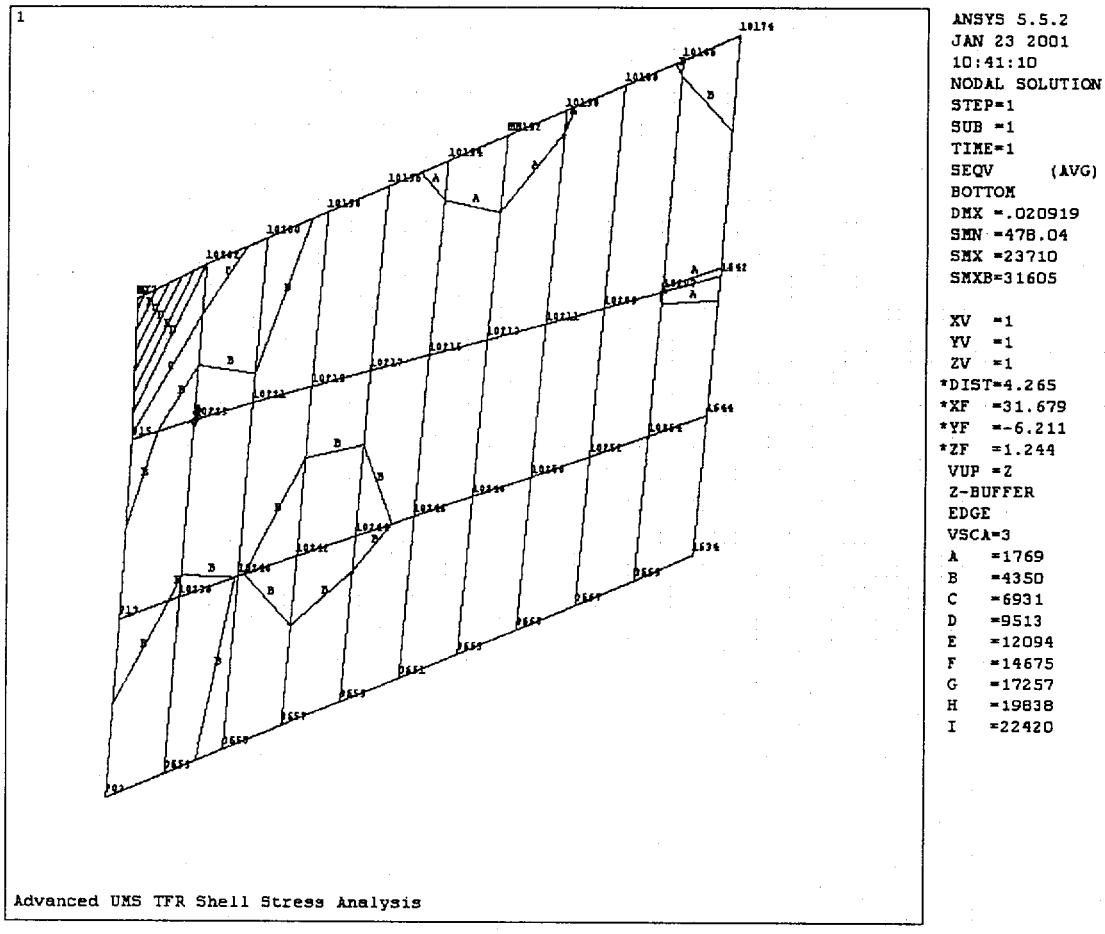

Table 3.4.3.4-1 Top 30 Stresses for Advanced Transfer Cask Outer Shell Element Top Surface

Node[1]	Principal Stresses (psi)			Nodal Von SeMisses Stressesqv (psi)	FS on Yield $(S_y)^2$	FS on Ultimate $(S_u)^2$
	S1	S2	S3			
815	3826.5	-213.1	-6617.3	9121.6	NA[3]	NA[3]
818	5489.8	-5.1	-4049.8	8293.3	NA	NA
820	4864.3	-1.9	-3634.4	7385.9	6.2	NA
827	5467.3	9.9	-2896.6	7354.7	6.2	NA
862	4847.2	3.3	-3530.7	7285.0	6.3	NA
825	5331.6	46.7	-2843.8	7180.6	6.4	NA
852	4708.0	0.3	-3275.8	6951.2	6.6	10.1
829	4163.6	-32.5	-3761.8	6867.6	6.6	10.2
871	7593.2	2376.9	-104.9	6805.5	6.7	10.3
822	4395.9	-0.3	-3328.5	6710.8	6.8	10.4
767	4460.2	129.3	-3077.8	6552.3	7.0	10.7
842	4289.1	0.2	-3001.4	6346.5	7.2	11.0
816	3994.4	-0.1	-3172.3	6220.2	7.3	11.3
943	3923.2	-0.1	-3167.1	6152.0	7.4	11.4
864	4384.5	9.7	-2590.9	6105.7	7.5	11.5
941	3858.7	-0.1	-3154.5	6083.8	7.5	11.5
2	3777.8	0.0	-3137.0	5997.0	7.6	11.7
832	3896.2	0.2	-2847.8	5864.0	7.8	11.9
854	4294.6	2.8	-2380.3	5858.9	7.8	11.9
703	3796.2	403.9	-2924.7	5820.5	7.8	12.0
964	3797.0	0.3	-2769.6	5710.0	8.0	12.3
873	6270.5	2019.3	-108.3	5625.3	8.1	12.4
954	3706.0	0.2	-2688.5	5561.1	8.2	12.6
844	3986.4	2.1	-2173.4	5410.7	8.4	12.9
8	3604.7	0.0	-2610.7	5405.5	8.4	12.9
780	3173.5	201.6	-3062.0	5402.0	8.4	13.0
47	3082.8	0.0	-2836.0	5127.3	8.9	13.7
717	5482.2	2416.5	-302.7	5012.8	9.1	14.0
834	3658.3	1.9	-2009.6	4977.0	9.2	14.1
866	3876.4	2.7	-1685.2	4939.0	9.2	14.2

Notes:

1. See Figure 3.4.3.4 -2 for node locations.
2. S_y = 45,600 psi, S_u = 70,000 psi.
3. Local stresses that are relieved by local material yielding. Therefore, stress design factors of 6 and 10 on material yield and ultimate strength are not applicable (ANSI N14.6, Section 4.2.1.2).

Table 3.4.3.4-2 Top 30 Stresses for Advanced Transfer Cask Outer Shell Element Bottom Surface

Node[1]Node	Principal Stresses (psi)Principal Stresses (psi)			Nodal Von Misses Stresses (psi)Nodal Seqv (psi)	FS on Yield $(S_y)^2$	FS on Ultimate $(S_u)^2$
	S1	S2	S3			
815	23117.0	2218.6	-178.6	22195.0	NA[3]	NA[3]
829	11968.0	5735.9	-18.9	10383.0	NA	NA
703	1423.8	-967.7	-9354.8	9804.1	NA	NA
818	9713.1	2279.0	-6.7	8802.4	NA	NA
871	94.9	-1212.6	-8374.4	7897.2	NA	NA
862	8885.1	3223.8	-10.3	7798.7	NA	NA
638	5557.4	114.7	-2341.4	7001.6	6.5	10.0
827	8016.0	3977.8	-8.5	6949.4	6.6	10.1
776	6510.7	508.4	-1100.0	6947.6	6.6	10.1
873	96.4	-763.0	-7125.6	6833.0	6.7	10.2
864	7722.7	2933.9	-9.0	6759.1	6.7	10.4
778	6789.6	1430.4	-446.1	6503.7	7.0	10.8
649	4028.8	-83.7	-3465.5	6500.5	7.0	10.8
820	7069.8	2942.0	-1.3	6152.4	7.4	11.4
825	7053.3	3670.3	-38.6	6143.9	7.4	11.4
780	6781.3	2682.2	-224.7	6096.5	7.5	11.5
875	100.3	-280.5	-6043.9	5963.0	7.6	11.7
767	6767.8	3530.1	-113.1	5962.5	7.6	11.7
852	6770.6	2764.7	-2.8	5898.5	7.7	11.9
866	6665.5	2211.1	-0.6	5881.0	7.8	11.9
651	2424.8	-291.8	-4029.7	5613.0	8.1	12.5
769	6045.8	1502.0	0.4	5451.9	8.4	12.8
854	6169.1	2215.3	-3.8	5415.8	8.4	12.9
715	42.8	-4696.1	-5838.1	5401.2	8.4	13.0
822	6062.5	2413.7	-0.2	5286.6	8.6	13.2
790	5610.4	835.1	-1.7	5244.1	8.7	13.3
717	356.3	-4113.9	-5392.7	5228.2	8.7	13.4
788	5221.9	112.3	-2.8	5168.2	8.8	13.5
842	5860.1	2239.1	-0.7	5122.3	8.9	13.7
786	4723.6	-2.7	-633.4	5071.1	9.0	13.8

Notes:

1. See Figure 3.4.3.4 -2 for node locations.
2. S_y = 45,600 psi, S_u = 70,000 psi.
3. Local stresses that are relieved by local material yielding. Therefore, stress design factors of 6 and 10 on material yield and ultimate strength are not applicable (ANSI N14.6, Section 4.2.1.2).

Table 3.4.3.4-3 Top 30 Stresses for Advanced Transfer Cask Inner Shell Element Top Surface

Node[1]	Principal Stresses (psi)			Nodal Von Misses Stresses (psi)Nodal Seqv (psi)	FS on Yield (S_y)[2]	FS on Ultimate (S_u)[2]
	S1	S2	S3			
1869	2012.7	-552.0	-16137.0	17013.0	NA[3]	NA[3]
1797	13166.0	-115.4	-3089.1	14991.0	NA	NA
1803	12734.0	4058.3	-311.4	11501.0	NA	NA
1801	11627.0	4490.2	-214.9	10327.0	NA	NA
10174	663.9	-6733.1	-10256.0	9653.6	NA	NA
1633	9836.1	2649.9	-31.5	8837.4	NA	NA
1799	8856.4	4640.1	-144.2	7799.9	NA	NA
1638	743.8	-1547.7	-6362.4	6282.1	7.3	11.1
1725	5909.8	4672.1	-118.6	5514.7	8.3	12.7
1666	5438.4	1119.1	-33.4	4996.2	9.1	14.0
1882	783.0	-2383.4	-4495.2	4601.4	9.9	15.2
1636	4276.1	128.5	-576.2	4541.2	10.0	15.4
1822	4908.4	3039.9	-24.4	4313.6	10.6	16.2
1879	385.8	-127.4	-4147.3	4299.6	10.6	16.3
1731	4586.7	3239.6	-100.4	4179.6	10.9	16.7
1642	370.6	-17.7	-3713.0	3904.0	11.7	17.9
1838	4243.3	3272.0	-43.6	3893.2	11.7	18.0
1742	4389.1	2373.4	-14.5	3818.2	11.9	18.3
1886	99.4	-3236.9	-4024.2	3791.7	12.0	18.5
1884	444.8	-1827.8	-3719.9	3611.7	12.6	19.4
1676	3632.1	460.2	-25.6	3440.7	13.3	20.3
1854	3092.7	2724.2	-63.9	2989.4	15.3	23.4
1729	3305.4	1609.1	-110.0	2957.8	15.4	23.7
1652	2282.5	-2.8	-959.2	2884.9	15.8	24.3
1650	1868.2	46.8	-1388.3	2826.8	16.1	24.8
1644	576.4	-30.5	-2481.9	2804.5	16.3	25.0
1782	3124.2	1561.5	-8.7	2713.2	16.8	25.8
1120	4.1	-1046.1	-2882.0	2530.1	18.0	27.7
1648	1619.2	131.3	-1221.8	2461.3	18.5	28.4
1122	3.6	-824.2	-2582.3	2287.2	19.9	30.6

Notes:

1. See Figure 3.4.3.4-3 for node locations.
2. S_y = 45,600 psi, S_u = 70,000 psi.
3. Local stresses that are relieved by local material yielding. Therefore, stress design factors of 6 and 10 on material yield and ultimate strength are not applicable (ANSI N14.6, Section 4.2.1.2).

Table 3.4.3.4-4 Top 30 Stresses for Advanced Transfer Cask Inner Shell Element Bottom Surface

Node[1]	Principal Stresses (psi)			Nodal Von Misses Stresses (psi)Nodal Seqv (psi)	FS on Yield (S_y)[2]	FS on Ultimate (S_u)[2]
	S1	S2	S3			
1869	21448.0	632.6	-1960.3	22226.0	NA[3]	NA[3]
1882	8980.2	1059.9	-688.5	8923.9	NA	NA
10174	8109.4	7767.7	-819.1	8762.6	NA	NA
1797	1665.5	195.3	-7189.2	8218.8	NA	NA
1633	34.4	-2893.9	-8886.1	7875.8	NA	NA
1884	7160.2	652.9	-518.7	7165.3	6.4	NA
1731	1798.5	-157.2	-5950.2	6979.4	6.5	10.0
1803	501.1	-4651.7	-6891.7	6565.9	6.9	10.7
1725	819.9	-847.5	-6386.4	6534.2	7.0	10.7
1729	2571.3	-23.3	-4710.5	6392.4	7.1	11.0
1801	451.5	-4185.3	-6697.8	6282.0	7.3	11.1
1886	6799.4	2900.0	-79.4	5975.0	7.6	11.7
1879	5957.9	215.5	-205.1	5963.8	7.6	11.7
1638	5833.9	814.9	-647.9	5888.3	7.7	11.9
1799	450.0	-2722.7	-6304.4	5853.1	7.8	12.0
1742	1683.1	-3.7	-4630.1	5661.5	8.1	12.4
1822	1331.5	5.0	-4781.8	5569.8	8.2	12.6
1782	2155.7	-3.5	-4010.0	5418.9	8.4	12.9
1727	2988.1	35.3	-2969.9	5159.9	8.8	13.6
1766	2423.2	-1.0	-3317.9	4992.0	9.1	14.0
1784	2724.4	-2.3	-2938.1	4905.0	9.3	14.3
1838	1172.3	36.4	-4115.5	4821.3	9.5	14.5
1740	2640.2	-5.1	-2772.6	4688.0	9.7	14.9
1768	2402.5	-0.5	-2701.2	4422.5	10.3	15.8
1806	4006.7	141.6	-771.3	4393.2	10.4	15.9
1750	2260.4	0.0	-2725.3	4323.9	10.5	16.2
1666	18.8	-2100.4	-4642.2	4042.1	11.3	17.3
1786	2648.7	1.1	-1951.0	3998.6	11.4	17.5
1636	418.4	-283.5	-3777.7	3892.9	11.7	18.0
1646	2917.4	117.6	-1523.0	3888.9	11.7	18.0

Notes:

1. See Figure 3.4.3.4-3 for node locations.
2. S_y = 45,600 psi, S_u = 70,000 psi.
3. Local stresses that are relieved by local material yielding. Therefore, stress design factors of 6 and 10 on material yield and ultimate strength are not applicable (ANSI N14.6, Section 4.2.1.2).

Table 3.4.3.4-5 Top 30 Stresses for Advanced Transfer Cask Stiffener Plate Element Top Surface

Node[1]	Principal Stresses (psi)			Nodal Von Misses Stresses (psi)Nodal Seqv (psi)	FS on Yield $(S_y)^2$	FS on Ultimate $(S_u)^2$
	S1	S2	S3			
717	21871.0	0.0	-3327.1	23710.0	NA[3]	NA[3]
10202	10380.0	2355.3	0.0	9425.9	NA	NA
703	0.0	-2611.0	-7384.1	6485.5	7.0	10.8
715	2540.9	0.0	-4590.8	6260.7	7.3	11.2
10174	0.0	-331.0	-6322.5	6163.7	7.4	11.4
10200	5583.6	0.0	-327.2	5754.1	7.9	12.2
3653	0.0	-234.7	-5162.0	5048.8	9.0	13.9
10238	1540.5	0.0	-3784.2	4745.8	9.6	14.7
10186	0.0	-353.6	-4708.3	4541.8	10.0	15.4
10242	2112.4	0.0	-3100.6	4541.5	10.0	15.4
10244	2350.2	0.0	-2849.7	4510.2	10.1	15.5
10240	1634.9	0.0	-3271.9	4327.5	10.5	16.2
10246	2401.3	0.0	-2507.3	4251.3	10.7	16.5
10217	2848.4	0.0	-2000.3	4220.5	10.8	16.6
10219	3030.0	0.0	-1779.4	4211.7	10.8	16.6
10215	2588.3	0.0	-2137.9	4099.2	11.1	17.1
3657	1182.4	0.0	-3351.0	4073.1	11.2	17.2
10221	3249.6	0.0	-1287.2	4049.6	11.3	17.3
10213	2350.3	0.0	-2163.4	3910.1	11.7	17.9
10198	3889.7	51.5	0.0	3864.2	11.8	18.1
10248	2329.7	0.0	-2066.7	3809.6	12.0	18.4
3659	1493.7	0.0	-2771.5	3748.6	12.2	18.7
3655	0.0	-122.0	-3793.1	3733.6	12.2	18.7
10211	2126.4	0.0	-2015.8	3587.7	12.7	19.5
3661	1862.2	0.0	-2213.6	3534.1	12.9	19.8
3669	3134.7	0.0	-384.7	3343.7	13.6	20.9
3663	2090.4	0.0	-1721.4	3306.3	13.8	21.2
10250	2173.3	0.0	-1540.2	3231.5	14.1	21.7
3665	2305.8	0.0	-1283.8	3150.4	14.5	22.2
10209	1909.7	0.0	-1598.9	3042.5	15.0	23.0

Notes:

1. See Figure 3.4.3.4-4 for node locations.
2. S_y = 45,600 psi, S_u = 70,000 psi.
3. Local stresses that are relieved by local material yielding. Therefore, stress design factors of 6 and 10 on material yield and ultimate strength are not applicable (ANSI N14.6, Section 4.2.1.2).

Table 3.4.3.4-6 Top 30 Stresses for Advanced Transfer Cask Stiffener Plate Element Bottom Surface

Node[1]	Principal Stresses (psi)			Nodal Von Misses Stresses (psi)Nodal Seqv (psi)	FS on Yield (S_y)[2]	FS on Ultimate (S_u)[2]
	S1	S2	S3			
717	21871.0	0.0	-3327.1	23710.0	NA[3]	NA[3]
10202	10380.0	2355.3	0.0	9425.9	NA	NA
703	0.0	-2611.0	-7384.1	6485.5	7.0	10.8
715	2540.9	0.0	-4590.8	6260.7	7.3	11.2
10174	0.0	-331.0	-6322.5	6163.7	7.4	11.4
10200	5583.6	0.0	-327.2	5754.1	7.9	12.2
3653	0.0	-234.7	-5162.0	5048.8	9.0	13.9
10238	1540.5	0.0	-3784.2	4745.8	9.6	14.7
10186	0.0	-353.6	-4708.3	4541.8	10.0	15.4
10242	2112.4	0.0	-3100.6	4541.5	10.0	15.4
10244	2350.2	0.0	-2849.7	4510.2	10.1	15.5
10240	1634.9	0.0	-3271.9	4327.5	10.5	16.2
10246	2401.3	0.0	-2507.3	4251.3	10.7	16.5
10217	2848.4	0.0	-2000.3	4220.5	10.8	16.6
10219	3030.0	0.0	-1779.4	4211.7	10.8	16.6
10215	2588.3	0.0	-2137.9	4099.2	11.1	17.1
3657	1182.4	0.0	-3351.0	4073.1	11.2	17.2
10221	3249.6	0.0	-1287.2	4049.6	11.3	17.3
10213	2350.3	0.0	-2163.4	3910.1	11.7	17.9
10198	3889.7	51.5	0.0	3864.2	11.8	18.1
10248	2329.7	0.0	-2066.7	3809.6	12.0	18.4
3659	1493.7	0.0	-2771.5	3748.6	12.2	18.7
3655	0.0	-122.0	-3793.1	3733.6	12.2	18.7
10211	2126.4	0.0	-2015.8	3587.7	12.7	19.5
3661	1862.2	0.0	-2213.6	3534.1	12.9	19.8
3669	3134.7	0.0	-384.7	3343.7	13.6	20.9
3663	2090.4	0.0	-1721.4	3306.3	13.8	21.2
10250	2173.3	0.0	-1540.2	3231.5	14.1	21.7
3665	2305.8	0.0	-1283.8	3150.4	14.5	22.2
10209	1909.7	0.0	-1598.9	3042.5	15.0	23.0

Notes:

1. See Figure 3.4.3.4-4 for node locations.
2. S_y = 45,600 psi, S_u = 70,000 psi.
3. Local stresses that are relieved by local material yielding. Therefore, stress design factors of 6 and 10 on material yield and ultimate strength are not applicable (ANSI N14.6, Section 4.2.1.2).

3.4.4 Normal Operating Conditions Analysis

The Universal Storage System is evaluated using individual finite element models for the fuel basket, canister, and vertical concrete cask. Because the individual components are free to expand without interference, the structural finite element models need not be connected.

3.4.4.1 Canister and Basket Analyses

The evaluations presented in this Section are based on consideration of the bounding conditions for each aspect of the analysis. Generally, the bounding condition is represented by the component, or combination of components, of each configuration that is the heaviest. The bounding thermal condition is established by the configuration having the largest thermal gradient in normal use. Some cases require the evaluation of both a PWR and a BWR configuration because of differences in the design of these systems. For reference, the bounding case used in each of the structural evaluations is:

Section	Aspect Evaluated	Bounding Condition	Configuration
3.4.4.1.1	Canister Thermal Stress	Largest temperature gradient	Temperature[a] distribution
3.4.4.1.2	Canister Dead Weight	Heaviest loaded canister	BWR Class 5
3.4.4.1.3	Canister Pressure	Bounding pressure 15 psig, smallest canister	PWR Class 1 BWR Class 4
3.4.4.1.4	Canister Handling	Shortest canister dimensions w/ heaviest canister load [b]	PWR Class 1 BWR Class 5
3.4.4.1.5	Canister Load Combinations	Bounding pressure 15 psig + shortest canister dimensions w/ heaviest loaded canister[b] (handling) + shortest canister dimensions w/ heaviest loaded canister [b] (dead load) largest temperature gradient (thermal)	PWR Class 3 PWR Class 1 BWR Class 5 PWR Class 1 BWR Class 5 Temperature[a] distribution
3.4.4.1.6	Canister Fatigue	Bounding thermal excursions (58°F)	Not Applicable
3.4.4.1.7	Canister Pressure Test	Loaded canister (smallest canister)	PWR Class 1
3.4.4.1.8	PWR Basket Support Disk	Loaded PWR Canister	PWR fuel basket
	BWR Basket Support Disk	Loaded BWR Canister	BWR fuel basket [c]
3.4.4.1.9	PWR Basket Weldment	Loaded PWR Canister	PWR Class 2
	BWR Basket Weldment	Loaded BWR Canister	BWR Class 5
3.4.4.1.10	PWR Fuel Tube	Loaded PWR Canister (Longest)	PWR Class 3
	BWR Fuel Tube	Loaded BWR Canister (Longest)	BWR Class 5
3.4.4.1.11	Canister Closure Weld	Same as 3.4.4.1.5	Same as 3.4.4.1.5

[a] See Section 3.4.4.1.1 for an explanation of the composite temperature distribution used in the analyses. The shortest canister, PWR Class 1, has the fewest number of fuel basket support disks.

[b] When combined with the heaviest fuel assembly/fuel basket weight (BWR Class 5), the load per support disk or weldment disk is maximized.

[c] The evaluation of the BWR basket uses the analysis presented in the UMS Transport SAR [2].

3.4.4.1.1 Canister Thermal Stress Analysis

A three-dimensional finite element model of the canister was constructed using ANSYS SOLID45 elements. By taking advantage of the symmetry of the canister, the model represents one-half (180° section) of the canister including the canister shell, bottom plate, structural lid, and shield lid. Contact between the structural and shield lids is modeled using COMBIN40 combination elements in the axial (UY) degree of freedom. Simulation of the spacer ring is accomplished using a ring of COMBIN40 gap/spring elements connecting the shield lid and the canister in the axial direction at the lid lower outside radius. In addition, CONTAC52 elements are used to model the interaction between the structural lid and the canister shell and between the shield lid and canister shell, just below the respective lid weld joints as shown in Figure 3.4.4.1-2. The size of the CONTAC52 gaps is determined from nominal dimensions of contacting components. The gap size is defined by the "Real Constant" of the CONTAC52 element. Due to the relatively large gaps resulting from the nominal geometry, these gaps remain open during all loadings considered. The COMBIN40 elements used between the structural and shield lids and for the spacer ring are assigned small gap sizes of 1×10^{-8} in. All gap/spring elements are assigned a stiffness of 1×10^{8} lb/in. The three-dimensional finite element model of the canister used in the thermal stress evaluation is shown in Figure 3.4.4.1-1 through Figure 3.4.4.1-3.

The model is constrained in the Z-direction for all nodes in the plane of symmetry. For the stability of the solution, one node at the center of the bottom plate is constrained in the Y-direction, and all nodes at the centerline of the canister are constrained in the X-direction. The directions of the coordinate system are shown in Figure 3.4.4.1-1.

This model represents a "bounding" combination of geometry and loading that envelopes the Universal Storage System PWR and BWR canisters. Specifically, the shortest canister (PWR Class 1) is modeled in conjunction with the heaviest fuel and fuel basket combination (BWR Class 5). By using the shortest canister (PWR Class 1), which has the fewest number of support disks, in combination with the weight of the heaviest loaded fuel basket, the load per support disk and weldment disk is maximized. Thus, the analysis yields very conservative results relative to the expected performance of the actual canister configurations.

3.4.4.1.2 Canister Dead Weight Load Analysis

The canister is structurally analyzed for dead weight load using the finite element model described in Section 3.4.4.1.1. The canister temperature distribution discussed in Section 3.4.4.1.1 is used in the dead load structural analysis to evaluate the material properties at temperature. The fuel and fuel basket assembly contained within the canister are not explicitly modeled but are included in the analysis by applying a uniform pressure load representing their combined weight to the top surface of the canister bottom plate. The nodes on the bottom surface of the bottom plate are restrained in the axial direction in conjunction with the constraints described in Section 3.4.4.1.1. The evaluation is based on the weight of the BWR Class 5 canister, which has the highest weight, and the length of the PWR Class 1 canister, which is the shortest configuration. An acceleration of 1g is applied to the model in the axial direction (Y) to simulate the dead load.

The resulting maximum canister dead load stresses are summarized in Table 3.4.4.1-2 and Table 3.4.4.1-3 for primary membrane and primary membrane plus bending stresses, respectively. The sectional stresses at 16 axial locations are obtained for each angular division of the model (a total of 19 angular locations for each axial location). The locations for the stress sections are shown in Figure 3.4.4.1-4.

The lid support ring is evaluated for the dead load condition using classical methods. The ring, which is made of ASTM A-479, Type 304 stainless steel, is welded to the inner surface of the canister shell to support the shield lid. For conservatism, a temperature of 400°F, which is higher than the anticipated temperature at this location, is used to determine the material allowable stress. The total weight, W, imposed on the lid support ring is conservatively considered to be the weight of the auxiliary shielding and the shield lid. A 10% load factor is also applied to ensure that the analysis bounds all normal operating loads. The stresses on the support ring are the bearing stresses and shear stresses at its weld to the canister shell.

The bearing stress $\sigma_{bearing}$ is:

$$\sigma_{bearing} = \frac{W}{area} = \frac{14{,}200\,\text{lb}}{102.6\,\text{in}^2} = 138\ \text{psi}$$

where:

W = (7,000 lb + 5,890 lb) × 1.1 = 14,179 lb, use 14,200 lb
where the weight of the auxiliary shielding (W_s) can be comprised of three 2-inch-thick stainless steel plates resting on the shield lid, or

W_s = .291 x (π/4) x 65.5^2 x 6 = 5,883 lb, use 5,890 lb

$$A = \frac{\pi}{4}(D^2 - (D-2t)^2)\,\text{in}^2 = 102.6\ \text{in}^2$$

D = lid support ring diameter = 65.81 in.

t = radial thickness of support ring = 0.5 in.

The yield strength, S_y, for A-479, Type 304 stainless steel = 20,700 psi, and the ultimate allowable tensile stress, S_u = 64,400 psi at 400°F. The allowable bearing stress is 1.0 S_y per ASME Code, Section III, Subsection NB. The acceptability of the support ring design is evaluated by comparing the allowable stresses to the maximum calculated stress:

$$MS = \frac{20{,}700\ \text{psi}}{138\ \text{psi}} - 1 = +\text{Large}$$

Therefore, the support ring is structurally adequate.

The attachment weld for the lid support ring is a 1/8-in. partial penetration groove weld. The total shear force on the weld is considered to be the weight of the shield lid, the structural lid, and the lid support ring. The total effective area of each weld is A_{eff} = .125 × π × 65.81 in. = 25.8 in^2. The average shear stress in the weld is:

$$\sigma_w = \frac{W}{A_{eff}} = \frac{14{,}200\ \text{lb}}{25.8\ \text{in}^2} = 550\ \text{psi}$$

The allowable stress on the weld is 0.30 × the nominal tensile strength of the weld material [Ref.23, Table J2.5]. The nominal tensile strength of E308-XX filler material is 80,000 psi [Ref.28, SFA-5.4, Table 5]. However, for conservatism, S_y and S_u for the base metal, are used. The acceptability of the support ring weld is evaluated by comparing the allowable stress to the maximum calculated stress:

$$MS = \frac{0.3 \times 20{,}700\ \text{psi}}{550\ \text{psi}} - 1 = +\text{Large}$$

3.4.4.1.3 Canister Maximum Internal Pressure Analysis

The canister is structurally analyzed for a maximum internal pressure load using the finite element model and temperature distribution and restraints described in Section 3.4.4.1.1. A maximum internal pressure of 15 psig is applied as a surface load to the elements along the internal surface of the canister shell, bottom plate, and shield lid. This pressure bounds the calculated pressure of 7.1 psig that occurs in the smallest canister, PWR Class 1, under normal conditions. The PWR Class 1 canister internal pressure bounds the internal pressures of the other four canister configurations because it has the highest quantity of fission-gas-to-volume ratio.

The resulting maximum canister stresses for maximum internal pressure load are summarized in Table 3.4.4.1-9 and Table 3.4.4.1-10 for primary membrane and primary membrane plus primary bending stresses, respectively. The sectional stresses at 16 axial locations are obtained for each angular division of the model (a total of 19 angular locations for each axial location). The locations of the stress sections are shown in Figure 3.4.4.1-4.

3.4.4.1.4 Canister Handling Analysis

The canister is structurally analyzed for handling loads using the finite element model and conditions described in Section 3.4.4.1.1. Normal handling is simulated by restraining the model at nodes on the structural lid simulating three lift points and applying a 1.1g acceleration, which includes a 10% dynamic load factor, to the model in the axial direction. The canister is lifted at six points; however, a three-point lifting configuration is conservatively used in the handling analysis. Since the model represents a one-half section of the canister, the three-point lift is simulated by restraining two nodes 120° apart (one node at the symmetry plane and a second node 120° from the first) along the bolt diameter at the top of the structural lid in the axial direction. Additionally, the nodes along the centerline of the lids and bottom plate are restrained in the radial direction, and the nodes along the symmetry face are restrained in the direction normal to the symmetry plane.

The maximum stresses occur for the BWR class 5 canister handling, which is the heaviest configuration. Thus, the BWR class 5 canister analysis is the bounding condition for handling loads.

The resulting maximum stresses in the canister are summarized in Table 3.4.4.1-4 and Table 3.4.4.1-5 for primary membrane and primary membrane plus primary bending stresses, respectively. The sectional stresses at 16 axial locations are obtained for each angular division of the model (a total of 19 angular locations for each axial location). The locations of the stress sections are shown in Figure 3.4.4.1-4.

3.4.4.1.5 Canister Load Combinations

The canister is structurally analyzed for combined thermal, dead, maximum internal pressure, and handling loads using the finite element model and the conditions described in Section 3.4.4.1.1. Loads are applied to the model as discussed in Sections 3.4.4.1.1 through 3.4.4.1.4. A maximum internal pressure of 15.0 psi is used in conjunction with a positive axial acceleration of 1.1g. Two nodes 120° apart (one node at the symmetry plane and a second node 120° from the first) are restrained along the bolt diameter at the top of the structural lid in the axial direction. Additionally, the nodes along the centerline of the lids and bottom plate are restrained in the radial direction, and the nodes along the symmetry face are restrained in the direction normal to the symmetry plane.

The resulting maximum stresses in the canister for combined loads are summarized in Table 3.4.4.1-6, Table 3.4.4.1-7, and Table 3.4.4.1-8, for primary membrane, primary membrane plus primary bending, and primary plus secondary stresses, respectively. The sectional stresses at 16 axial locations are obtained for each angular division of the model (a total of 19 angular locations for each axial location). The locations for the stress sections are shown in Figure 3.4.4.1-4.

As shown in Table 3.4.4.1-6 through Table 3.4.4.1-8, the canister maintains positive margins of safety for the combined load conditions.

3.4.4.1.6 Canister and Basket Fatigue Evaluation

The purpose of this section is to evaluate whether an analysis for cyclic service is required for the Universal Storage System components. The requirements for analysis for cyclic operation of components designed to ASME Code criteria are presented in ASME Section III, Subsection NB-3222.4 [5] for the canister and Subsection NG-3222.4 [6] for the fuel basket. Guidance for components designed to AISC standards is in the Manual of Steel Construction, Table A-K4.1 [23].

The maximum stress intensity and the margin of safety for the weldments are shown in Table 3.4.4.1-17. Note that the nodal stress intensity is conservatively used for the evaluation. The P_m stresses for the weldments for normal conditions are essentially zero since there are no loads in the plane of the weldments. The weldments satisfy the stress criteria in the ASME Code Section III, Subsection NG [6].

3.4.4.1.10 Fuel Tube Analysis

Under normal storage conditions, the fuel tubes, Figure 3.4.4.1-9 (PWR) and Figure 3.4.4.1-17 (BWR), support only their own weight. The fuel assemblies are supported by the canister bottom plate, not by the fuel tubes. Thermal stresses are considered to be negligible since the tubes are free to expand axially and radially. The handling load is taken as 10% of the dead load.

The weight of the fuel tube, with a load of 1.1g (to account for both the dead load and handling load) is carried by the tube cross-section. The cross sectional area of a PWR fuel tube is:

$$\text{Area} = (8.9\text{ in})^2 - (8.9\text{ in.} - 2 \times 0.048\text{ in.})^2 = 1.7\text{ in}^2$$

The bounding weight of the heaviest PWR fuel tube is about 200 pounds. Considering a g-load of 1.1, the maximum compressive and bearing stress in the fuel tube is about 129 psi (200 lb × 1.1 / 1.7 in^2). Limiting the compressive stress level in the tube to the material yield strength ensures the tube remains in position in storage conditions. The yield strength of Type 304 stainless steel is 17,300 psi at a conservatively high temperature of 750°F.

$$\text{MS} = 17{,}300/129 - 1 = +\text{Large}$$

The minimum cross-sectional area of a BWR fuel tube and oversized fuel tube is:

$$\text{Area} = (5.996\text{ in})^2 - (5.9969\text{ in.} - 2 \times 0.048\text{ in.})^2 = 1.14\text{ in}^2$$

The bounding weight of the heaviest BWR fuel tube and oversized fuel tube is about 100 pounds. Considering a g-load of 1.1, the maximum compressive and bearing stress in the fuel tube is about 96 psi (100 lb × 1.1 / 1.14 in.^{2}). Limiting the compressive stress level in the tube to the material yield strength ensures the tube remains in position in storage conditions. The yield strength of Type 304 stainless steel is 17,300 psi at a conservatively high temperature of 750°F.

Margin of Safety = 17,300/96 - 1 = +Large

Thus, the tubes are structurally adequate under normal storage and handing conditions.

3.4.4.1.11 Canister Closure Weld Evaluation

The closure weld for the canister is a 0.9-inch groove weld between the structural lid and the canister shell. The evaluation of this weld incorporates a 0.8 stress reduction factor in accordance with NRC Interim Staff Guidance (ISG) No. 15, Revision 0. The use of this factor is in accordance with ISG No. 15, since the strength of the weld material (E308) is greater than that of the base material (Type 304 or 304L stainless steel).

The stresses for the canister closure weld are evaluated using sectional stresses as permitted by Subsection NB of the ASME Code. The location of the section for the canister closure weld evaluation is shown in Figure 3.4.4.1-4 and corresponds to Section 13. The governing P_m, P_m+ P_b, and P + Q stress intensities for Section 13, and the associated allowables, are listed in Table 3.4.4.1-6, Table 3.4.4.1-7, and Table 3.4.4.1-8, respectively. The factored allowables, incorporating the 0.8 stress reduction factor, and the resulting controlling Margins of Safety are shown below.

This evaluation confirms that the canister closure weld is acceptable for normal operation conditions.

Stress Category	Analysis Stress Intensity (ksi)	0.8 × Allowable Stress (ksi)	Margin of Safety
P_m	1.77	13.36	6.5
$P_m + P_b$	2.47	20.04	8.1
P + Q	5.86	40.08	6.8

Critical Flaw Size for the Canister Closure Weld

The closure weld for the canister is comprised of multiple weld beads using a compatible weld material for Type 304L stainless steel. An allowable (critical) flaw evaluation has been performed to determine the critical flaw size in the weld region. The result of the flaw evaluation is used to define the minimum flaw size, which must be identifiable in the nondestructive examination of the weld. Due to the inherent toughness associated with Type 304L stainless steel, a limit load analysis is used in conjunction with a J-integral/tearing modulus approach.

The safety factor used in this evaluation is that defined in Section XI of the ASME Code.

The stress component used in the evaluation for the critical flaw size is the radial stress component in the weld region of the structural lid. For the normal operation condition, in accordance with ASME Code Section XI, a safety factor of 3 is required. For the purpose of identifying the stress for the flaw evaluation, the weld region corresponding to Section 13 in Figure 3.4.4.1-4 is considered. The radial stress corresponds to SX in Tables 3.4.4.1-1 through 3.4.4.1-10. The maximum reported radial tensile stress is 1.11 ksi.

To perform the flaw evaluation, a 10 ksi stress is conservatively used, resulting in a significantly larger actual safety factor than the required safety factor of 3. Using a 10 ksi stress as the basis for the evaluation of the structural lid weld, the critical flaw size is 0.52 inch for a flaw that extends 360 degrees around the circumference of the structural lid weld. Stress components for the circumferential (Z) and axial (Y) directions are also reported in Tables 3.4.4.1-1 through 3.4.4.1-10, which would be associated with flaws oriented in the radial or horizontal directions, respectively. As shown in Table 3.4.4.1-7 at Section No. 13 (the structural lid weld), the maximum tensile stress reported for these components (SY and SZ) is 1.8 ksi, which is also enveloped by the value of 10 ksi used in the critical flaw evaluation for stresses in the radial direction.

The 360-degree flaw employed for the circumferential direction is considered to be bounding with respect to any partial flaw in the weld, which could occur in the radial and horizontal directions. Therefore, using a minimum detectable flaw size of 0.375 inch is acceptable, since it is less than the very conservatively determined 0.52-inch critical flaw size.

The Type 304L stainless steel structural lid may be forged (SA-182 material), or fabricated from plate (SA-240 material). Since the forged material is required to have ultimate and yield strengths that are equal to, or greater than, the plate material, the critical flaw size determination is applicable to both materials.

Figure 3.4.4.1-1 Canister Composite Finite Element Model

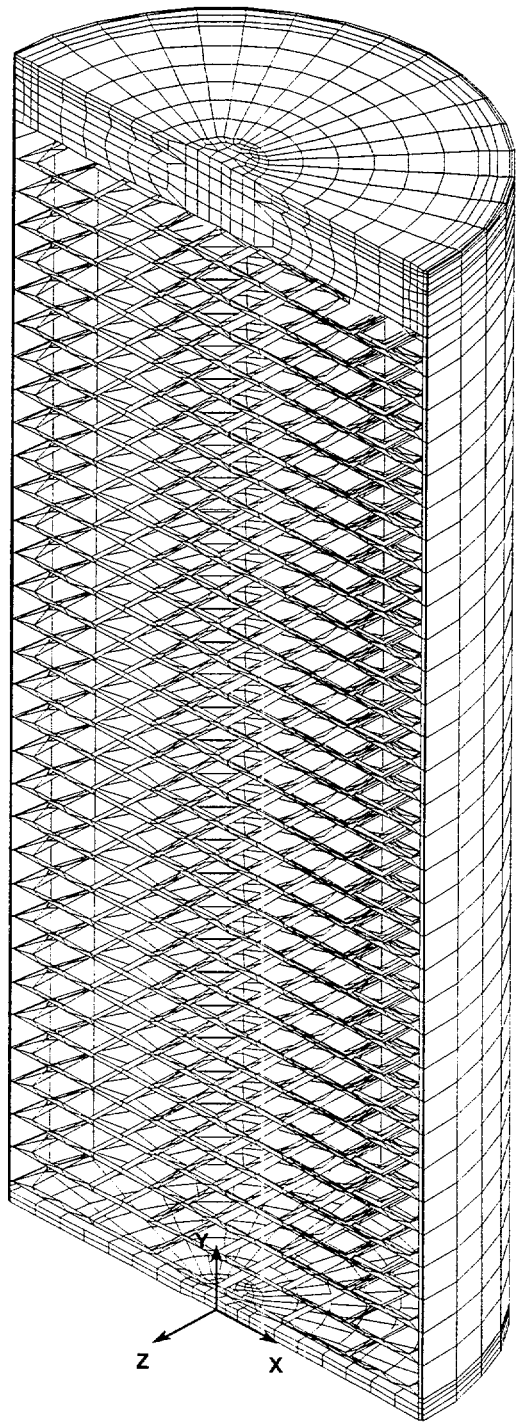

Table 3.4.4.1-1 Canister Secondary (Thermal) Stresses (ksi)

Section No.[1]	SX	SY	SZ	SXY	SYZ	SXZ	Stress Intensity
1	-0.29	0.06	1.17	-0.10	0.03	0.13	1.52
2	0.16	-2.23	0.48	-0.18	0.03	0.03	2.73
3	-0.28	3.08	1.43	0.07	-0.02	0.14	3.38
4	-0.01	0.01	0.00	0.00	0.01	0.00	0.03
5	0.00	0.12	-0.05	0.01	-0.01	0.00	0.17
6	0.00	0.15	-0.05	-0.01	0.01	0.00	0.20
7	0.00	0.01	0.00	0.00	-0.01	0.00	0.03
8	0.01	0.16	-0.13	0.00	-0.01	0.01	0.29
9	3.44	1.68	1.40	1.20	-0.14	-0.04	3.02
10	-2.06	3.97	0.46	-0.78	-0.09	-0.16	6.24
11	1.96	-8.57	-1.93	0.57	-0.07	-0.29	10.61
12	-6.20	-1.44	-2.54	-0.80	0.02	0.21	5.04
13	-3.39	1.40	-0.47	-0.57	-0.07	-0.23	4.94
14	-22.62	-13.47	-21.29	-0.06	-1.29	-0.70	9.70
15	-7.65	-6.44	-7.18	0.00	-0.47	-0.20	1.54
16	0.38	-0.08	0.39	0.00	0.00	0.00	0.47

1. See Figure 3.4.4.1-4 for definition of locations of stress sections.

Table 3.4.4.1-2 Canister Dead Weight Primary Membrane (P_m) Stresses (ksi), $P_{internal}$ = 0 psig

Section No.[1]	SX	SY	SZ	SXY	SYZ	SXZ	Stress Intensity
1	0.00	-0.05	-0.01	-0.01	0.00	0.00	0.05
2	0.01	-0.11	-0.02	-0.01	0.00	0.00	0.12
3	0.00	-0.13	-0.03	0.00	0.00	0.00	0.12
4	0.00	-0.12	0.00	0.00	0.00	0.00	0.12
5	0.00	-0.11	0.00	0.00	0.00	0.00	0.11
6	0.00	-0.10	0.00	0.00	0.00	0.00	0.10
7	0.00	-0.09	0.00	0.00	0.00	0.00	0.09
8	0.00	-0.06	0.00	0.00	0.00	0.00	0.06
9	-0.03	-0.04	-0.02	-0.01	0.01	-0.01	0.03
10	0.03	-0.02	-0.02	0.00	0.00	0.00	0.05
11	-0.03	0.01	-0.01	0.00	0.00	0.00	0.04
12	-0.01	0.03	0.01	0.00	-0.01	0.00	0.04
13	0.01	-0.04	-0.02	0.00	0.00	0.00	0.04
14	0.00	-0.02	0.00	0.00	0.00	0.00	0.02
15	0.01	0.00	0.01	0.00	0.00	0.00	0.01
16	0.00	0.00	0.00	0.00	0.00	0.00	0.00

1. See Figure 3.4.4.1-4 for definition of locations of stress sections.

Table 3.4.4.1-3 Canister Dead Weight Primary Membrane plus Bending ($P_m + P_b$) Stresses (ksi), $P_{internal} = 0$ psig

Section No.[1]	SX	SY	SZ	SXY	SYZ	SXZ	Stress Intensity
1	0.01	-0.06	-0.01	-0.01	0.00	0.00	0.07
2	0.01	-0.14	-0.03	0.00	0.00	0.00	0.15
3	0.00	-0.13	-0.03	0.00	0.00	0.00	0.13
4	0.00	-0.12	0.00	0.00	0.00	0.00	0.12
5	0.00	-0.11	0.00	0.00	0.00	0.00	0.11
6	0.00	-0.10	0.00	0.00	0.00	0.00	0.10
7	0.00	-0.09	0.00	0.00	0.00	0.00	0.09
8	0.01	-0.06	0.00	0.00	0.00	0.00	0.07
9	-0.05	-0.08	-0.01	0.00	0.01	0.00	0.08
10	-0.02	-0.10	-0.01	0.00	0.00	-0.03	0.12
11	-0.02	0.09	0.01	-0.01	0.00	0.00	0.11
12	0.05	0.05	0.01	0.02	0.00	0.00	0.06
13	0.04	-0.01	0.00	-0.01	0.00	0.00	0.06
14	0.00	-0.02	0.00	0.00	0.00	0.00	0.02
15	0.07	0.00	0.07	0.00	0.00	0.00	0.06
16	-0.03	0.00	-0.03	0.00	0.00	0.00	0.03

1. See Figure 3.4.4.1-4 for definition of locations of stress sections.

Table 3.4.4.1-4 Canister Normal Handling With No Internal Pressure Primary Membrane (P_m) Stresses, (ksi)

Section No.[1]	SX	SY	SZ	SXY	SYZ	SXZ	Stress Intensity
1	0.12	1.80	0.70	-0.26	0.01	0.05	1.76
2	1.17	-1.15	-1.68	-0.27	0.02	-0.22	2.92
3	-0.20	0.53	-2.62	0.48	-0.04	-0.22	3.42
4	0.00	0.51	0.01	0.00	0.00	0.00	0.51
5	0.01	0.55	0.00	0.00	0.00	0.00	0.55
6	0.01	0.62	-0.01	0.00	0.01	0.00	0.63
7	0.01	0.74	-0.01	0.00	0.01	0.00	0.75
8	0.02	1.14	-0.02	0.00	0.07	-0.01	1.17
9	0.00	1.54	0.30	0.02	0.15	0.03	1.56
10	-0.21	1.96	0.32	0.05	0.22	0.05	2.20
11	-0.53	1.06	0.84	-0.49	0.13	0.10	1.91
12	-0.10	2.35	0.55	0.17	0.12	0.09	2.49
13	0.26	-0.07	1.25	-0.59	0.04	0.18	1.82
14	0.30	-0.01	0.30	-0.02	-0.14	0.00	0.41
15	-0.03	0.00	-0.03	0.00	0.00	0.00	0.03
16	0.01	0.00	0.01	0.00	0.01	0.00	0.02

1. See Figure 3.4.4.1-4 for definition of locations of stress sections.

Table 3.4.4.1-5 Canister Normal Handling With No Internal Pressure Primary Membrane plus Bending ($P_m + P_b$) Stresses (ksi)

Section No.[1]	SX	SY	SZ	SXY	SYZ	SXZ	Stress Intensity
1	1.32	4.36	-0.05	-0.02	0.02	-0.07	4.42
2	0.57	-8.37	-3.98	-0.60	0.04	-0.38	9.05
3	-0.85	11.91	0.54	0.62	-0.04	0.08	12.82
4	0.00	0.50	-0.06	0.00	0.00	0.01	0.55
5	0.01	0.51	-0.14	0.00	0.01	-0.01	0.65
6	0.01	0.56	-0.19	0.00	0.01	-0.02	0.75
7	0.01	0.67	-0.21	0.00	0.01	-0.02	0.88
8	0.03	1.10	-0.14	0.00	0.06	-0.02	1.24
9	-0.11	1.49	0.20	-0.07	0.21	0.00	1.65
10	-0.31	3.50	0.79	0.21	0.14	0.13	3.85
11	-0.76	1.69	0.98	-0.98	0.21	0.11	3.17
12	-0.34	3.20	0.71	0.20	0.13	0.12	3.58
13	1.11	-0.68	1.79	-0.23	-0.07	0.30	2.61
14	6.65	0.18	6.66	-0.03	-0.12	0.00	6.48
15	-0.18	0.00	-0.18	0.00	0.00	0.00	0.18
16	0.80	0.02	0.79	0.00	0.01	-0.01	0.78

1. See Figure 3.4.4.1-4 for definition of locations of stress sections.

Table 3.4.4.1-6 Summary of Canister Normal Handling plus Normal Internal Pressure Primary Membrane (P_m) Stresses (ksi)

Section No.[1]	SX	SY	SZ	SXY	SYZ	SXZ	Stress Intensity	Stress Allowable[2]	Margin of Safety
1	0.22	3.26	1.27	-0.47	0.03	0.09	3.19	16.70	4.23
2	2.15	-2.10	-2.90	-0.48	0.04	-0.38	5.16	16.70	2.24
3	-0.38	0.95	-4.49	0.90	-0.08	-0.38	5.94	16.70	1.81
4	0.00	0.90	0.80	0.00	0.00	0.07	0.91	16.14	16.72
5	0.00	0.94	0.78	0.00	0.00	0.07	0.94	14.92	14.81
6	0.01	1.01	0.78	0.00	0.01	0.07	1.01	14.84	13.68
7	0.01	1.13	0.78	0.00	0.01	0.07	1.13	15.97	13.20
8	0.02	1.52	0.37	-0.01	0.07	0.03	1.51	16.70	10.08
9	0.05	1.80	0.51	0.06	0.15	0.04	1.77	16.70	8.42
10	-0.34	2.10	0.45	0.02	0.22	0.08	2.48	16.70	5.73
11	-0.36	1.01	0.90	-0.48	0.13	0.09	1.72	16.70	8.70
12	-0.16	2.05	0.57	0.10	0.12	0.10	2.24	16.70	6.45
13	0.23	0.09	1.31	-0.56	0.03	0.19	1.77	16.70	8.45
14	0.54	-0.02	0.54	-0.04	-0.25	0.00	0.75	16.70	21.28
15	-0.05	-0.01	-0.05	0.00	0.00	0.00	0.05	16.70	361.65
16	0.04	0.00	0.04	0.00	0.01	0.00	0.04	16.70	380.80

1. See Figure 3.4.4.1-4 for definition of locations of stress sections.
2. ASME Code Service Level A is used for material allowable stresses.

Table 3.4.4.1-7 Summary of Canister Normal Handling, Plus Normal Pressure Primary Membrane plus Bending ($P_m + P_b$) Stresses (ksi)

Section No.[1]	SX	SY	SZ	SXY	SYZ	SXZ	Stress Intensity	Stress Allowable[2]	Margin of Safety
1	2.44	7.90	0.07	-0.04	0.04	-0.12	7.83	25.05	2.20
2	1.04	-15.17	-7.06	-1.08	0.07	-0.67	16.41	25.05	0.53
3	-1.56	21.42	1.19	1.14	-0.08	0.17	23.10	25.05	0.08
4	0.00	0.95	0.86	0.00	0.00	0.08	0.96	24.22	24.26
5	0.01	0.98	0.90	0.00	0.00	0.08	0.98	22.38	21.82
6	0.01	1.07	0.95	0.00	0.01	0.08	1.07	22.27	19.87
7	0.01	1.20	0.97	0.00	0.01	0.09	1.20	23.96	19.03
8	0.03	1.54	0.28	-0.01	0.06	0.02	1.51	25.05	15.58
9	-0.06	2.08	0.51	0.02	0.20	0.02	2.17	25.05	10.53
10	-0.47	2.95	0.72	0.11	0.15	0.13	3.45	25.05	6.26
11	-0.56	1.94	1.14	-0.97	0.21	0.11	3.20	25.05	6.82
12	-0.52	2.67	0.63	0.10	0.14	0.13	3.22	25.05	6.79
13	0.88	-0.59	1.75	-0.20	-0.07	0.31	2.47	25.05	9.13
14	11.75	0.33	11.75	-0.06	-0.21	0.00	11.44	25.05	1.19
15	-0.25	-0.02	-0.25	0.00	0.00	0.00	0.24	25.05	103.94
16	0.81	0.02	0.80	0.00	0.01	-0.01	0.80	25.05	30.51

1. See Figure 3.4.4.1-4 for definition of locations of stress sections.
2. ASME Code Service Level A is used for material allowable stresses.

Table 3.4.4.1-8 Summary of Maximum Canister Normal Handling, plus Normal Pressure, plus Secondary (P + Q) Stresses (ksi)

Section No.[1]	SX	SY	SZ	SXY	SYZ	SXZ	Stress Intensity	Stress Allowable[2]	Margin of Safety
1	3.73	11.31	2.84	0.12	0.05	0.02	8.47	50.10	4.91
2	1.25	-18.35	-6.84	-1.23	0.11	-0.67	19.81	50.10	1.53
3	-1.83	25.12	2.83	1.23	-0.10	0.33	27.08	50.10	0.85
4	0.00	0.97	0.86	0.00	0.01	0.08	0.98	48.43	48.53
5	-0.01	1.04	0.88	0.01	-0.02	-0.08	1.05	44.76	41.43
6	0.00	1.10	0.55	0.01	0.02	0.05	1.10	44.53	39.52
7	0.01	1.21	0.97	0.00	0.00	0.09	1.21	47.91	38.53
8	0.03	1.67	0.33	-0.01	0.07	0.03	1.65	50.10	29.38
9	1.30	3.28	1.07	1.35	0.06	0.00	3.35	50.10	13.97
10	-6.74	1.20	-1.92	-0.70	0.16	0.34	8.09	50.10	5.19
11	2.32	-10.26	-2.29	-0.69	-0.12	0.33	12.67	50.10	2.95
12	-6.74	1.20	-1.92	-0.70	0.16	0.34	8.09	50.10	5.19
13	-4.01	1.66	-0.41	-0.67	-0.08	-0.29	5.86	50.10	7.56
14	-13.20	-0.14	-12.97	-0.02	0.05	-0.20	13.18	50.10	2.80
15	-7.99	-6.46	-7.52	0.01	-0.46	-0.20	1.80	50.10	26.88
16	0.03	-0.50	0.06	0.00	0.05	-0.02	0.59	50.10	84.54

1. See Figure 3.4.4.1-4 for definition of locations of stress sections.
2. ASME Code Service Level A is used for material allowable stresses.

Table 3.4.4.1-9 Canister Normal Internal Pressure Primary Membrane (P_m) Stresses (ksi)

Section No.[1]	SX	SY	SZ	SXY	SYZ	SXZ	Stress Intensity
1	0.10	1.46	0.57	-0.21	0.02	0.04	1.43
2	0.98	-0.95	-1.22	-0.21	0.02	-0.16	2.24
3	-0.18	0.42	-1.86	0.42	-0.04	-0.16	2.52
4	0.00	0.39	0.79	0.00	0.00	0.07	0.80
5	0.00	0.39	0.78	0.00	0.00	0.07	0.80
6	0.00	0.39	0.78	0.00	0.00	0.07	0.80
7	0.00	0.39	0.78	0.00	0.00	0.07	0.80
8	0.00	0.39	0.40	-0.01	0.00	0.04	0.41
9	0.04	0.29	0.20	0.03	0.00	0.02	0.26
10	-0.13	0.19	0.13	-0.04	0.00	0.02	0.34
11	0.14	-0.04	0.12	0.01	-0.01	-0.04	0.21
12	0.03	-0.19	-0.07	-0.01	0.06	0.02	0.25
13	-0.02	0.19	0.11	0.01	-0.01	0.01	0.22
14	0.25	-0.01	0.25	-0.02	-0.10	0.00	0.34
15	-0.03	-0.01	-0.03	0.00	0.00	0.00	0.02
16	0.02	0.00	0.02	0.00	0.00	0.00	0.03

1. See Figure 3.4.4.1-4 for definition of locations of stress sections.

Table 3.4.4.1-10 Canister Normal Internal Pressure Primary Membrane plus Bending ($P_m + P_b$) Stresses (ksi)

Section No.[1]	SX	SY	SZ	SXY	SYZ	SXZ	Stress Intensity
1	1.12	3.53	0.12	-0.01	0.02	-0.05	3.41
2	0.47	-6.80	-3.08	-0.48	0.03	-0.29	7.36
3	-0.71	9.51	0.66	0.53	-0.04	0.09	10.28
4	-0.01	0.38	0.80	0.00	0.00	0.07	0.81
5	0.00	0.39	0.79	0.00	0.00	0.07	0.81
6	0.00	0.39	0.79	0.00	0.00	0.07	0.81
7	-0.01	0.39	0.79	0.00	0.00	0.07	0.81
8	0.00	0.44	0.42	-0.01	0.00	0.04	0.44
9	0.04	0.59	0.29	0.08	-0.01	0.02	0.58
10	-0.10	0.74	0.30	0.02	0.00	0.03	0.85
11	-0.04	-0.45	0.14	0.00	-0.02	0.00	0.59
12	-0.05	-0.35	-0.18	-0.02	0.10	0.02	0.36
13	-0.22	0.08	0.03	0.03	-0.01	0.02	0.31
14	5.09	0.13	5.09	-0.02	-0.09	0.00	4.97
15	-0.33	-0.02	-0.33	0.00	0.00	0.00	0.32
16	0.17	0.00	0.17	0.00	0.00	0.00	0.17

1. See Figure 3.4.4.1-4 for definition of locations of stress sections.

Chapter 4

Table of Contents

4.0 THERMAL EVALUATION 4.1-1

4.1 Discussion 4.1-1

4.2 Summary of Thermal Properties of Materials 4.2-1

4.3 Technical Specifications for Components 4.3-1

4.4 Thermal Evaluation for Normal Conditions of Storage 4.4-1

4.4.1 Thermal Models 4.4.1-1

4.4.1.1 Two-Dimensional Axisymmetric Air Flow and Concrete Cask Models 4.4.1-3

4.4.1.2 Three-Dimensional Canister Models 4.4.1-13

4.4.1.3 Three-Dimensional Transfer Cask and Canister Models 4.4.1-26

4.4.1.4 Three-Dimensional Periodic Canister Internal Models 4.4.1-30

4.4.1.5 Two-Dimensional Fuel Models 4.4.1-34

4.4.1.6 Two-Dimensional Fuel Tube Models 4.4.1-37

4.4.1.7 Two-Dimensional Forced Air Flow Model for Transfer Cask Cooling 4.4.1-43

4.4.2 Test Model 4.4.2-1

4.4.3 Maximum Temperatures for PWR and BWR Fuel 4.4.3-1

4.4.3.1 Maximum Temperatures at Reduced Total Heat Loads 4.4.3-2

4.4.3.2 Preferential Fuel Loading 4.4.3-5

4.4.4 Minimum Temperatures 4.4.4-1

4.4.5 Maximum Internal Pressures 4.4.5-1

4.4.5.1 Maximum Internal Pressure for PWR Fuel Canister 4.4.5-1

4.4.5.2 Maximum Internal Pressure for BWR Fuel Canister 4.4.5-3

4.4.6 Maximum Thermal Stresses 4.4.6-1

4.4.7 Maximum Allowable Cladding Temperature and Canister Heat Load 4.4.7-1

4.4.7.1 Maximum Allowable Cladding Temperature 4.4.7-2

4.4.7.2 Maximum Allowable Canister Heat Load 4.4.7-5

4.4.8 Evaluation of System Performance for Normal Conditions of Storage 4.4.8-1

Table of Contents (Continued)

4.5 Thermal Evaluation for Site Specific Spent Fuel 4.5-1
4.5.1 Maine Yankee Site Specific Spent Fuel 4.5-1
4.5.1.1 Thermal Evaluation for Maine Yankee Site Specific Spent Fuel 4.5-3
4.5.1.2 Maximum Allowable Heat Loads for Maine Yankee Site Specific Spent Fuel 4.5-17

4.6 References 4.6-1

List of Figures

Figure 4.3-1 PWR Heat Transfer Disk Model for Normal Handling Condition 4.3-2
Figure 4.3-2 BWR Heat Transfer Disk Model for Normal Handling Condition 4.3-3
Figure 4.4.1.1-1 Two-Dimensional Axisymmetric Air Flow and Concrete Cask Model: PWR 4.4.1-9
Figure 4.4.1.1-2 Two-Dimensional Axisymmetric Air Flow and Concrete Cask Finite Element Model: PWR 4.4.1-10
Figure 4.4.1.1-3 Axial Power Distribution for PWR Fuel 4.4.1-11
Figure 4.4.1.1-4 Axial Power Distribution for BWR Fuel 4.4.1-12
Figure 4.4.1.2-1 Three-Dimensional Canister Model for PWR Fuel 4.4.1-18
Figure 4.4.1.2-2 Three-Dimensional Canister Model for PWR Fuel - Cross Section 4.4.1-19
Figure 4.4.1.2-3 Three-Dimensional Canister Model for BWR Fuel 4.4.1-20
Figure 4.4.1.2-4 Three-Dimensional Canister Model for BWR Fuel - Cross Section 4.4.1-21
Figure 4.4.1.3-1 Three-Dimensional Transfer Cask and Canister Model - PWR 4.4.1-28
Figure 4.4.1.3-2 Three-Dimensional Transfer Cask and CanisterModel – BWR 4.4.1-29
Figure 4.4.1.4-1 Three-Dimensional Periodic Canister Internal Model - PWR 4.4.1-32
Figure 4.4.1.4-2 Three-Dimensional Periodic Canister Internal Model - BWR 4.4.1-33
Figure 4.4.1.5-1 Two-Dimensional PWR (17 × 17) Fuel Model 4.4.1-36
Figure 4.4.1.6-1 Two-Dimensional Fuel Tube Model: PWR Fuel 4.4.1-40
Figure 4.4.1.6-2 Two-Dimensional Fuel Tube Model: BWR Fuel Tube with Neutron Absorber 4.4.1-41
Figure 4.4.1.6-3 Two-Dimensional Fuel Tube Model: BWR Fuel Tube without Neutron Absorber 4.4.1-42
Figure 4.4.1.7-1 Two-Dimensional Axisymmetric Finite Element Model for Transfer Cask Forced Air Cooling 4.4.1-44
Figure 4.4.1.7-2 Two-Dimensional Axisymmetric Outlet Air Flow Model for Transfer Cask Cooling 4.4.1-45

List of Figures (continued)

Figure 4.4.1.7-3 Two-Dimensional Axisymmetric Inlet Air Flow Model for Transfer Cask Cooling 4.4.1-46
Figure 4.4.1.7-4 Non-Uniform Heat Load from Canister Contents 4.4.1-47
Figure 4.4.1.7-5 Maximum Canister Temperature Versus Air Volume Flow Rate 4.4.1-48
Figure 4.4.3-1 Temperature Distribution (°F) for the Normal Storage Condition: PWR Fuel 4.4.3-8
Figure 4.4.3-2 Air Flow Pattern in the Concrete Cask in the Normal Storage Condition: PWR Fuel 4.4.3-9
Figure 4.4.3-3 Air Temperature (°F) Distribution in the Concrete Cask During the Normal Storage Condition: PWR Fuel 4.4.3-10
Figure 4.4.3-4 Concrete Temperature (°F) Distribution During the Normal Storage Condition: PWR Fuel 4.4.3-11
Figure 4.4.3-5 History of Maximum Component Temperature (°F) for Transfer Conditions for PWR Fuel with Design Basis 23 kW Uniformly Distributed Heat Load 4.4.3-12
Figure 4.4.3-6 History of Maximum Component Temperature (°F) for Transfer Conditions for BWR Fuel with Design Basis 23 kW Uniformly Distributed Heat Load 4.4.3-13
Figure 4.4.3-7 Basket Location for the Thermal Analysis of PWR Reduced Heat Load Cases 4.4.3-14
Figure 4.4.3-8 BWR Fuel Basket Location Numbers 4.4.3-15
Figure 4.4.3-9 PWR Basket Fuel Loading Positions 4.4.3-16
Figure 4.4.3-10 BWR Basket Fuel Loading Positions 4.4.3-17
Figure 4.4.7-1 PWR Fuel Dry Storage Temperature versus Cladding Stress 4.4.7-6
Figure 4.4.7-2 BWR Fuel Dry Storage Temperature versus Cladding Stress 4.4.7-6
Figure 4.4.7-3 PWR and BWR Fuel Cladding Dry Storage Temperature versus Basket Heat Load 4.4.7-7
Figure 4.5.1.1-1 Quarter Symmetry Model for Maine Yankee Consolidated Fuel 4.5-12
Figure 4.5.1.1-2 Maine Yankee Three-Dimensional Periodic Canister Internal Model 4.5-13

List of Figures (continued)

Figure 4.5.1.1-3 Evaluated Locations for the Maine Yankee Consolidated Fuel Lattice in the PWR Fuel Basket 4.5-14
Figure 4.5.1.1-4 Active Fuel Region in the Three-Dimensional Canister Model 4.5-15
Figure 4.5.1.1-5 Fuel Debris and Damaged Fuel Regions in the Three-Dimensional Canister Model 4.5-16
Figure 4.5.1.2-1 Canister Basket Preferential Loading Plan 4.5-22
Figure 4.5.1.2-2 Maximum Allowable Cladding Temperature at Initial Storage versus Cladding Stress (50,000 MWD/MTU) 4.5-23

List of Tables

Table 4.1-1 Summary of Thermal Design Conditions for Storage 4.1-4
Table 4.1-2 Summary of Thermal Design Conditions for Transfer 4.1-5
Table 4.1-3 Maximum Allowable Material Temperatures 4.1-6
Table 4.1-4 Summary of Thermal Evaluation Results for the Universal Storage System: PWR Fuel 4.1-7
Table 4.1-5 Summary of Thermal Evaluation Results for the Universal Storage System: BWR Fuel 4.1-8
Table 4.2-1 Thermal Properties of Solid Neutron Shield (NS-4-FR and NS-3) 4.2-2
Table 4.2-2 Thermal Properties of Stainless Steel 4.2-2
Table 4.2-3 Thermal Properties of Carbon Steel 4.2-3
Table 4.2-4 Thermal Properties of Chemical Copper Lead 4.2-3
Table 4.2-5 Thermal Properties of Type 6061-T651 Aluminum Alloy 4.2-3
Table 4.2-6 Thermal Properties of Helium 4.2-4
Table 4.2-7 Thermal Properties of Dry Air 4.2-4
Table 4.2-8 Thermal Properties of Zircaloy and Zircaloy-4 Cladding 4.2-5
Table 4.2-9 Thermal Properties of Fuel (UO_2) 4.2-5
Table 4.2-10 Thermal Properties of BORAL Composite Sheet 4.2-6
Table 4.2-11 Thermal Properties of Concrete 4.2-6
Table 4.2-12 Thermal Properties of Water 4.2-7
Table 4.2-13 Thermal Properties of METAMIC 4.2-7
Table 4.4.1.2-1 Effective Thermal Conductivities for PWR Fuel Assemblies 4.4.1-22
Table 4.4.1.2-2 Effective Thermal Conductivities for BWR Fuel Assemblies 4.4.1-23
Table 4.4.1.2-3 Effective Thermal Conductivities for PWR Fuel Tubes 4.4.1-24
Table 4.4.1.2-4 Effective Thermal Conductivities for BWR Fuel Tubes 4.4.1-25
Table 4.4.3-1 Maximum Component Temperatures for the Normal Storage Condition - PWR 4.4.3-18
Table 4.4.3-2 Maximum Component Temperatures for the Normal Storage Condition - BWR 4.4.3-19

List of Tables (continued)

Table 4.4.3-3 Maximum Component Temperatures for the Transfer Condition – PWR Fuel with Design Basis 23 kW Uniformly Distributed Heat Load 4.4.3-20
Table 4.4.3-4 Maximum Component Temperatures for the Transfer Condition – BWR Fuel with Design Basis 23 kW Uniformly Distributed Heat Load 4.4.3-20
Table 4.4.3-5 Maximum Limiting Component Temperatures in Transient Operations for the Reduced Heat Load Cases for PWR Fuel 4.4.3-21
Table 4.4.3-6 Maximum Limiting Component Temperatures in Transient Operations for the Reduced Heat Load Cases for PWR Fuel after In-Pool Cooling 4.4.3-22
Table 4.4.3-7 Maximum Limiting Component Temperatures in Transient Operations for the Reduced Heat Load Cases for PWR Fuel after Forced-Air Cooling 4.4.3-22
Table 4.4.3-8 Maximum Limiting Component Temperatures in Transient Operations for BWR Fuel 4.4.3-23
Table 4.4.3-9 Maximum Limiting Component Temperatures in Transient Operations after Vacuum for BWR Fuel after In-Pool Cooling 4.4.3-24
Table 4.4.3-10 Maximum Limiting Component Temperatures in Transient Operations after Vacuum for BWR Fuel after Forced-Air Cooling. 4.4.3-24
Table 4.4.3-11 Maximum Limiting Component Temperatures in Transient Operations after Helium for BWR Fuel after In-Pool Cooling..... 4.4.3-25
Table 4.4.3-12 Maximum Limiting Component Temperatures in Transient Operations after Helium for BWR Fuel after Forced-Air Cooling.. 4.4.3-25
Table 4.4.3-13 Temperature Summary for PWR Fuel Preferential Loading 4.4.3-26
Table 4.4.3-14 Temperature Summary for BWR Fuel Preferential Loading 4.4.3-27
Table 4.4.5-1 PWR Per Assembly Fuel Generated Gas Inventory..... 4.4.5-4
Table 4.4.5-2 PWR Canister Free Volume (No Fuel or Inserts) 4.4.5-4
Table 4.4.5-3 PWR Maximum Normal Condition Pressure Summary..... 4.4.5-4
Table 4.4.5-4 BWR Per Assembly Fuel Generated Gas Inventory 4.4.5-5
Table 4.4.5-5 BWR Canister Free Volume (No Fuel or Inserts)..... 4.4.5-5
Table 4.4.5-6 BWR Maximum Normal Condition Pressure Summary 4.4.5-5

List of Tables (continued)

Table 4.4.7-1 PWR Cladding Stress Level Comparison Chart 4.4.7-8
Table 4.4.7-2 BWR Cladding Stress Level Comparison Chart 4.4.7-8
Table 4.4.7-3 Cladding Stress as a Function of Fuel Assembly Average Burnup and Temperature 4.4.7-9
Table 4.4.7-4 Maximum Allowable Initial Storage Temperature (°C) As a Function of Initial Cladding Stress and Initial Cool Time 4.4.7-9
Table 4.4.7-5 Maximum Allowable Cladding Temperature for PWR and BWR Fuel Assemblies 4.4.7-10
Table 4.4.7-6 Cladding Maximum Temperature as a Function of Basket Heat Load (PWR) 4.4.7-10
Table 4.4.7-7 Cladding Maximum Temperature as a Function of Basket Heat Load (BWR) 4.4.7-10
Table 4.4.7-8 Maximum Allowable Decay Heat for UMS® PWR and BWR Systems 4.4.7-11
Table 4.4.7-9 Temperature Bias Applied to Maximum Allowable Decay Heats... 4.4.7-11
Table 4.5.1.2-1 Cladding Stress for 50,000 MWD/MTU Burnup Fuel 4.5-24
Table 4.5.1.2-2 Maximum Allowable Cladding Temperature for 50,000 MWD/MTU Burnup Fuel 4.5-24
Table 4.5.1.2-3 Maximum Allowable Canister Heat Load for 50,000 MWD/MTU Burnup Fuel 4.5-24
Table 4.5.1.2-4 Heat Load for Interior Assemblies for the Configuration with 0.958 kW Assemblies in Peripheral Locations 4.5-25
Table 4.5.1.2-5 Heat Load Limit for Interior Assemblies for the Configuration with 1.05 kW Assemblies in Peripheral Locations 4.5-25

Table 4.4.1.2-4 Effective Thermal Conductivities for BWR Fuel Tubes

	Conductivity	**Temperature (°F)**			
Tubes with Neutron Absorber	**(Btu/hr-in-°F)**	**200**	**400**	**600**	**800**
In CS disk region					
	Kxx	0.017	0.022	0.027	0.032
	Kyy	1.665	1.759	1.815	1.830
	Kzz	1.665	1.759	1.815	1.830
In AL disk region					
	Kxx	0.017	0.022	0.027	0.033
	Kyy	1.665	1.759	1.815	1.830
	Kzz	1.665	1.759	1.815	1.830
Tubes without Neutron Absorber		**200**	**400**	**600**	**800**
In CS disk region					
	Kxx	0.012	0.015	0.018	0.021
	Kyy	0.191	0.202	0.218	0.236
	Kzz	0.191	0.202	0.218	0.236
In AL disk region					
	Kxx	0.012	0.015	0.019	0.023
	Kyy	0.191	0.202	0.218	0.236
	Kzz	0.191	0.202	0.218	0.236

Note: Kxx is in the direction across the thickness of fuel tube wall.
Kyy is in the direction parallel to fuel tube wall.
Kzz is in the canister axial direction.

4.4.1.3 Three-Dimensional Transfer Cask and Canister Models

The three-dimensional half-symmetry transfer cask model is a representation of the canister and transfer cask assembly. The model is used to perform a transient thermal analysis to determine the maximum water temperature in the canister for the period beginning immediately after removing the transfer cask and canister from the spent fuel pool. The model is also used to calculate the maximum temperature of the fuel cladding, the transfer cask and canister components during the vacuum drying condition and after the canister is back-filled with helium. The transfer cask is evaluated separately for PWR or BWR fuel using two models. For each fuel type, the class of fuel with the shortest associated canister and transfer cask is modeled in order to maximize the contents heat generation rate per unit volume and minimize the heat rejection from the external surfaces. The models for PWR and BWR fuel are shown in Figures 4.4.1.3-1 and 4.4.1.3-2, respectively. ANSYS SOLID70 three-dimensional conduction elements, LINK31 (PWR model) and MATRIX50 (BWR model) radiation elements are used. The model includes the transfer cask and the canister and its internals. The details of the canister and contents are modeled using the same methodology as that presented in Section 4.4.1.2 (Three-Dimensional Canister Models). Effective thermal properties for the fuel regions and the fuel tube regions are established using the fuel models and fuel tube models presented in Sections 4.4.1.5 and 4.4.1.6 respectively. The effective specific heat and density are calculated on the basis of material mass and volume ratio, respectively.

Radiation across the gaps was represented by the LINK31 elements or the MATRIX50 elements, which used the gray body emissivities for stainless and carbon steels. Convection is considered at the top of the canister lid, the exterior surfaces of the transfer cask, as well as at the annulus between the canister and the inner surface of the transfer cask. The combination of radiation and convection at the transfer cask exterior vertical surfaces and canister lid top surface is taken into account in the model using the same method described in Section 4.4.1.2 for the three-dimensional canister models. The bottom of the transfer cask is modeled as being in contact with the concrete floor. Volumetric heat generation (Btu/hr-in^3) is applied to the active fuel region based on a total heat load of 23 kW for both PWR and BWR fuel. The model considers the active fuel length of 144 inches and an axial power distribution, as shown in Figure 4.4.1.1-3 and 4.4.1.1-4 for PWR and BWR fuel, respectively.

An initial temperature of 100°F is considered in the model on the basis of typical maximum average water temperature in the spent fuel pool. For the design basis heat loads, the water inside the canister is drained within 17 hours and the canister is back-filled with helium immediately after the vacuum drying and transferred to the concrete cask. The design basis heat load transient analysis is performed for 17 hours with the water inside the canister, 32 hours (PWR) and 25 hours (BWR) for the vacuum-dried condition, and 10 hours (PWR) and 16 hours (BWR) for the helium condition, followed by a steady state analysis (in helium condition). The 10 hour duration for PWR fuel in the helium condition is used to obtain the peak (maximum) basket temperature after the helium backfill. Different time durations are used for the transient analyses for the reduced heat load cases, as specified in Section 4.4.3.1. The temperature history of the fuel cladding and the basket components, as well as the transfer cask components, is determined and compared with the short-term temperature limits presented in Table 4.1-3.

Figure 4.4.1.3-1 Three-Dimensional Transfer Cask and Canister Model - PWR

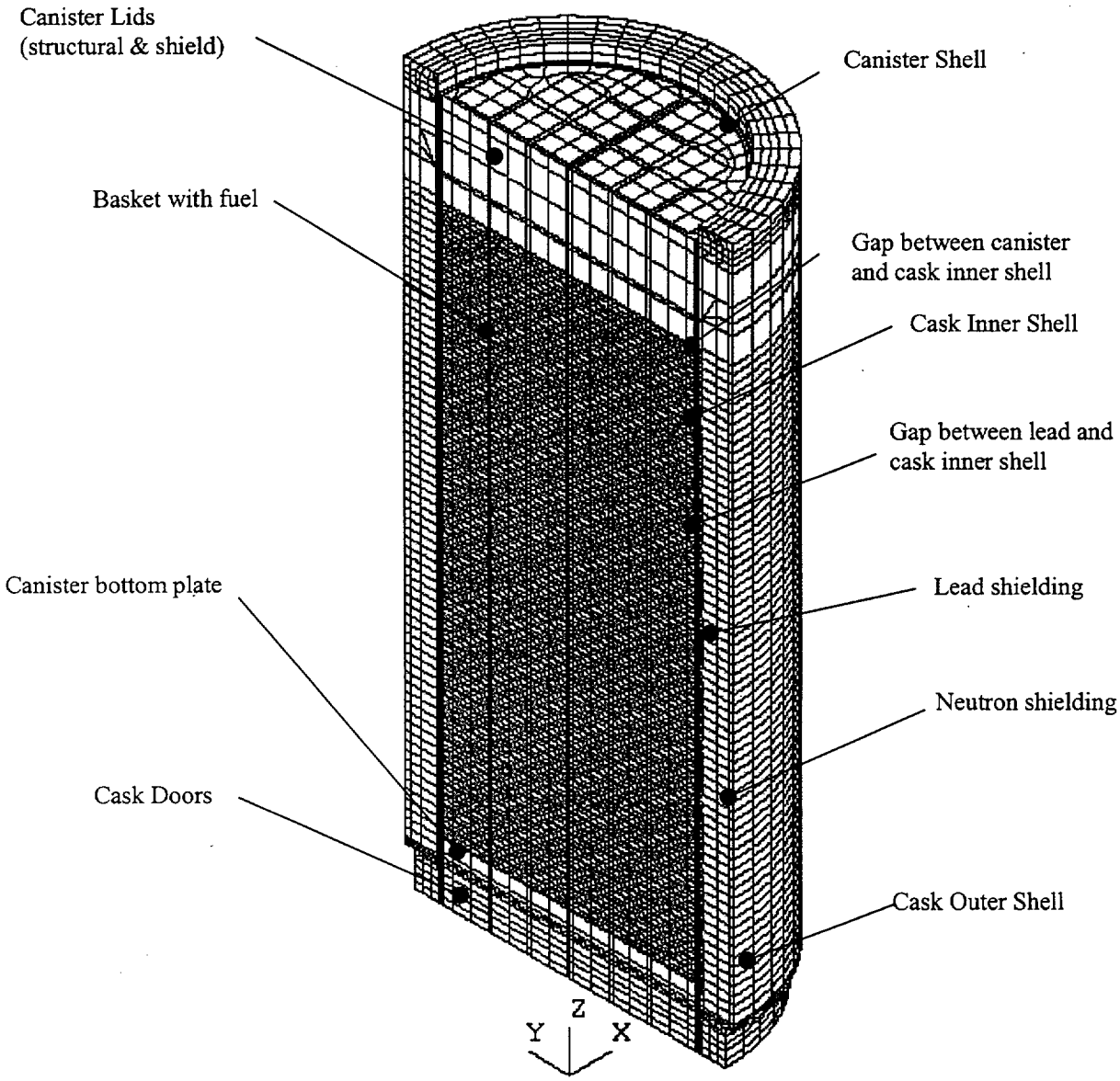

Figure 4.4.1.3-2 Three-Dimensional Transfer Cask and Canister Model - BWR

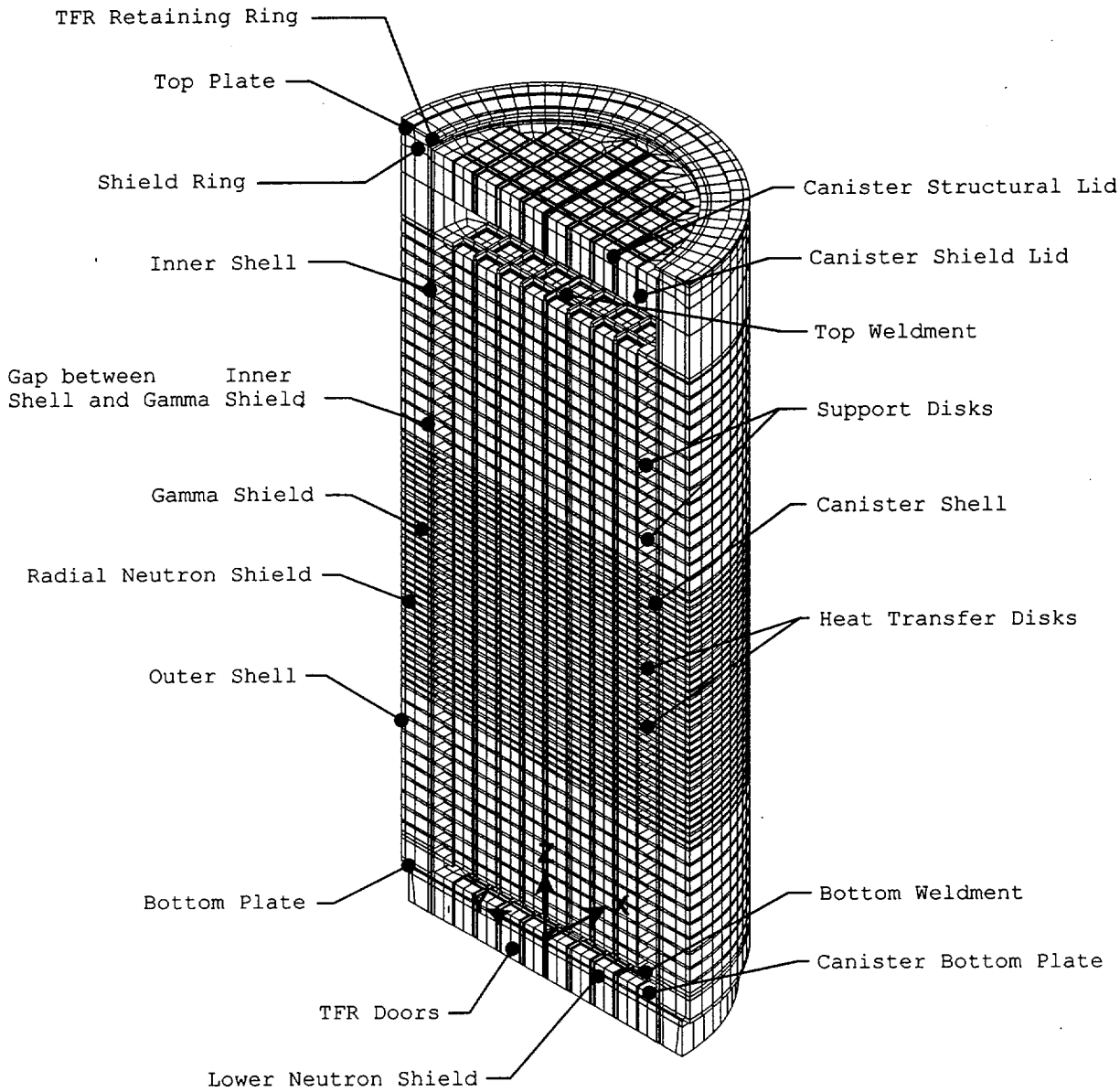

Canister and transfer cask media (water/helium) not shown for clarity.

4.4.1.4 Three-Dimensional Periodic Canister Internal Models

The three-dimensional periodic canister internal model consists of a periodic section of the canister internals. A total of three models are used: one for PWR fuel and two for BWR fuel. For the PWR canister, the model contains one support disk with two heat transfer disks (half thickness) on its top and bottom, the fuel assemblies, the fuel tubes and the media in the canister, as shown in Figure 4.4.1.4-1. The first BWR model, shown in Figure 4.4.1.4-2, represents the central region of the BWR canister, which contains one heat transfer disk with two support disks (half thickness) on its top and bottom, the fuel assemblies, the fuel tubes and the media in the canister. The second BWR model (not shown), for the region without heat transfer disks, contains two support disks (half thickness), the fuel assemblies, the fuel tubes and the media in the canister. The difference between the two BWR models is that the second model does not have the heat transfer disk. The purpose of these models is to determine the effective thermal conductivity of the canister internals in the canister radial direction. The effective conductivities are used in the two-dimensional axisymmetric air flow and concrete cask models. The media in the canister is considered to be helium. The fuel assemblies and fuel tubes in this model are represented by homogeneous regions with effective thermal properties. The effective conductivities for the fuel assemblies and the fuel tubes are determined by the two-dimensional fuel models (Section 4.4.1.5) and the two-dimensional fuel tube models (Section 4.4.1.6) respectively. The properties corresponding to the PWR 14 × 14 assemblies are used for the PWR model, since the 14 × 14 assemblies have the lowest conductivities as compared to other PWR assemblies. For the same reason, the properties corresponding to the BWR 9 × 9 assemblies are used for the BWR models.

The effective thermal conductivity (k_{eff}) of the fuel region in the radial direction is determined by considering the canister internals as a solid cylinder with heat generation. The temperature distribution in the cylinder may be expressed as [17]:

$$T - T_o = \frac{q'''R^2}{4k_{eff}}[1 - (\frac{r}{R})^2]$$

where:

T_o = the surface temperature of the cylinder
T = temperature at radius "r" of the cylinder
R = the outer radius of the cylinder,
r = radius
q''' = the heat generation rate = $\frac{Q}{\pi R^2 H}$

where: Q = total heat generated in the cylinder
H = length of the cylinder

Considering the temperature at the center of the canister to be T_{max}, the above equation can be simplified and used to compute the effective thermal conductivity (k_{eff}):

$$k_{eff} = \frac{Q}{4\pi H(T_{max} - T_o)} = \frac{Q}{4\pi H \Delta T}$$

where:

Q = total heat generated by the fuel
H = length of the active fuel region
T_o = temperature at outer surface internals (inside surface of the canister)
$\Delta T = T_{max} - T_o$

The value of ΔT is obtained from thermal analysis using the three-dimensional periodic canister internal model with the boundary temperature constrained to be T_o. The effective conductivity (k_{eff}) is then determined by using the above formula. Analysis is repeated by applying different boundary temperatures so that temperature-dependent conductivities can be determined.

Figure 4.4.1.4-1 Three-Dimensional Periodic Canister Internal Model - PWR

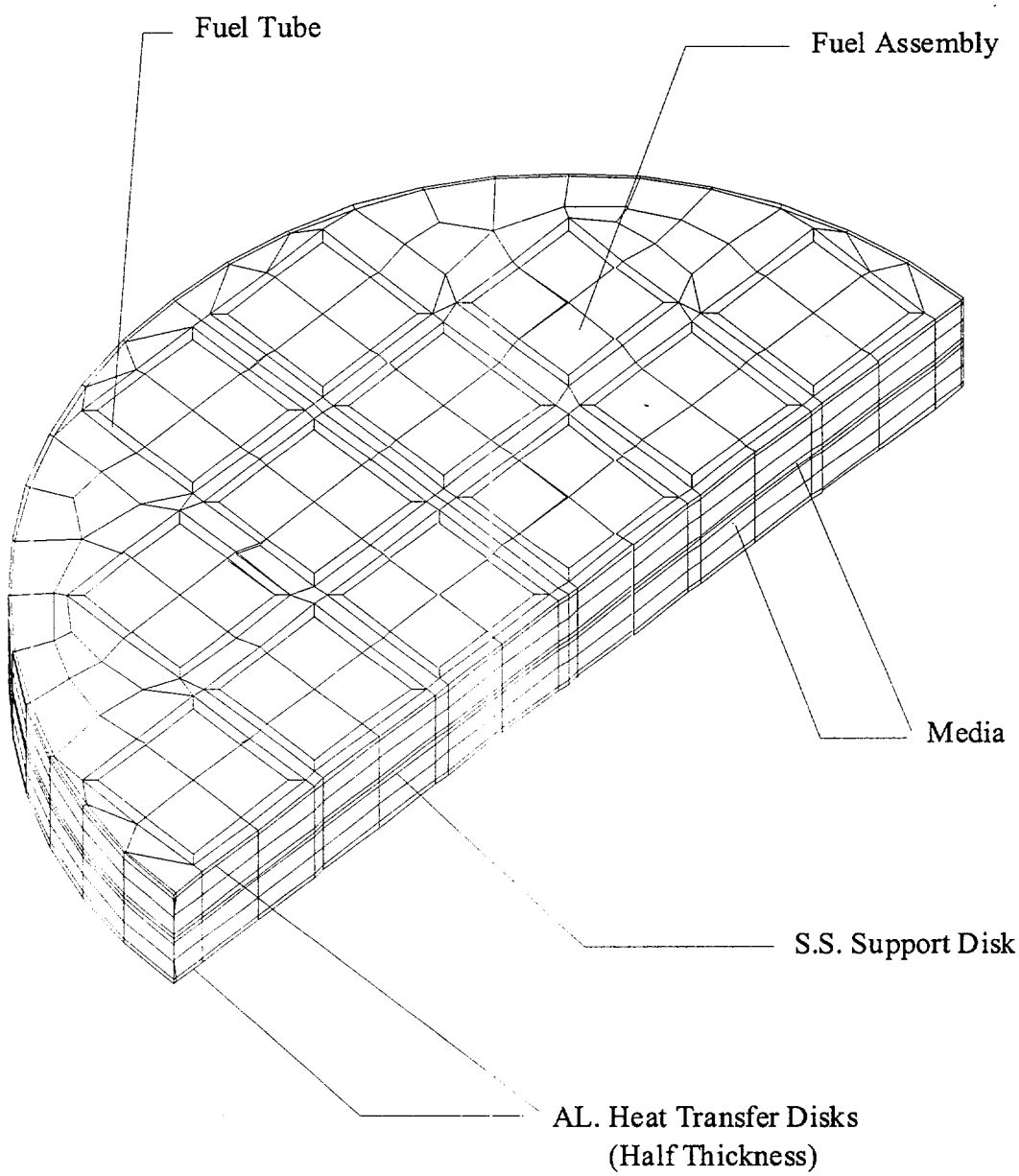

Figure 4.4.1.4-2 Three-Dimensional Periodic Canister Internal Model - BWR

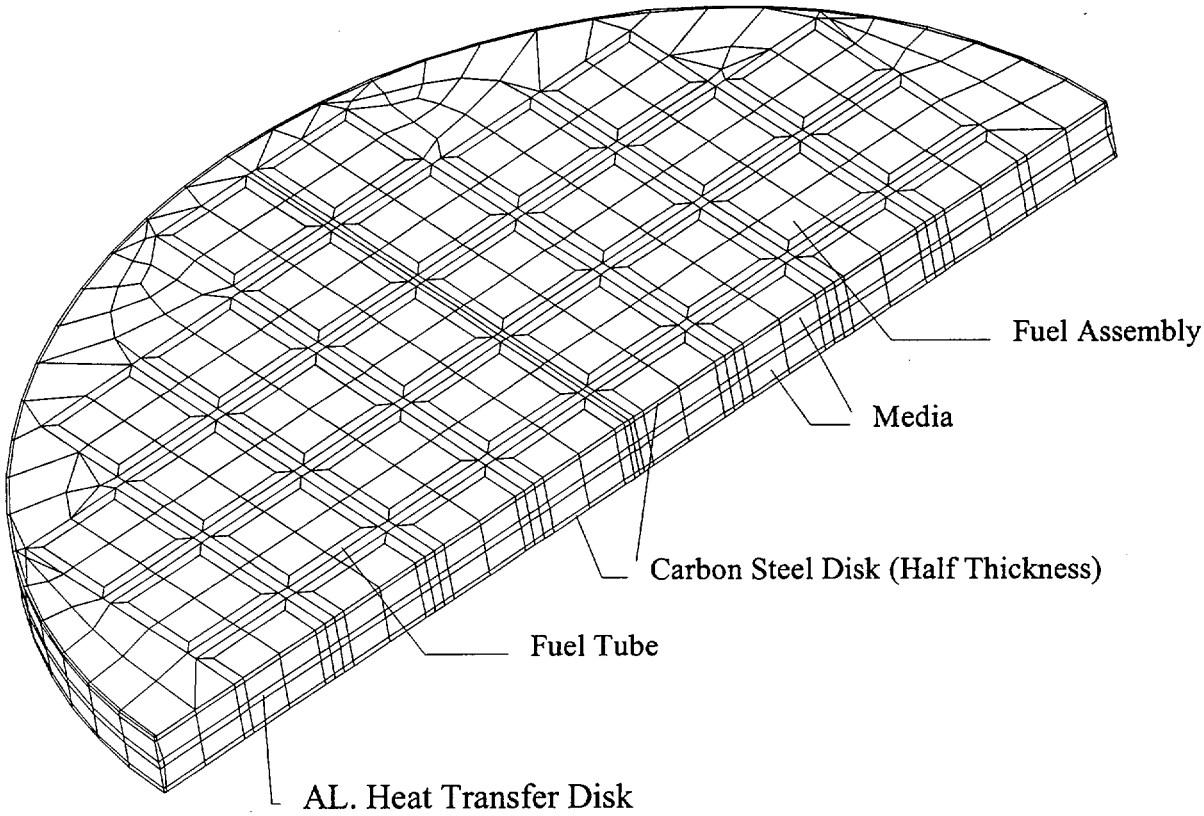

4.4.1.5 Two-Dimensional Fuel Models

The effective conductivity of the fuel is determined by the two-dimensional finite element model of the fuel assembly. The effective conductivity is used in the three-dimensional canister models (Section 4.4.1.2) and the three-dimensional periodic canister internal models (Section 4.4.1.4). A total of seven models are required: four models for the 14×14, 15×15, 16×16 and 17×17 PWR fuels and three models for the 7×7, 8×8 and 9×9 BWR fuels. Because of similarity, only the figure for the PWR 17×17 model is shown in this section (Figure 4.4.1.5-1). All models contain a full cross-section of an assembly to accommodate the radiation elements.

The model includes the fuel pellets, cladding, media between fuel rods, media between the fuel rods and the inner surface of the fuel tube (PWR) or fuel channel (BWR), and helium at the gap between the fuel pellets and cladding. Three types of media are considered: helium, water and a vacuum. Modes of heat transfer modeled include conduction and radiation between individual fuel rods for the steady-state condition. ANSYS PLANE55 conduction elements and MATRIX50 radiation elements are used to model conduction and radiation. Radiation elements are defined between fuel rods and from rods to the wall. Radiation at the gap between the pellets and the cladding is conservatively ignored.

The effective conductivity for the fuel is determined by using an equation defined in a Sandia National Laboratory Report [30]. The equation is used to determine the maximum temperature of a square cross-section of an isotropic homogeneous fuel with a uniform volumetric heat generation. At the boundary of the square cross-section, the temperature is constrained to be uniform. The expression for the temperature at the center of the fuel is given by:

$$T_c = T_e + 0.29468\,(Qa^2 / K_{eff})$$

where: T_c = the temperature at the center of the fuel (°F)
T_e = the temperature applied to the exterior of the fuel (°F)
Q = volumetric heat generation rate (Btu/hr-in^3)
a = half length of the square cross-section of the fuel (inch)
K_{eff} = effective thermal conductivity for the isotropic homogeneous fuel material (Btu/hr-in-°F)

Volumetric heat generation (Btu/hr-in^3) based on the design heat load is applied to the pellets. The effective conductivity is determined based on the heat generated and the temperature difference from the center of the model to the edge of the model. Temperature-dependent effective properties are established by performing multiple analyses using different boundary temperatures. The effective conductivity in the axial direction of the fuel assembly is calculated on the basis of the material area ratio.

Figure 4.4.1.5-1 Two-Dimensional PWR (17×17) Fuel Model

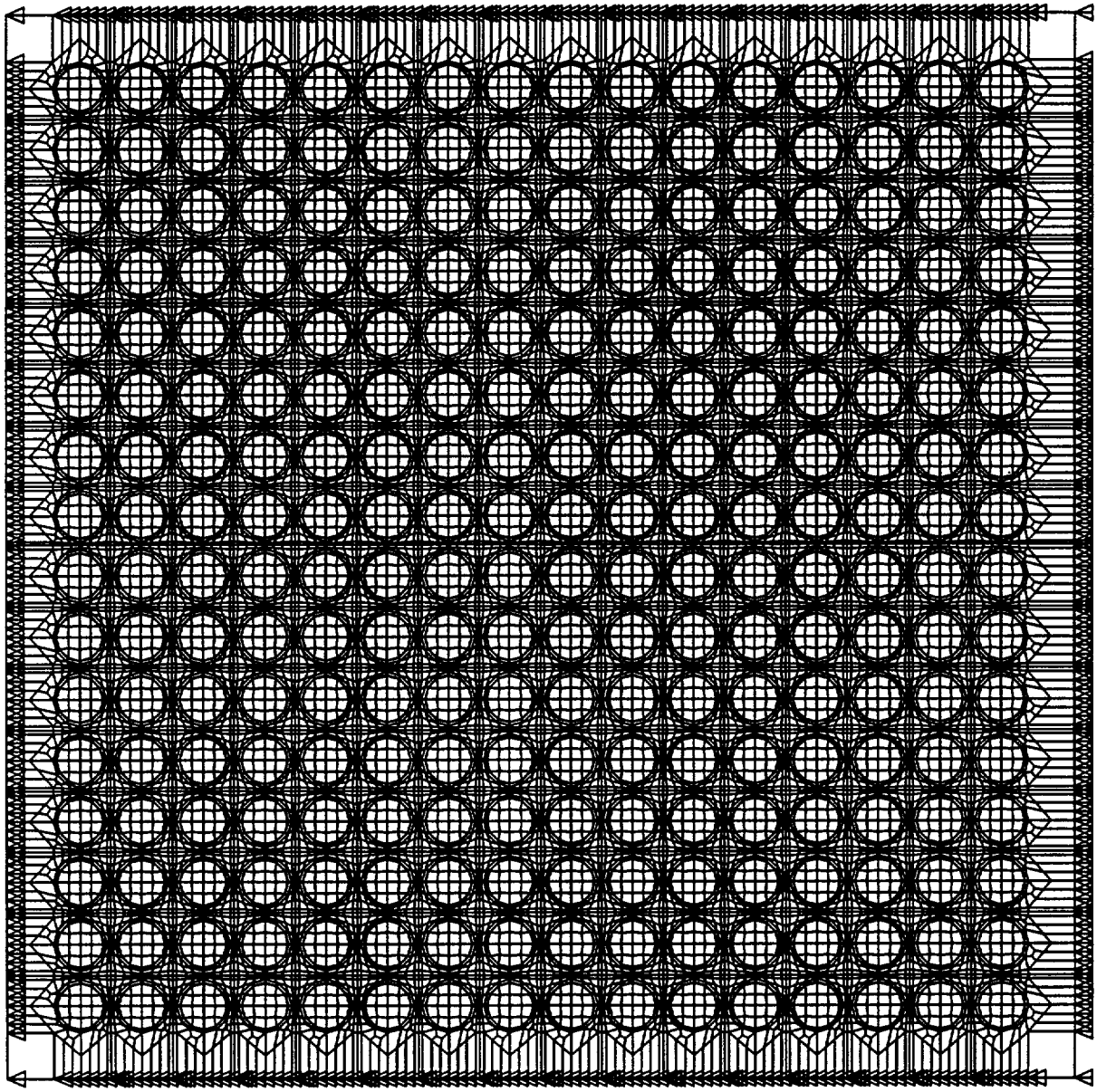

4.4.1.6 Two-Dimensional Fuel Tube Models

The two-dimensional fuel tube model is used to calculate the effective conductivities of the fuel tube wall and BORAL plate. These effective conductivities are used in the three-dimensional canister models (Section 4.4.1.2), the three-dimensional transfer cask and canister models (Section 4.4.1.3) and the three-dimensional periodic canister internal models (Section 4.4.1.4). A total of three models are required: one PWR model and two BWR models (one with the neutron absorber plate, one without the neutron absorber plate), corresponding to the enveloping configurations of the 7×7, 8×8 and 9×9 BWR fuels.

Two forms of the neutron absorber plates are evaluated. The configuration shown in the fuel tube models in Figures 4.4.1.6-1 and 4.4.1.6-2 (for PWR and BWR fuel, respectively) incorporates the BORAL core matrix sandwiched between two layers of aluminum cladding. An alternate design substitutes a single layer of METAMIC for the BORAL. The properties of these materials are presented in Tables 4.2-10 and 4.2-13, respectively. The difference in thermal performance between the two neutron absorber materials is considered to be insignificant, since the primary thermal resistance in the fuel tube design is not the neutron absorber material, but rather the gaps between the fuel tube and the disks.

As shown in Figure 4.4.1.6-1, the PWR model includes the fuel tube, the BORAL plate (including the core matrix sandwiched by aluminum cladding), the stainless steel cladding and the gap between the stainless steel cladding and the support disk or heat transfer disk. Three conditions of media are considered in the gaps: helium, water and a vacuum.

ANSYS PLANE55 conduction elements and LINK31 radiation elements are used to construct the model. The model consists of six layers of conduction elements and two radiation elements (radiation elements are not used for water condition) that are defined at the gaps (two for each gap). The thickness of the model (x-direction) is the distance measured from the outside face of the fuel assembly to the inside face of the slot in the support disk (assuming the fuel tube is centered in the hole in the disk). The tolerance of the neutron absorber plate thickness, 0.003 inch, is used as the gap size between the neutron absorber plate and the stainless steel cladding. The height of the model is defined as equal to the width of the model.

The fuel tubes in the BWR fuel basket differ from those in the PWR fuel basket in that not all sides of the fuel tubes contain neutron absorber. In addition, the BWR fuel assembly is contained in a fuel channel. Therefore, two effective conductivity models are necessary, one fuel tube model with the neutron absorber plate (a total of eight layers of materials) and another fuel tube model with a gap replacing the neutron absorber plate (a total of four layers of materials).

As shown in Figure 4.4.1.6-2, the BWR fuel tube model with neutron absorber includes the fuel channel, the gap between the fuel channel and fuel tube, the fuel tube, the neutron absorber plate (including the core matrix sandwiched by aluminum claddings), and a gap between the stainless steel cladding for the neutron absorber plate and the support disk or heat transfer disk. The effective conductivity of the fuel tube without the neutron absorber plate is determined using the second BWR fuel tube model. As shown in Figure 4.4.1.6-3, this model includes the gap between fuel assembly and the fuel channel, the fuel channel, gap between the fuel channel and stainless steel fuel tube, the fuel tube, and a gap between the fuel tube and the support disk or heat transfer disk. An emissivity value of 0.0001 is conservatively used for the BWR support disk in the model.

Heat flux is applied at the left side of the model (fuel tube for PWR models and fuel channel for BWR models), and the temperature at the right boundary of the model is constrained. The heat flux is determined based on the design heat load. The maximum temperature of the model (at the left boundary) and the temperature difference (ΔT) across the model are calculated by the ANSYS model. The effective conductivity (K_{xx}) is determined using the following formula:

$$q = K_{xx} (A/L) \Delta T$$

or

$$K_{xx} = q \ L / (A \ \Delta T)$$

where:

K_{xx} = effective conductivity (Btu/hr-in-°F) in X direction in Figure 4.4.1.6-1.
q = heat rate (Btu/hr)
A= area (in^2)
L= length (thickness) of model (in)
ΔT = temperature difference across the model (°F)

The temperature-dependent conductivity is determined by varying the temperature constraints at one boundary of the model and resolving for the heat rate (q) and temperature difference. The effective conductivity for the parallel path (the Y direction in Figure 4.4.1.6-1) is calculated by:

$$K_{yy} = \frac{\sum K_i t_i}{L}$$

where:

K_i = thermal conductivity of each layer
t_i = thickness of each layer
L = total length (thickness) of the model

Figure 4.4.1.6-1 Two-Dimensional Fuel Tube Model: PWR Fuel

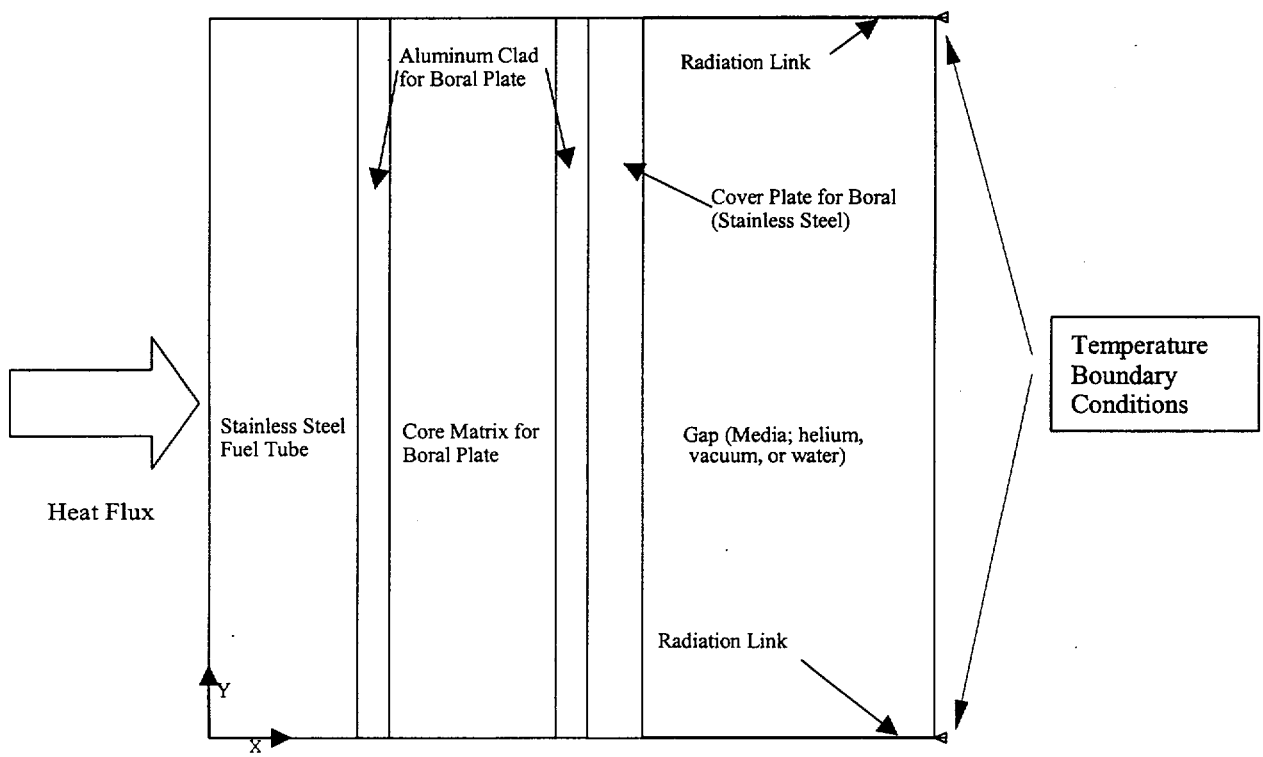

*Media can be water, vacuum, or helium.

Figure 4.4.1.6-2 Two-Dimensional Fuel Tube Model: BWR Fuel Tube with Neutron Absorber

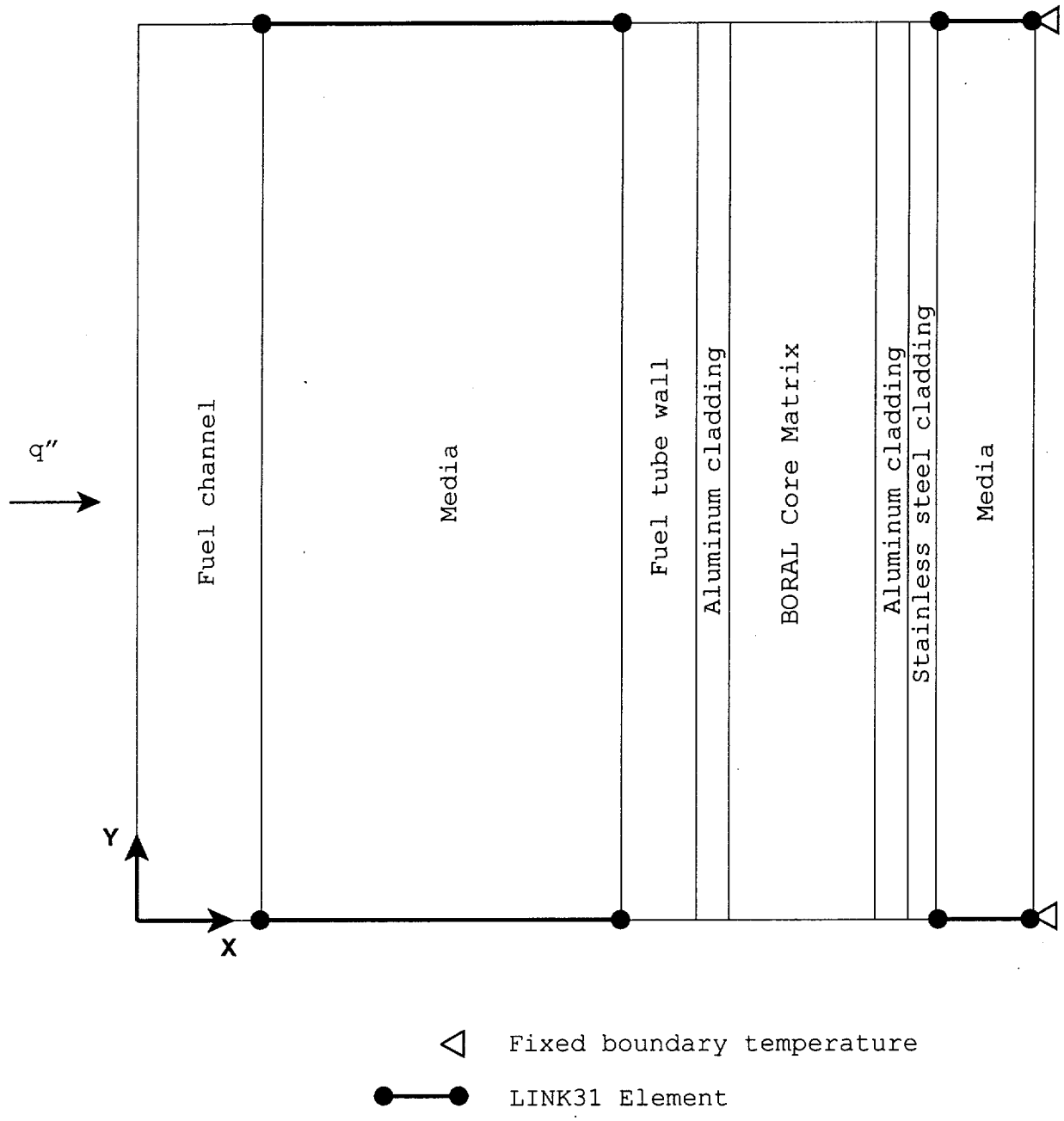

*Media can be water, vacuum, or helium.

Figure 4.4.1.6-3 Two-Dimensional Fuel Tube Model: BWR Fuel Tube without Neutron Absorber

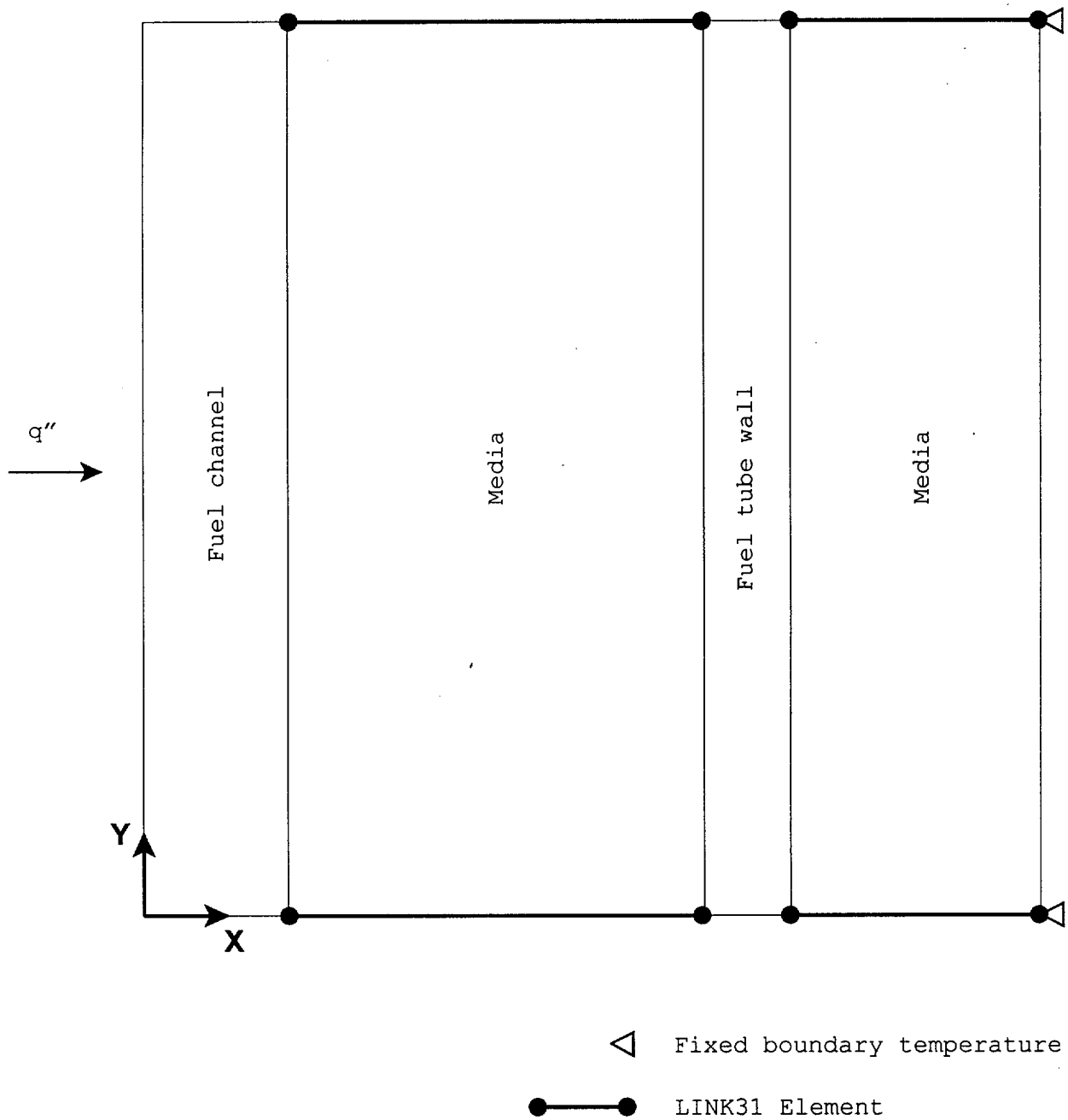

*Media can be water, vacuum, or helium.

4.4.1.7 Two-Dimensional Forced Air Flow Model for Transfer Cask Cooling

A two-dimensional axisymmetric air flow model is used to determine the air flow rate needed to ensure that the maximum temperature of the canister shell and canister components inside the transfer cask do not exceed those presented in Tables 4.4.3-3 and 4.4.3-4 for the helium condition. This air flow model considers a 0.34-inch air annulus between the outer surface of the canister shell and the inner surface of the transfer cask, and has a total length of 191-inches. The fuel canister is cooled by forced convection in the air annulus resulting from air pumped in through fill/drain ports in the body of the transfer cask. The radiation heat transfer between the vertical annulus surfaces (the canister shell outer surface and the transfer cask inner surface) is conservatively neglected. All heat is considered to be removed by the air flow.

ANSYS FLOTRAN FLUID141 fluid thermal elements are used to construct the two-dimensional axisymmetric air flow finite element model for transfer cask cooling. The model and the boundary conditions applied to the model, are shown in Figures 4.4.1.7-1, 4.4.1.7-2 and 4.4.1.7-3.

As shown in Tables 4.4.3-3 and 4.4.3-4, the temperature margin of the governing component (the heat transfer disk) for the PWR fuel configuration is lower than the margin for the BWR fuel configuration; therefore, the thermal loading for the PWR configuration is used. The non-uniform heat generation applied in the model, shown in Figure 4.4.1.7-4, is based on the axial power distribution shown in Figure 4.4.1.1-3 for PWR fuel.

The inlet air velocity is specified based on the volume flow rate. Room temperature (76°F) is applied to the inlet nodes, while zero air velocity, in both the X and Y directions, is defined as the boundary condition for the vertical solid sides.

Results of the analyses of forced air cooling of the canister inside the transfer cask are shown in Figure 4.4.1.7-5. As shown in the figure, the maximum canister shell temperature is less than 416°F for a forced air flow rate of 275 ft^3/minute, or higher, where 416°F is the calculated maximum canister shell temperature for the typical transfer operation for the PWR configuration (Table 4.4.3-3). A forced air volume flow rate of 375 ft^3/minute is conservatively specified for cooling the canister in the event that forced air cooling is required. Evaluation of a forced air volume flow rate of 375 ft^3/minute, results in a maximum canister shell temperature of 321°F, which is significantly less than the design basis temperature of 416°F.

Figure 4.4.1.7-1 Two-Dimensional Axisymmetric Finite Element Model for Transfer Cask Forced Air Cooling

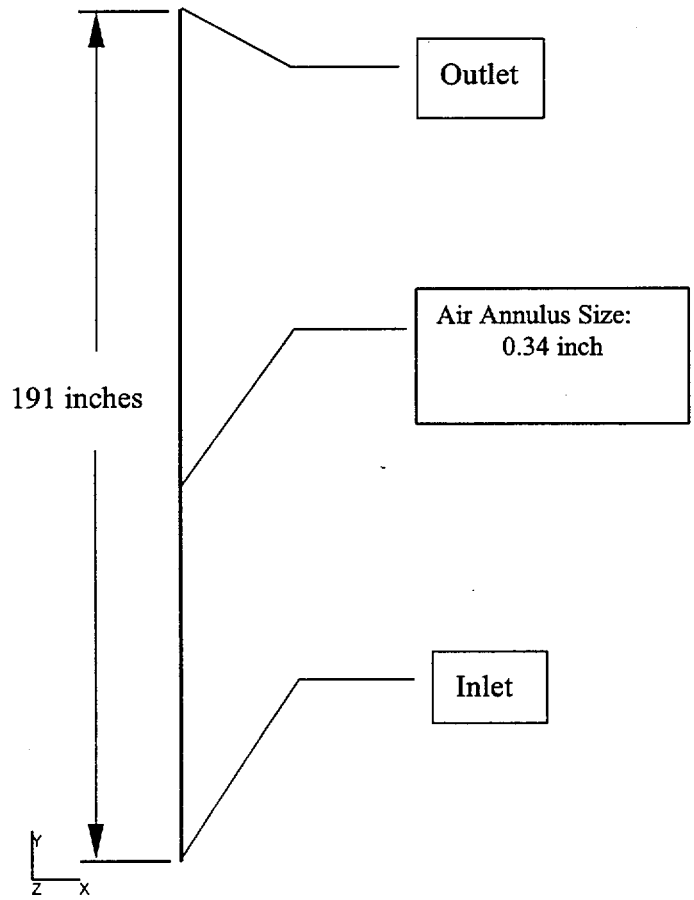

Figure 4.4.1.7-2 Two-Dimensional Axisymmetric Outlet Air Flow Model for Transfer Cask Cooling

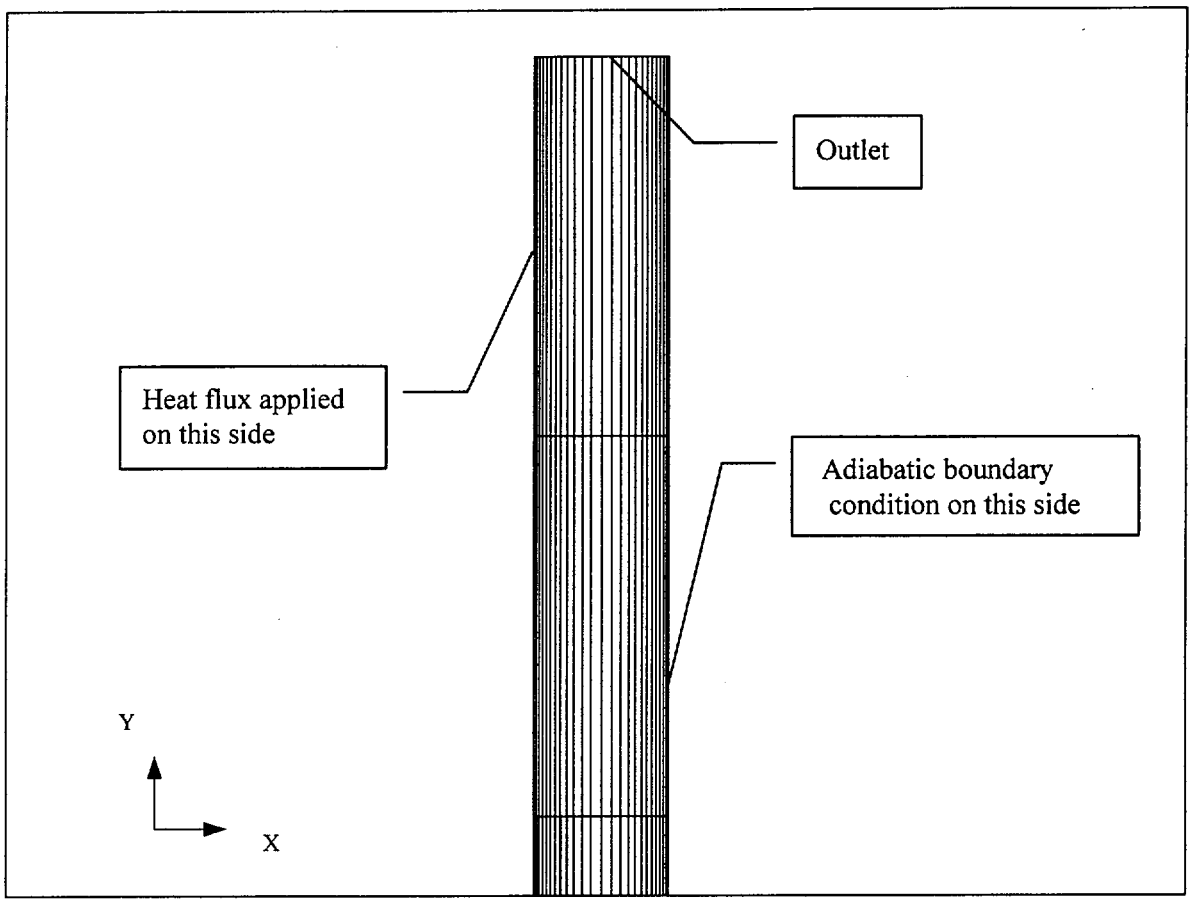

Figure 4.4.1.7-3 Two-Dimensional Axisymmetric Inlet Air Flow Model for Transfer Cask Cooling

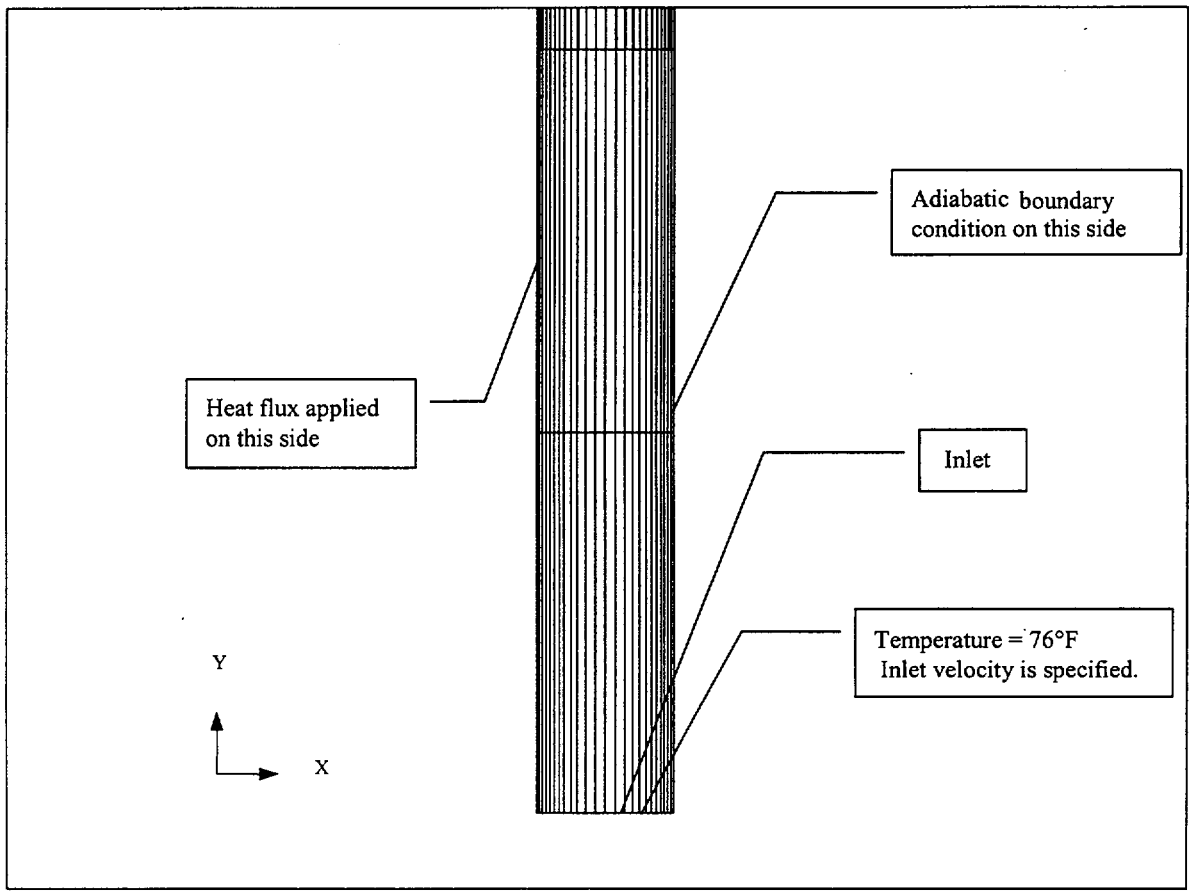

Figure 4.4.1.7-4 Non-Uniform Heat Load from Canister Contents

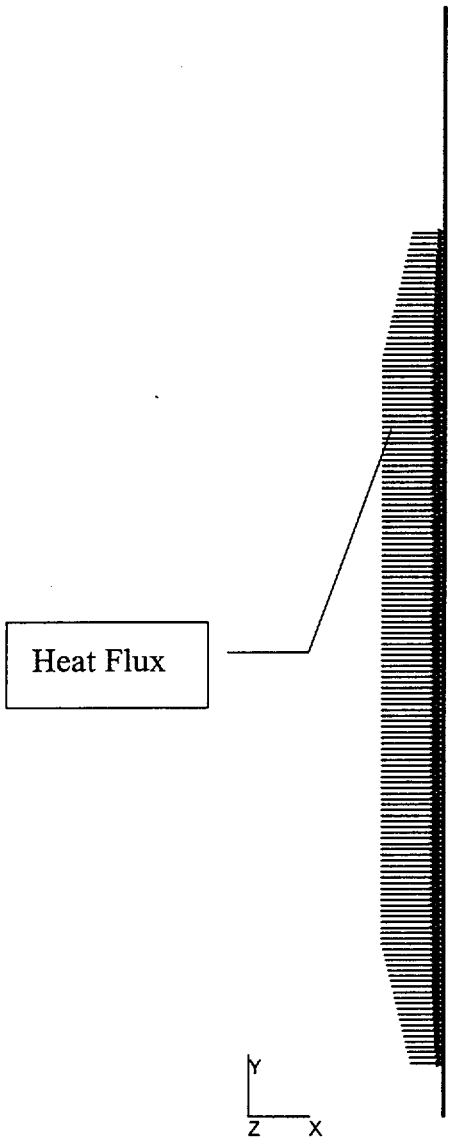

Figure 4.4.1.7-5 Maximum Canister Temperature Versus Air Volume Flow Rate

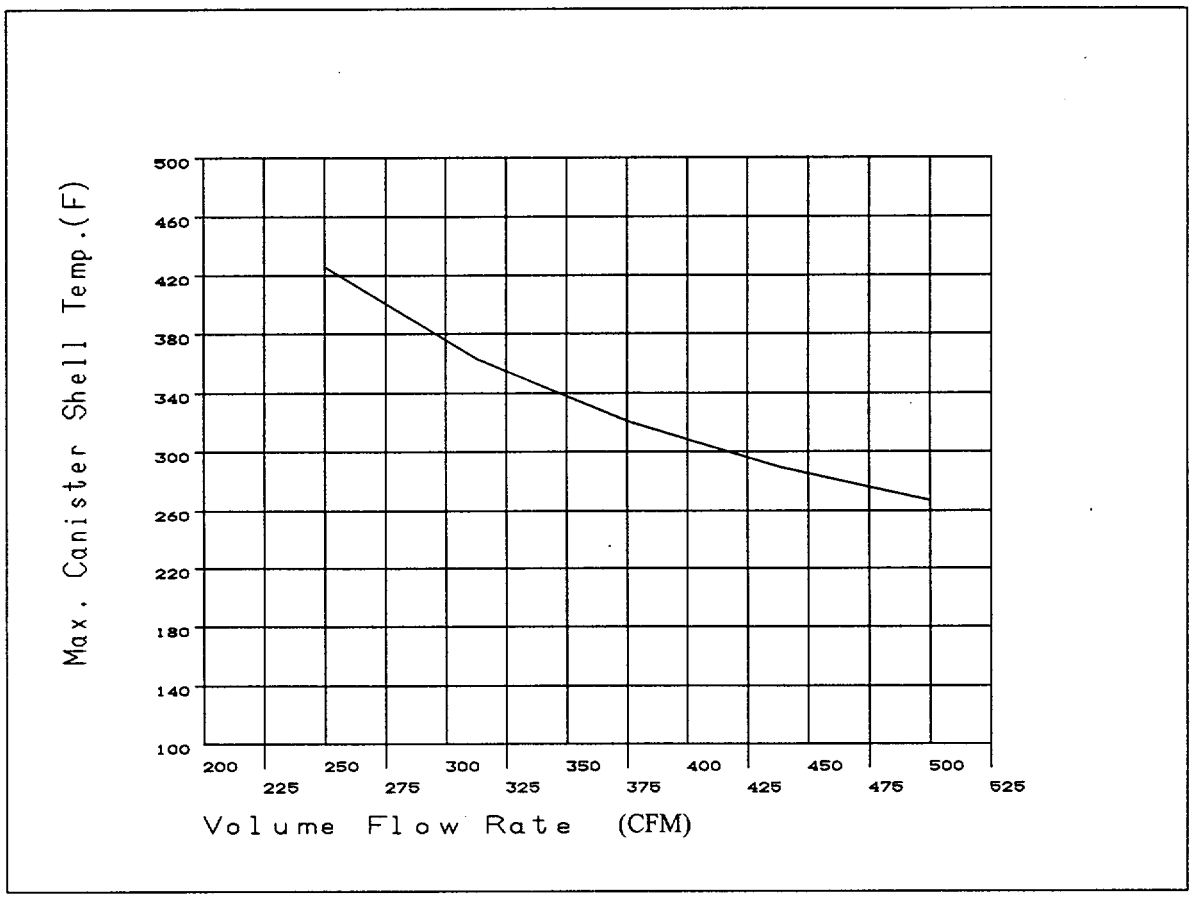

4.4.3 Maximum Temperatures for PWR and BWR Fuel

Temperature distribution and maximum component temperatures for the Universal Storage System under the normal conditions of storage and transfer, based on the use of the Standard transfer cask, are provided in this section. The thermal evaluation is identical for the Advanced transfer cask. Components of the Universal Storage System containing PWR and BWR fuels are addressed separately. Temperature distributions for the evaluated off-normal and accident conditions are presented in Sections 11.1 and 11.2.

Figure 4.4.3-1 shows the temperature distribution of the Vertical Concrete Cask and the canister containing the PWR design basis fuel for the normal, long-term storage condition. The air flow pattern and air temperatures in the annulus between the PWR canister and the concrete cask liner for the normal condition of storage are shown in Figures 4.4.3-2 and 4.4.3-3, respectively. The temperature distribution in the concrete portion of the concrete cask for the PWR assembly is shown in Figure 4.4.3-4. The temperature distribution for the BWR design basis fuel is similar to that of the PWR fuel and is, therefore, not presented. Table 4.4.3-1 shows the maximum component temperatures for the normal condition of storage for the PWR design basis fuel. The maximum component temperatures for the normal condition of storage for the BWR design basis fuel are shown in Table 4.4.3-2.

As shown in Figure 4.4.3-3, a high-temperature gradient exists near the wall of the canister and the liner of the concrete cask, while the air in the center of the annulus exhibits a much lower temperature gradient, indicating significant boundary layer features of the air flow. The temperatures at the concrete cask steel liner surface are higher than the air temperature, which indicates that salient radiation heat transfer occurs across the annulus. As shown in Figure 4.4.3-4, the local temperature in the concrete, directly affected by the radiation heat transfer across the annulus, can reach 186°F (less than the 200°F allowable temperature). The bulk temperature in the concrete, as determined using volume average of the temperatures in the concrete region, is 135°F, less than the allowable value of 150°F.

Under typical operations, the transient history of maximum component temperatures for the transfer conditions (canister, inside the transfer cask, containing water for 17 hours, vacuum for 32 hours for PWR and 25 hours for BWR and for steady state condition (unlimited time) helium for PWR and 16 hours in helium for BWR) is shown in Figures 4.4.3-5 and 4.4.3-6 for PWR and BWR fuels, respectively. The maximum component temperatures for the transfer conditions (vacuum and helium conditions) are shown in Tables 4.4.3-3 and 4.4.3-4, for PWR and BWR

fuels, respectively. The maximum calculated water temperature is 204°F and 203°F for PWR and BWR fuels, respectively, at the end of 17 hours based on an initial water temperature of 100°F. Using the three-dimensional transfer cask and canister models as described in Section 4.4.1.3, the thermal transient analysis is performed for the 100-ton transfer cask in the horizontal position. The maximum temperatures for the fuel cladding and heat transfer disk are calculated to be 761°F and 701°F, respectively. These temperatures are below the results for the vertical configuration due to contact between components. However, the maximum temperature difference between the center and the edge of the support disk increased from 388°F to 394°F. This temperature remains bounded by the ΔT (425°F) used in Section 3.4.4.1.8.1 for the thermal stress evaluation for the PWR support disk. Based on the results for the PWR configuration, it is expected that the maximum ΔT for the BWR support disk for the 100-ton transfer cask in the horizontal position will remain bounded by the ΔT (400°F) used in Section 3.4.4.1.8.2 for the thermal stress evaluation for the BWR support disk. Note that the maximum ΔT for the BWR support disk for the 100-ton transfer cask in the vertical position is 356°F, which is well below 400°F.

4.4.3.1 Maximum Temperatures at Reduced Total Heat Loads

This section provides the evaluation of component temperatures for fuel heat loads less than the design basis heat load of 23 kW. Transient thermal analyses are performed for PWR fuel heat loads of 20, 17.6, 14, 11 and 8 kW to establish the allowable time limits for the vacuum condition in the canister as described in the Technical Specifications (Chapter 12) for the Limiting Conditions of Operation (LCO), LCOs 3.1.1 and 3.1.4. The time limits ensure that the allowable temperatures of the limiting components – the heat transfer disks and the fuel cladding - are not exceeded. A steady state evaluation is also performed for heat loads of 11 kW and 8 kW in the vacuum condition and all heat load cases in the helium condition. If the steady state temperature calculated is less than the limiting component allowable temperature, then the allowable time duration in the vacuum or helium conditions is defined to be 600 hours (25 days) based on the 30 day time test for abnormal regimes as described in PNL-4835 [34].

The three-dimensional transfer cask and canister model for the PWR fuel configuration, described in Section 4.4.1.3, is used for the transient and steady state thermal analysis for the reduced heat load cases. To obtain the bounding temperatures for all possible loading configurations, thermal analyses are performed for a total of fourteen (14) cases as tabulated below. The basket locations are shown in Figure 4.4.3-7. Since the maximum temperature for the limiting components (fuel cladding and heat transfer disk) always occurs at the central region

of the basket, hotter fuels (maximum allowable heat load for 5-year cooled fuel: 0.958 kW = 23 kW/24) are specified at the central basket locations. The bounding cases for each heat load condition are noted with an asterisk (*) in the tabulation which follows. Six cases (cases 3 through 8) are evaluated for the 17.6 kW heat load condition. The first four cases (cases 3 through 6) represent standard UMS system fuel loadings. The remaining two cases (cases 7 and 8) account for the preferential loading configuration for Maine Yankee site specific high burnup fuel (Section 4.5.1.2.2), with case 8 being the bounding case for the Maine Yankee high burnup fuel. Based on the analysis results of the 17.6 kW heat load cases, only two loading cases are required to establish the bounding condition for the 20, 14, 11 and 8 kW heat loads.

Canister Heat Load (kW)	Heat Load Case	Heat Load (kW) Evaluated in Each Basket Location (See Figure 4.4.3-7)					
		1	2	3	4	5	6
20	1	0.958	0.958	0.709	0.958	0.709	0.709
20*	2	0.958	0.958	0.958	0.958	0.958	0.210
17.6	3	0.958	0.958	0.509	0.958	0.509	0.509
17.6*	4	0.958	0.958	0.568	0.958	0.958	0.000
17.6	5	0.958	0.958	0.958	0.958	0.568	0.000
17.6	6	0.958	0.958	0.284	0.958	0.958	0.284
17.6	7	0.958	0.146	1.050	0.146	1.050	1.050
17.6	8	0.958	0.958	1.050	0.384	1.050	0.000
14	9	0.958	0.958	0.209	0.958	0.209	0.209
14*	10	0.958	0.958	0.000	0.958	0.626	0.000
11	11	0.958	0.896	0.000	0.896	0.000	0.000
11*	12	0.958	0.958	0.000	0.834	0.000	0.000
8	13	0.958	0.521	0.000	0.521	0.000	0.000
8*	14	0.958	0.958	0.000	0.084	0.000	0.000

The heat load (23 kW/24 Assemblies = 0.958 kW) at the four (4) central basket locations corresponds to the maximum allowable canister heat load for 5-year cooled fuel (Table 4.4.7-8). The non-uniform heat loads evaluated in this section bound the equivalent uniform heat loads, since they result in higher maximum temperatures of the fuel cladding and heat transfer disk.

Volumetric heat generation (Btu/hr-in^3) is applied to the active fuel region in each fuel assembly location of the model using the axial power distribution for PWR fuel (Figure 4.4.1.1-3) in the axial direction.

The thermal analysis results for the closure and transfer of a loaded PWR fuel canister in the transfer cask for the reduced heat load cases are shown in Table 4.4.3-5, with a comparison to the results for the design basis heat load case. The temperatures shown are the maximum

temperatures for the limiting components (fuel cladding and heat transfer disk). The maximum temperatures of the fuel cladding and the heat transfer disk are less than the allowable temperatures (Table 4.1-3) of these components for the short-term conditions of vacuum drying and helium backfill. As shown in Table 4.4.3-5, a time limit of 600 hours is specified for moving the canister out of the transfer cask for all of the heat load cases, after the canister is filled with helium. For all heat load cases, the maximum fuel cladding/heat transfer disk temperatures for the steady state condition are below the short-term allowable temperatures of the fuel cladding and the heat transfer disk. Similarly, a time limit of 600 hours is specified for the vacuum stage for the heat load cases at or below 11 kW. Note that the maximum water temperature at the end of the "water period" is considered to be the volumetric average temperature of the calculated cladding temperatures in the active fuel region of the hottest fuel assembly. The results indicate that the volumetric average water temperature is below 212°F for all cases evaluated. This is consistent with the thermal model that only considers conduction in the fuel assembly region and between the disks. This approach does not include consideration of convection of the water or the energy absorbed by latent heat of vaporization.

The Technical Specifications specify the remedial actions, either in-pool or forced air cooling, required to ensure that the fuel cladding and basket component temperatures do not exceed their short-term allowable temperatures, if the time limits are not met. LCOs 3.1.1 and 3.1.4 incorporate the operating times for heat loads that are less than the design basis heat loads as evaluated in this section.

Using the same three-dimensional transfer cask/canister models, analysis is performed for the conditions of in-pool cooling and forced air cooling followed by the vacuum drying and helium backfill operation (LCO 3.1.1). The conditions at the end of the vacuum drying as shown in Tables 4.4.3-5 (PWR) and 4.4.3-8 (BWR) are used as the initial conditions of the analyses. The LCO 3.1.1 "Action" analysis results are shown in Tables 4.4.3-6 and 4.4.3-7 for the PWR configuration and Tables 4.4.3-9 and 4.4.3-10 for the BWR configuration. Note that the duration of the second vacuum (after completion of the in-pool or forced air cooling) is limited (calculated based on the heat-up rate of the first vacuum), so the maximum temperatures at the end of the second vacuum cycle will not exceed those at the end of the first vacuum cycle. The maximum temperatures at the end of the first vacuum (Table 4.4.3-5 for PWR and Table 4.4.3-8 for BWR) are conservatively presented as the maximum temperatures for the second vacuum condition. The maximum temperatures for the fuel cladding and the heat transfer disk are below the short-term allowable temperatures.

The in-pool cooling and the forced-air cooling followed by the helium backfill operation in LCO 3.1.4 are also evaluated for the BWR configuration for 23 kW and 20 kW cases. The condition at the end of the helium condition, as shown in Table 4.4.3-8, is used as the initial condition. The results are shown in Tables 4.4.3-11 and 4.4.3-12 for the in-pool cooling and forced-air cooling, respectively. Note that the time limit for the first helium backfill condition is used for second helium backfill condition (after completion of the in-pool or forced air cooling). Based on the heat-up rate of the first helium condition, the maximum component temperatures at the end of the second helium are well below the maximum temperatures at the end of the first helium condition. The maximum temperatures at the end of the first helium (Table 4.4.3-8) are conservatively presented as the maximum temperatures for the second helium backfill condition, as shown in Tables 4.4.3-11 and 4.4.3-12.

4.4.3.2 Preferential Fuel Loading

This section provides the evaluation of preferential fuel loading in accordance with Section 12B 2.1.2 for PWR and BWR fuel. As stated in Section 12B2.1.2, loading of the fuel assemblies designated for a given canister must be administratively controlled to ensure that the fuel cladding temperature limits are not exceeded for any fuel assembly, unless all of the designated fuel assemblies have a cooling time of 7 years or more. Fuel with the shortest cooling time (and, therefore, having a higher allowable cladding temperature) is placed in the center of the basket. Fuel with the longest cooling time (and, therefore, having a lower allowable cladding temperature) is placed in the periphery of the basket. Canisters containing fuel assemblies, all of which have a cooling time of 7 years, or more, do not require preferential loading.

The three-dimensional half-symmetry (180-degree) canister models for PWR fuel and BWR fuel, as described in Section 4.4.1.2, are used to generate three-dimensional full (360-degree) models for the thermal analyses in this section. The full models are required to analyze the non-symmetric preferential loading patterns. The modeling methodology, material properties, and boundary conditions are the same for the half-symmetry models and the full models.

4.4.3.2.1 Preferential Loading of PWR Fuel

Thermal analyses are performed to evaluate the effect of preferential PWR fuel loading. The design heat load is 23 kW. Three cases for PWR fuel are considered to bound the maximum fuel clad temperature for preferential loading. The fuel basket positions referenced in the cases below are defined in Figure 4.4.3-9.

1. Case 1: Positions A, B and C contain fuel assemblies, each with a 5-year cool time and a heat load of 23/24 (0.958) kW. Position D and the remainder of the basket contain 6-year cooled fuel with a corresponding heat load of 22.4/24 (0.933) kW (Table 4.4.7-8 for 35,000 MWD/MTU) in each position. This case represents the worst case of 5-year and 6-year fuel mix according to the preferential loading requirement.

2. Case 2: Positions A, B and C contain fuel assemblies each with a 5-year cool time and a heat load of 23/24 (0.958) kW; Position D and the remainder of the basket contain 7-year cooled fuel with a corresponding heat load of 20.2/24 (0.842) kW (Table 4.4.7-8 for 35,000 MWD/MTU) in each position. This case represents the worst case of 5-year and 7-year fuel mix according to the preferential loading requirement.

3. Case 3: Positions A, B and C, and the remainder of the basket contain fuel assemblies each with a 7-year cool time and a heat load of 20.2/24 (0.842) kW (Table 4.4.7-8 for 35,000 MWD/MTU) each. Position D contains 15-year cooled fuel with a corresponding heat load of 19.1/24 (0.796) kW (Table 4.4.7-8 for 35,000 MWD/MTU). This case represents the worst case for the fuel assemblies having a cool time of 7 years or more.

The fuel cladding maximum temperatures for the three preferential loading cases are listed in Table 4.4.3-13. As shown in Table 4.4.3-13, the fuel cladding maximum temperatures for different cool times remain below the allowable temperature for each case.

Case 1 and Case 2 bound all possible PWR fuel preferential loading configurations. For example, even if the 7-year cooled fuel assemblies in Case 2 are replaced with 15-year cooled fuel assemblies, the maximum temperature of the 15-year cooled fuel assemblies will remain below their allowable temperature of 630°F (see Table 4.4.7.8 for 35,000 MWD/MTU) since the 7-year cooled fuel assemblies have a maximum temperature of 619°F (see Table 4.4.3-13). Additionally, maximum fuel cladding temperature for the 15-year cooled fuel would be lower than that for the 7-year cooled fuel since it has a lower heat generation rate. Case 3 bounds all possible configurations that do not require preferential loading (all fuel assemblies are of 7 years or more cool time).

4.4.3.2.2 Preferential Loading of BWR Fuel

Thermal analyses are performed to evaluate the effect of preferential BWR fuel loading. The design heat load is 23 kW. Three cases are presented, which are considered to bound the

maximum fuel clad temperature for preferential loading. The basket positions referenced in the following cases are defined in Figure 4.4.3-10.

1. Case 1: Positions A, B, C, D, and F contain fuel assemblies each with a 5-year cool time and a heat load of 23/56 (0.411) kW. Position E and the remainder of the basket contain 6-year cooled fuel, each with a heat load of 23/56 (0.411) kW (Table 4.4.7-8 for 35,000 MWD/MTU). This case is identical to the base loading configuration except the fuel assemblies in positions E and G have different allowable temperatures (6-year cooled). This case represents the worst case of 5-year and 6-year fuel mix according to the preferential loading requirement.

2. Case 2: Positions A, B, C, D, and F contain fuel assemblies each with a 5-year cool time and a heat load of 23/56 (0.441) kW. Position E and the remainder of the basket contain 7-year cooled fuel, each with a corresponding heat load of 22.1/56 (0.395) kW (Table 4.4.7-8 for 35,000 MWD/MTU). This case represents the worst case of 5-year and 7-year fuel mix according to the preferential loading requirement.

3. Case 3: Positions A, B, C, D, F, and the remainder of the basket contain fuel assemblies, each with a 7-year cool time and a heat load of 22.1/56 (0.395) kW (Table 4.4.7-8 for 35,000 MWD/MTU). Position E contains 15-year cooled fuel with a corresponding heat load of 21.1/56 (0.377) kW (Table 4.4.7-8 for 35,000 MWD/MTU). This case represents the worst case of the fuel assemblies having a cool time of 7 years or more.

The fuel cladding maximum temperatures for the three preferential loading cases for BWR fuels are listed in Table 4.4.3-14. As shown in Table 4.4.3-14, the fuel cladding maximum temperatures for different cool times remain below the allowable temperature for each case.

Case 1 and Case 2 bound all possible BWR fuel preferential loading configurations. For example, even if the 7-year cooled fuel assemblies in Case 2 are replaced with 15-year cooled fuel assemblies, the maximum temperature of the 15-year cooled fuel assemblies will remain below their allowable temperature of 642°F (see Table 4.4.7.8 for 35,000 MWD/MTU) since the 7-year cooled fuel assemblies have a maximum temperature of 637°F (see Table 4.4.3-14). Additionally, maximum fuel cladding temperature for the 15-year cooled fuel would be lower than that for the 7-year cooled fuel since it has a lower heat generation rate. Case 3 bounds all possible configurations that do not require preferential loading (all fuel assemblies are of 7 years or more cool time).

Figure 4.4.3-1 Temperature Distribution (°F) for the Normal Storage Condition: PWR Fuel

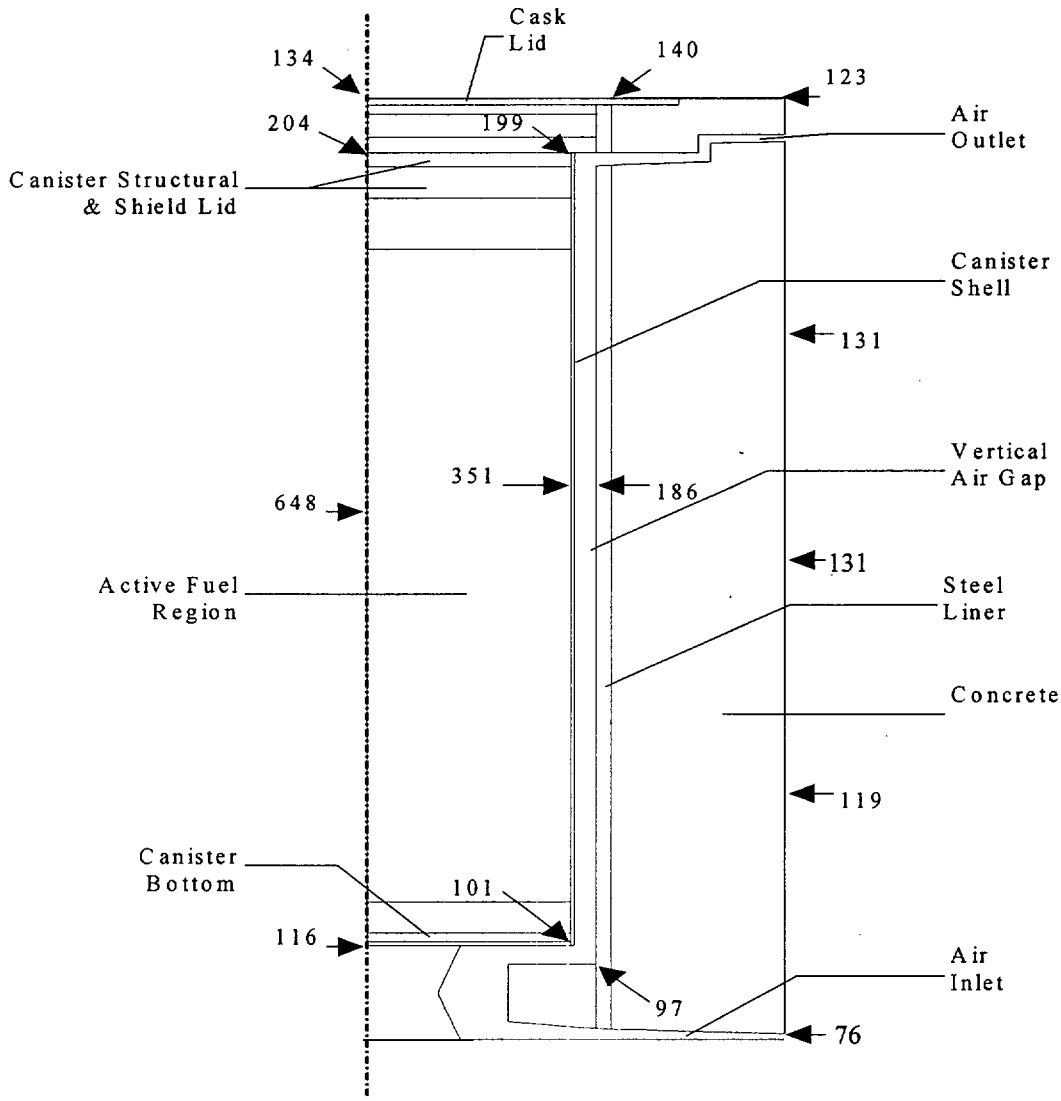

Figure 4.4.3-2 Air Flow Pattern in the Concrete Cask in the Normal Storage Condition: PWR Fuel

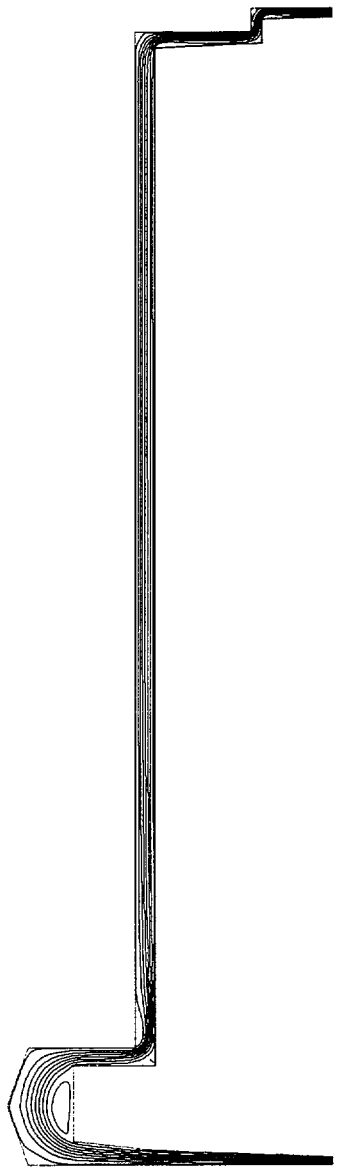

Figure 4.4.3-3 Air Temperature (°F) Distribution in the Concrete Cask During the Normal Storage Condition: PWR Fuel

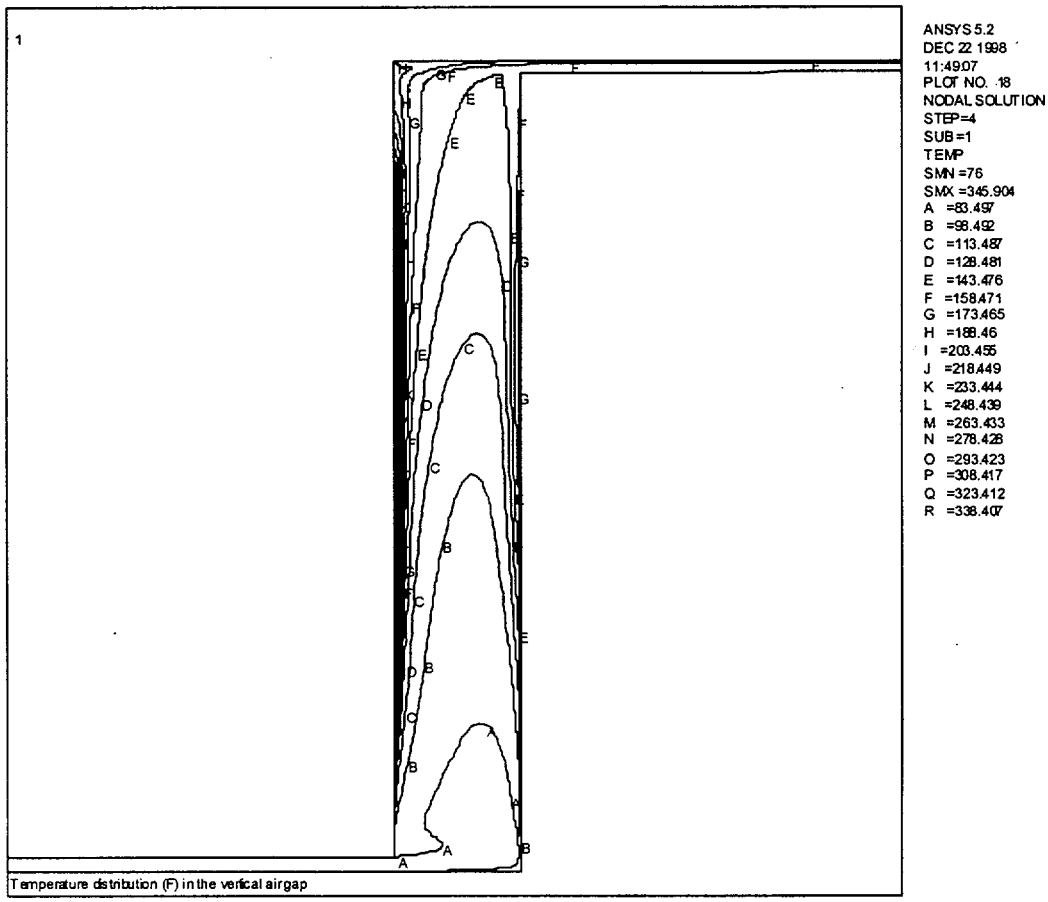

Figure 4.4.3-4 Concrete Temperature (°F) Distribution During the Normal Storage Condition: PWR Fuel

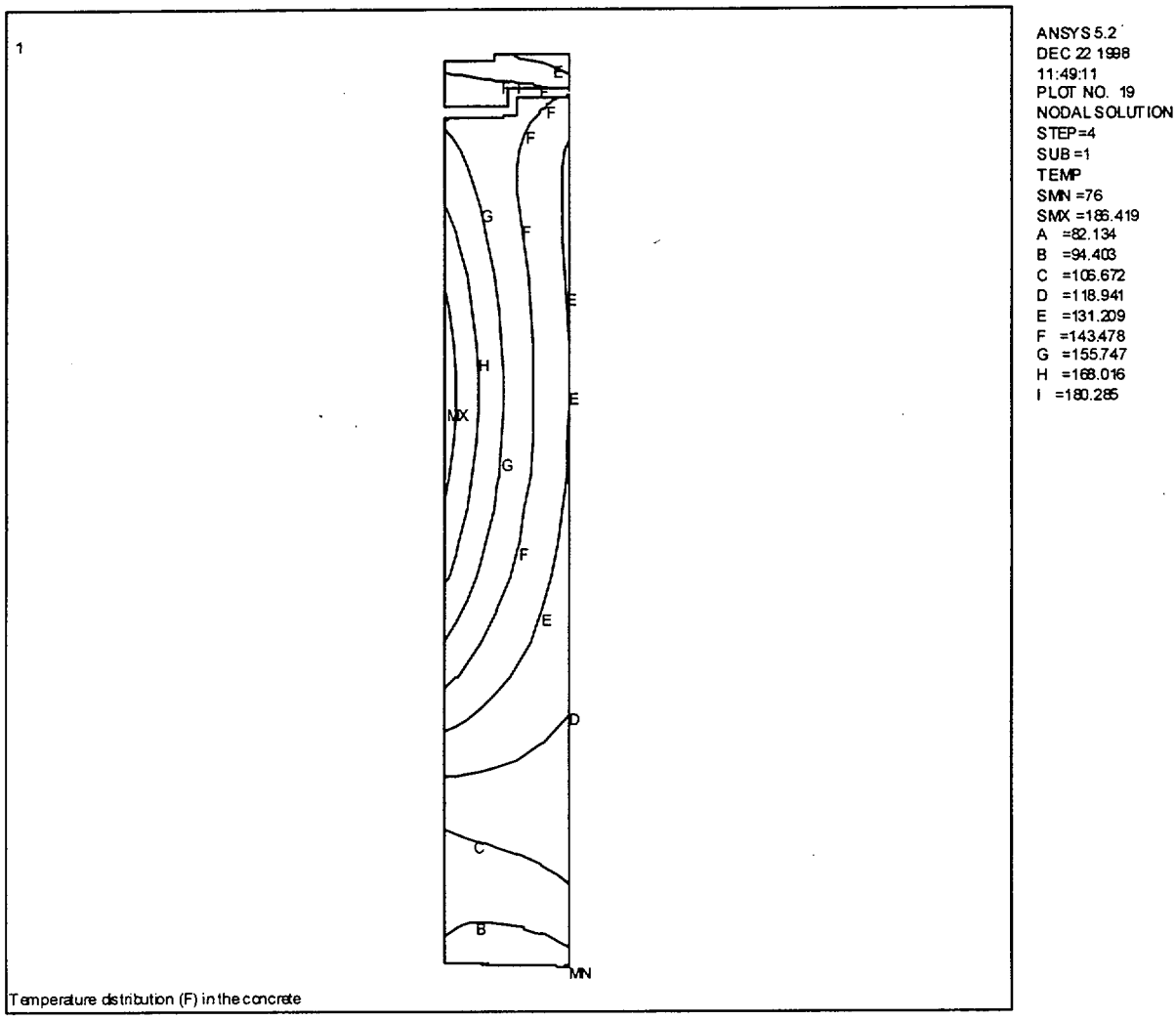

Figure 4.4.3-5 History of Maximum Component Temperature (°F) for Transfer Conditions for PWR Fuel with Design Basis 23 kW Uniformly Distributed Heat Load

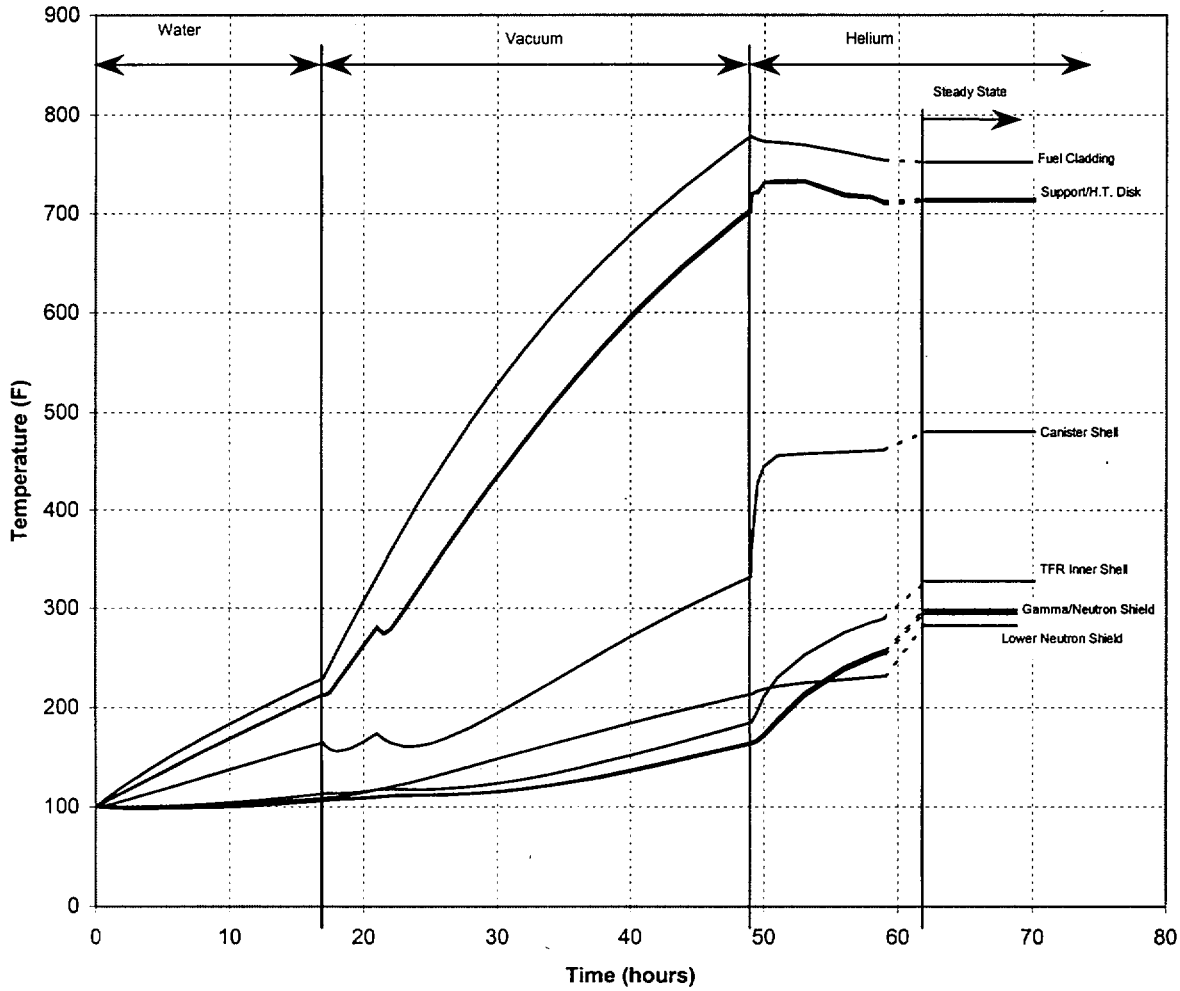

Notes:

1. This graph corresponds to a canister containing water for 17 hours, vacuum for 32 hours and 600 hours in the helium condition. The results correspond to a uniformly distributed decay heat load of 23 kW.
2. "TFR" refers to the standard transfer cask.

Figure 4.4.3-6 History of Maximum Component Temperature (°F) for Transfer Conditions for BWR Fuel with Design Basis 23 kW Uniformly Distributed Heat Load

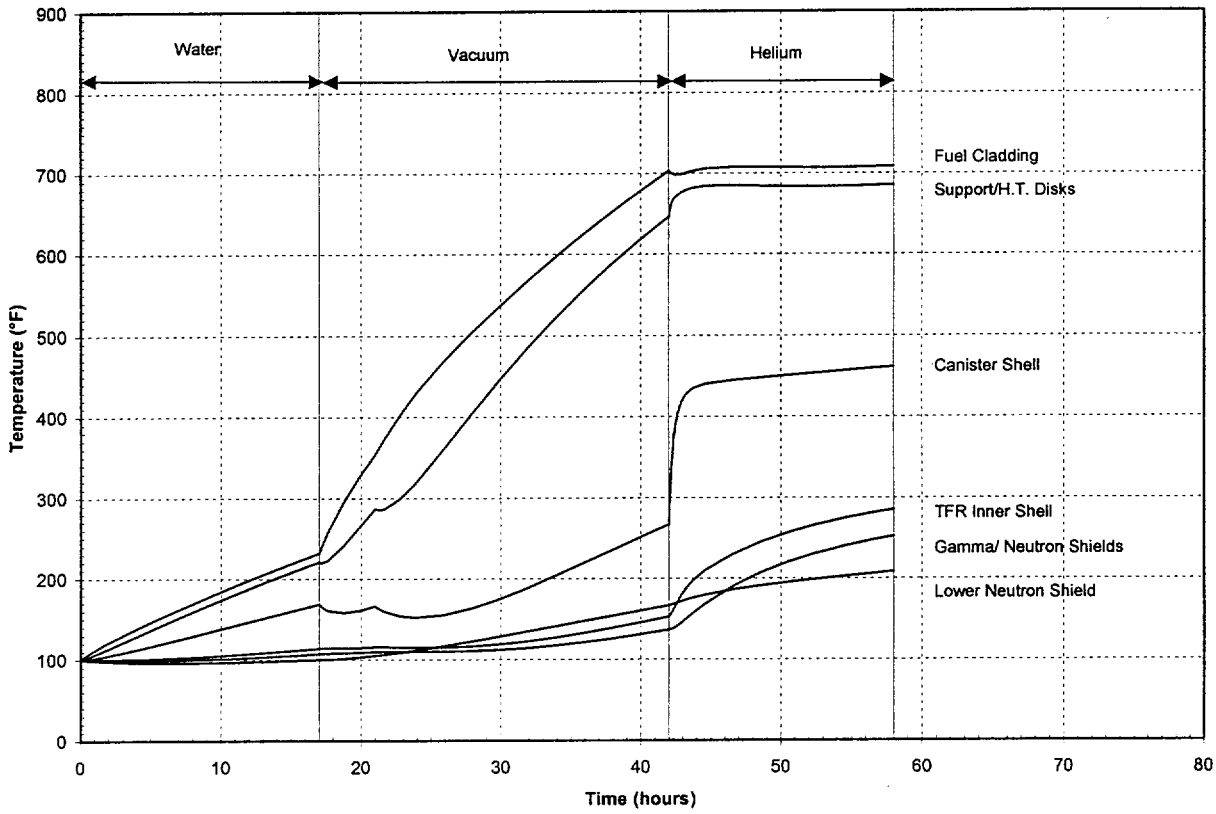

Notes:

1. This graph corresponds to a canister containing water for 17 hours, vacuum for 25 hours and 16 hours in the helium condition. The results correspond to a uniformly distributed decay heat load of 23 kW.
2. "TFR" refers to the standard transfer cask.

Figure 4.4.3-7 Basket Location for the Thermal Analysis of PWR Reduced Heat Load Cases

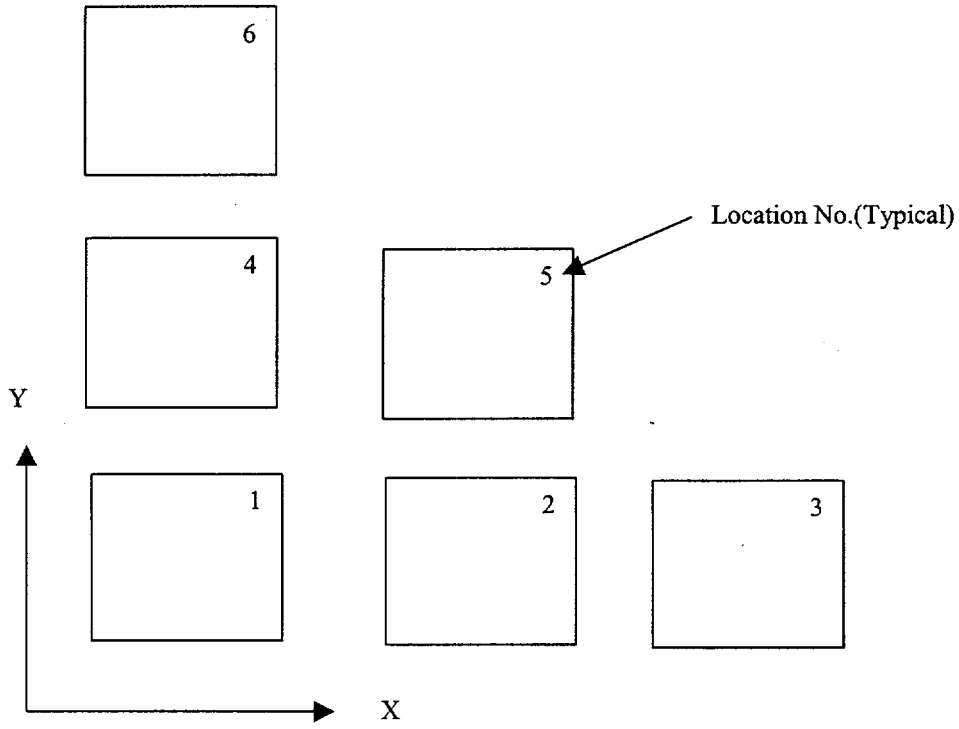

A quarter symmetry configuration is considered. X and Y axes are at the centerlines of the basket.

Figure 4.4.3-8 BWR Fuel Basket Location Numbers

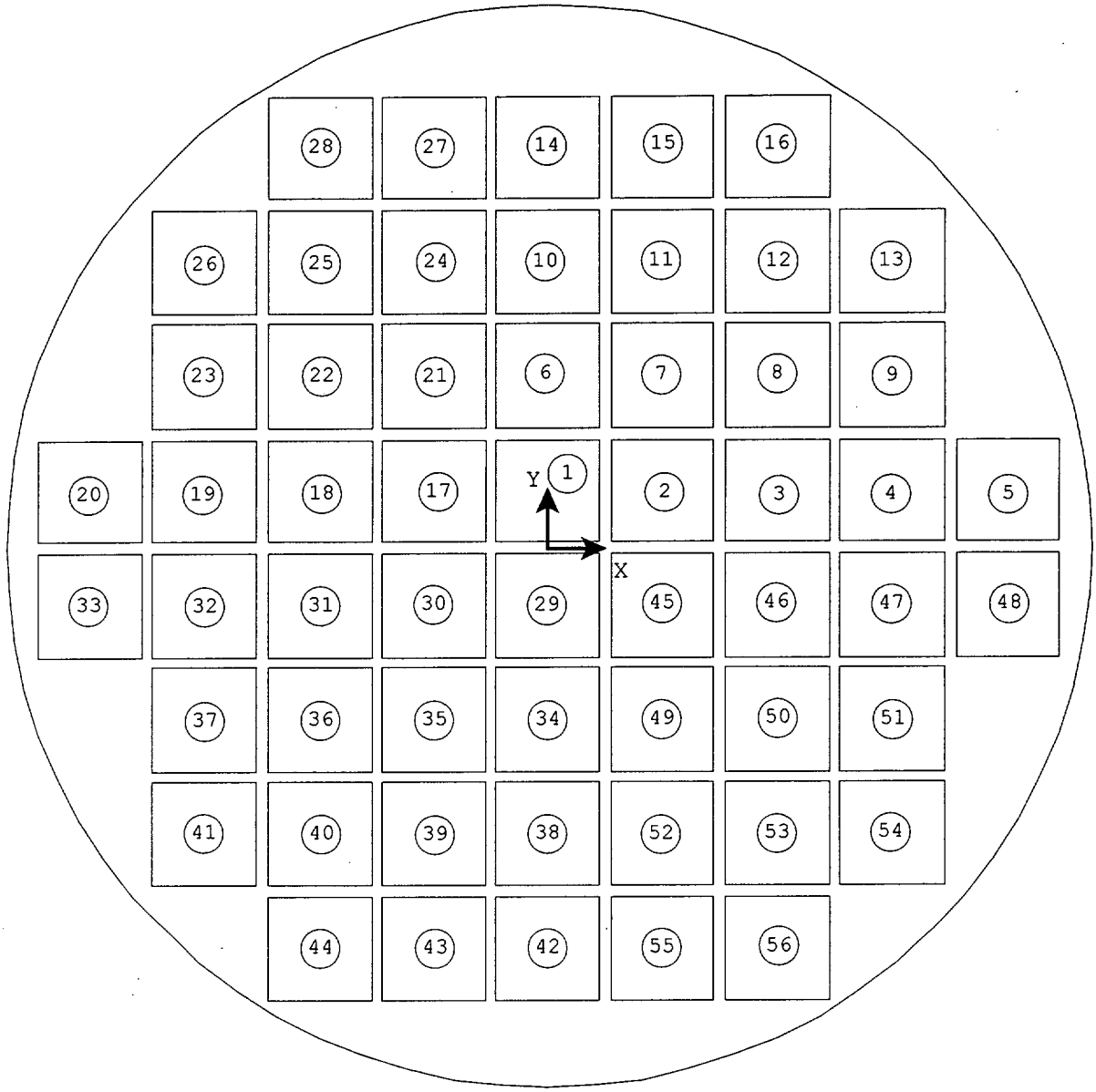

Figure 4.4.3-9 PWR Basket Fuel Loading Positions

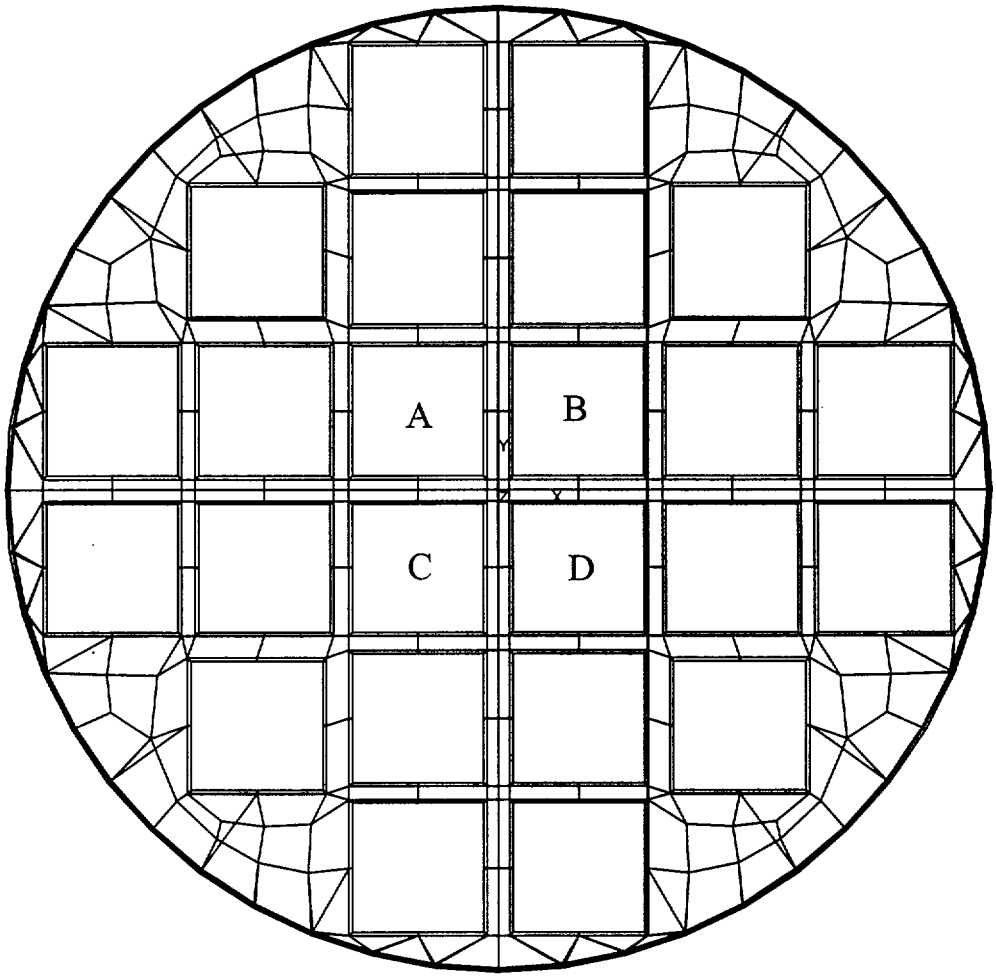

Figure 4.4.3-10 BWR Basket Fuel Loading Positions

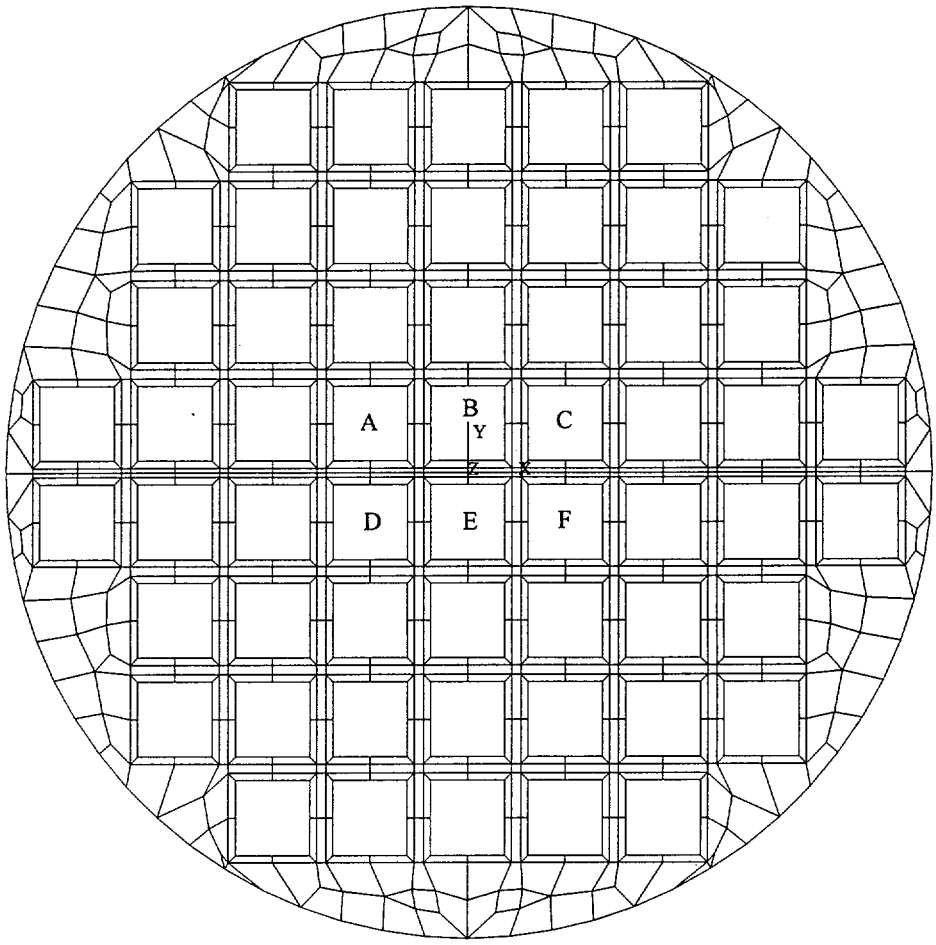

Table 4.4.3-1 Maximum Component Temperatures for the Normal Storage Condition - PWR

Component	Maximum Temperature (°F)	Allowable Temperatures (°F)
Fuel Cladding	648	716
Heat Transfer Disk	599	650
Support Disk	601	650
Top Weldment	399	800
Bottom Weldment	159	800
Canister Shell	351	800
Canister Structural Lid	204	800
Canister Shield Lid	212	800
Concrete	186 (local) 135 (bulk*)	300 (local) 150 (bulk)

* The volume average temperature of the concrete region is used as the bulk concrete temperature.

Table 4.4.3-2 Maximum Component Temperatures for the Normal Storage Condition - BWR

Component	Maximum Temperature (°F)	Allowable Temperatures (°F)
Fuel Cladding	642	716
Heat Transfer Disk	612	650
Support Disk	614	700
Top Weldment	361	800
Bottom Weldment	276	800
Canister Shell	376	800
Canister Structural Lid	180	800
Canister Shield Lid	185	800
Concrete	192 (local) 136 (bulk*)	300 (local) 150 (bulk)

*The volume average temperature of the concrete region is used as the bulk concrete temperature.

Table 4.4.3-3 Maximum Component Temperatures for the Transfer Condition – PWR Fuel with Design Basis 23 kW Uniformly Distributed Heat Load

Component	Maximum Temperature (°F)		Allowable Temperature (°F)
	Vacuum[1]	Helium[1]	
Fuel	779	779	1058
Lead	165	299	600
Neutron Shield	213	295	300
Heat Transfer Disk	702	732	750
Support Disk	705	734	800
Canister	332	481	800
Transfer Cask Shells	185	328	700

1. See Figure 4.4.3-5 for history of maximum component temperatures.

Table 4.4.3-4 Maximum Component Temperatures for the Transfer Condition – BWR Fuel with Design Basis 23 kW Uniformly Distributed Heat Load

Component	Maximum Temperature (°F)		Allowable Temperature (°F)
	Vacuum[1]	Helium[1]	
Fuel	703	708	1058
Lead	137	252	600
Neutron Shield	135	249	300
Heat Transfer Disk	645	683	750
Support Disk	646	686	700
Canister	267	462	800
Transfer Cask Shells	153	286	700

1. See Figure 4.4.3-6 for history of maximum component temperatures.

Table 4.4.3-5 Maximum Limiting Component Temperatures in Transient Operations for the Reduced Heat Load Cases for PWR Fuel

Heat Load (kW)	Water			Vacuum			Helium		
	Duration (hours)	Maximum Temperature (°F)		Duration (hours)	Maximum Temperature (°F)		Duration (hours)	Max. Temp. / Temp. at Steady-state (°F)	
		Fuel	Heat Transfer Disk		Fuel	Heat Transfer Disk		Fuel	Heat Transfer Disk
23.0	17	230	213	32	779	702	600[2]	779/752	732/713
20.0	18	232	214	37	785	695	600[2]	785/707	723/664
17.6	20	239	219	44	797	697	600[2]	797/672	725/625
17.6[1]	20	232	214	44	783	684	600[2]	783/658	703/611
14.0	22	240	219	68	811	700	600[2]	811/613	724/560
11.0	24	237	215	600[2]	822	702	600[2]	822/555	727/496
8.0	26	224	199	600[2]	751	588	600[2]	751/484	622/413

1. Preferential loading configuration 2, site specific case for Maine Yankee.
2. Duration is defined based on a test time of 30 days for abnormal regimes as described in PNL-4835 [34].

Table 4.4.3-6 Maximum Limiting Component Temperatures in Transient Operations for PWR Fuel after In-Pool Cooling

Heat Load (kW)	In-Pool (helium)			Vacuum			Helium		
	Duration (hours)	End Temperature (°F)		Duration[1] (hours)	Maximum Temperature (°F)[2]		Duration (hours)	Max. Temp. / Temp. at Steady-state (°F)	
		Fuel	Heat Transfer Disk		Fuel	Heat Transfer Disk		Fuel	Heat Transfer Disk
23.0	24	507	434	19	779	702	600[3]	779/752	732/713
20.0	24	489	407	26	785	695	600[3]	785/707	723/664
17.6	24	481	400	33	797	697	600[3]	797/672	725/625
14.0	24	468	385	61	811	700	600[3]	811/613	724/560

1. The maximum allowable time in the Technical Specification for this condition is equal to 2 hours less than the maximum allowable time shown in this table. This 2-hour reduction allows the handling time required to enter the next stage.
2. The maximum temperatures at the end of the first vacuum (Table 4.4.3-5) are conservatively presented.
3. Duration is defined based on a test time of 30 days for abnormal regimes as described in PNL-4835.

Table 4.4.3-7 Maximum Limiting Component Temperatures in Transient Operations for PWR Fuel after Forced-Air Cooling

Heat Load (kW)	Forced-Air (helium)			Vacuum			Helium		
	Duration (hours)	End Temperature (°F)		Duration[1] (hours)	Maximum Temperature (°F)		Duration (hours)	Max. Temp. / Temp. at Steady-state (°F)	
		Fuel	Heat Transfer Disk		Fuel	Heat Transfer Disk		Fuel	Heat Transfer Disk
23.0	24	648	594	9	779	702	600[3]	779/752	732/713
20.0	24	619	558	14	785	695	600[3]	785/707	723/664
17.6	24	600	544	21	797	697	600[3]	797/672	725/625
14.0	24	572	506	45	811	700	600[3]	811/613	724/560

1. The maximum allowable time in the Technical Specification for this condition is equal to 2 hours less than the maximum allowable time shown in this table. This 2-hour reduction allows the handling time required to enter the next stage.
2. The maximum temperatures at the end of the first vacuum (Table 4.4.3-5) are conservatively presented.
3. Duration is defined based on a test time of 30 days for abnormal regimes as described in PNL-4835.

Table 4.4.3-8 Maximum Limiting Component Temperatures in Transient Operations for BWR Fuel

Heat Load (kW)	Water			Vacuum			Helium		
	Duration (hours)	Maximum Temperature (°F)		Duration (hours)	Maximum Temperature (°F)		Duration (hours)	Max. Temp. / Temp. at Steady-state (°F)	
		Fuel	Heat Transfer Disk		Fuel	Heat Transfer Disk		Fuel	Heat Transfer Disk
23	17	232	221	25	703	645	16	708	683
20	18	234	222	27	694	627	30	694	661
17	19	234	221	33	701	629	600[1]	701/660	659/631
14	20	232	219	45	719	643	600[1]	719/606	671/574
11	23	234	220	72	733	653	600[1]	733/543	679/508
8	31	236	220	600[1]	724	639	600[1]	724/467	639/427

1. Duration is defined based on a test time of 30 days for abnormal regimes as described in PNL-4835.

Table 4.4.3-9 Maximum Limiting Component Temperatures in Transient Operations after Vacuum for BWR Fuel after In-Pool Cooling

Heat Load (kW)	In-Pool (helium)			Vacuum			Helium		
	Duration (hours)	End Temperature (°F)		Duration[1] (hours)	Maximum Temperature (°F)		Duration (hours)	Max. Temp. / Temp. at Steady-state (°F)	
		Fuel	Heat Transfer Disk		Fuel	Heat Transfer Disk		Fuel	Heat Transfer Disk
23	24	488	444	12	703	645	16	708	683
20	24	476	431	13	694	627	30	694	661
17	24	467	419	19	701	629	600[3]	701/660	659/631
14	24	455	404	28	719	643	600[3]	719/606	671/574
11	24	439	383	54	733	653	600[3]	733/543	679/508

1. The maximum allowable time in the Technical Specification for this condition is equal to 2 hours less than the maximum allowable time shown in this table. This 2-hour reduction allows the handling time required to enter the next stage.
2. The maximum temperatures at the end of the first vacuum (Table 4.4.3-8) are conservatively presented.
3. Duration is defined based on a test time of 30 days for abnormal regimes as described in PNL-4835.

Table 4.4.3-10 Maximum Limiting Component Temperatures in Transient Operations after Vacuum for BWR Fuel after Forced-Air Cooling

Heat Load (kW)	Forced-Air (helium)			Vacuum			Helium		
	Duration (hours)	End Temperature (°F)		Duration[1] (hours)	Maximum Temperature (°F)		Duration (hours)	Max. Temp. / Temp. at Steady-state (°F)	
		Fuel	Heat Transfer Disk		Fuel	Heat Transfer Disk		Fuel	Heat Transfer Disk
23	24	623	591	4	703	645	16	708	683
20	24	592	558	5	694	627	30	694	661
17	24	565	528	10	701	629	600[3]	701/660	659/631
14	24	541	503	20	719	643	600[3]	719/606	671/574
11	24	519	477	43	733	653	600[3]	733/543	679/508

1. The maximum allowable time in the Technical Specification for this condition is equal to 2 hours less than the maximum allowable time shown in this table. This 2-hour reduction allows the handling time required to enter the next stage.
2. The maximum temperatures at the end of the first vacuum (Table 4.4.3-8) are conservatively presented.
3. Duration is defined based on a test time of 30 days for abnormal regimes as described in PNL-4835.

Table 4.4.3-11 Maximum Limiting Component Temperatures in Transient Operations after Helium for BWR Fuel after In-Pool Cooling

Heat Load (kW)	In-Pool (helium)			Helium		
	Duration (hours)	End Temperature (°F)		Duration (hours)	Max. Temp. (°F)[1]	
		Fuel	Heat Transfer Disk		Fuel	Heat Transfer Disk
23	24	489	444	16	708	683
20	24	477	431	30	694	661

1. The maximum temperatures at the end of helium in Table 4.4.3-8 are conservatively used.

Table 4.4.3-12 Maximum Limiting Component Temperatures in Transient Operations after Helium for BWR Fuel after Forced-Air Cooling

Heat Load (kW)	Forced-Air (helium)			Helium		
	Duration (hours)	End Temperature (°F)		Duration (hours)	Max. Temp. (°F)[1]	
		Fuel	Heat Transfer Disk		Fuel	Heat Transfer Disk
23	24	630	598	16	708	683
20	24	601	566	30	694	661

1. The maximum temperatures at the end of helium in Table 4.4.3-8 are conservatively used.

Table 4.4.3-13 Temperature Summary for PWR Fuel Preferential Loading

Case	Total Heat Load (kW)	Parameter	Basket Position[1]				
			A	B	C	D	Remainder
1	22.48	Cool Time (years)	5	5	5	6	6
		Heat Load (kW)	0.958	0.958	0.958	0.933	0.933
		Allowable (°F) [2]	700	700	700	687	687
		Max. Temp. (°F)	644	644	644	642	600
2	20.55	Cool Time (years)	5	5	5	7	7
		Heat Load (kW)	0.958	0.958	0.958	0.842	0.842
		Allowable (°F) [2]	700	700	700	649	649
		Max. Temp. (°F)	629	629	629	619	580
3	20.15	Cool Time (years)	7	7	7	15	7
		Heat Load (kW)	0.842	0.842	0.842	0.796	0.842
		Allowable (°F) [2]	649	649	649	630	649
		Max. Temp. (°F)	613	613	613	609	575

Notes: (1) See Figure 4.4.3-9 for basket position locations.
(2) Allowable temperatures based on 45,000 MWD/MTU burnup (see Table 4.4.7-5).

Table 4.4.3-14 Temperature Summary for BWR Fuel Preferential Loading

Case	Total Heat Load (kW)	Parameter	Basket Position[1]						
			A	B	C	D	E	F	Remainder
1	23	Cool Time (years)	5	5	5	5	6	5	6
		Heat Load (kW)	0.411	0.411	0.411	0.411	0.411	0.411	0.411
		Allowable (°F)[2]	732	732	732	732	709	732	709
		Max. Temp. (°F)	633	642	633	633	641	633	623
2	22.18	Cool Time (years)	5	5	5	5	7	5	7
		Heat Load (kW)	0.411	0.411	0.411	0.411	0.395	0.411	0.395
		Allowable (°F)[2]	732	732	732	732	666	732	666
		Max. Temp. (°F)	628	639	629	628	637	629	618
3	22.08	Cool Time (years)	7	7	7	7	15	7	7
		Heat Load (kW)	0.395	0.395	0.395	0.395	0.377	0.395	0.395
		Allowable (°F)[2]	666	666	666	666	642	666	666
		Max. Temp. (°F)	625	634	625	624	633	625	616

Notes: (1) See Figure 4.4.3-10 for basket position locations.
(2) Allowable temperatures based on 45,000 MWD/MTU burnup (see Table 4.4.7-5).

THIS PAGE INTENTIONALLY LEFT BLANK

4.6 References

1. Code of Federal Regulations, "Licensing Requirements for the Independent Storage of Spent Nuclear Fuel and High Level Radioactive Waste," Part 72, Title 10, January 1996.

2. PNL-4835, Johnson, A.B., and Gilbert, E.R., "Technical Basis for Storage of Zircaloy-Clad Fuel in Inert Gases," 1985.

3. PNL-4555, "Results of Simulated Abnormal Heating Events for Full-Length Nuclear Fuel Rods," Gwenther, R.J., Pacific Northwest Laboratories, 1983.

4. ACI-349-85, American Concrete Institute, "Code Requirement for Nuclear Safety Related Concrete Structures and Commentary."

5. PNL-6189, Levy, et al., Pacific Northwest Laboratory, "Recommended Temperature Limits for Dry Storage of Spent Light-Water Zircalloy Clad Fuel Rods in Inert Gas," May 1987.

6. ANSYS Revision 5.2 and ANSYS Revision 5.5, Computer Program, ANSYS, Inc., Houston, PA.

7. MIL-HDBK-5G, Military Handbook, "Metallic Materials and Elements for Aerospace Vehicle Structures," U.S. Department of Defense, November 1994.

8. Genden Engineering Services & Construction Company, NS-4-FR Fire Resistant Neutron and/or Gamma Shielding Material - Product Technical Data.

9. Baumeister T. and Mark, L.S., Standard Handbook for Mechanical Engineers, 7th Edition, New York, McGraw-Hill Book Co., 1967.

10. The American Society of Mechanical Engineers, "ASME Boiler and Pressure Vessel Code," 1995, with 1995 Addenda.

11. ARMCO Product Data Bulletin No. S-22, "17-4PH, Precipitation Hardening Stainless Steel," ARMCO, Inc., 1988.

12. The American Society of Mechanical Engineers, "ASME Boiler and Pressure Vessel Code, Code Cases - Boilers and Pressure Vessels," Code Case N-71-17, 1996.

13. The American Society of Mechanical Engineers, "ASME Boiler and Pressure Vessel Code, Section II, Part D - Properties," 1995 Edition with 1995 Addenda.

14. Hanford Engineering Development Laboratory, "Nuclear Systems Materials Handbook," Volume 1, Design Data, Westinghouse Hanford Company, TID26666.

15. Bucholz, J.A., "Scoping Design Analyses for Optimized Shipping Casks Containing 1, 2-, 3-, 5-, 7-, or 10-Year-Old Spent Fuel, Oak Ridge National Library," ORNL/CSD/TM-149, 1983.

16. Ross R. B., "Metallic Specification Handbook," 4th Edition, London, Chapman and Hall, 1992.

17. Kreith, F., and Bohn, M. S., "Principles of Heat Transfer," 5th Edition, West Publishing Company, 1993.

18. Edwards, "TRUMP, A Computer Program for Transient and Steady State Temperature Distributions in Multimensional Systems," Lawrence Radiation Laboratory, Livermore, Rept, UCLR-14754, Rev. 1, May 1968.

19. Kreith, F., "Principles of Heat Transfer," 3rd Edition, New York, Intext Educational Publishers.

20. Vargaftik, Natan B., et al., "Handbook of Thermal Conductivity of Liquids and Gases," CRC Press, October 1993.

21. Chapman, A.J., "Heat Transfer," 4th Edition, MacMillan Publishing Company, New York, 1987.